Local Time Dependence of Jupiter's Polar Auroral Emissions Observed by Juno UVS

Greathouse Thomas K.[1], Gladstone Randy[1], Versteeg Maarten H.[1], Hue Vincent[1], Kammer Joshua[2], Giles Rohini S[1], Davis Michael W.[1], Bolton Scott J[1], Levin Steven M.[3], Connerney John E. P.[4], Gérard Jean-Claude M.C.[5], Grodent Denis[5], Bonfond Bertrand[5], Bunce Emma[6], and Vogt Marissa F.[7]

[1]Southwest Research Institute
[2]SWRI
[3]Jet Propulsion Laboratory
[4]NASA Goddard Space Flight Center
[5]Université de Liège
[6]University of Leicester
[7]Boston University

November 16, 2022

Abstract

Auroral brightness and color ratio imagery, captured using the Juno mission's Ultraviolet Spectrograph, display intense emissions poleward of Jupiter's northern main emission, and these are split into two distinctly different spectral or "color ratio" regimes. The most poleward region, designated the "swirl region" by Grodent et al. (2003), exhibits a high color ratio, while low color ratio emissions are found within the collar around the swirl region but still poleward of the main emission. We confirm the apparent strong magnetospheric local time control within the polar collar (Grodent et al., 2003), with the dusk side bright "active region" emissions extending from ~11 to 22 hr of magnetospheric local time. These bright emissions dim by at least an order of magnitude between ~0 and 11 hr magnetospheric local time, in the midnight to dawn side "dark region". This magnetospheric local time structure holds true even when the entire northern oval is located on the night side of the planet (in ionospheric local time), a geometry unstudied prior to Juno, as it is unobservable from Earth. The swirl region brightens at ionospheric dawn (~5-7 ionospheric local time) and diminishes or completely disappears at ionospheric local times of ~20 to 22 hrs. Finally, the southern auroral polar emissions appear to share all of the local time dependencies of its northern counterpart, but at a reduced intensity.

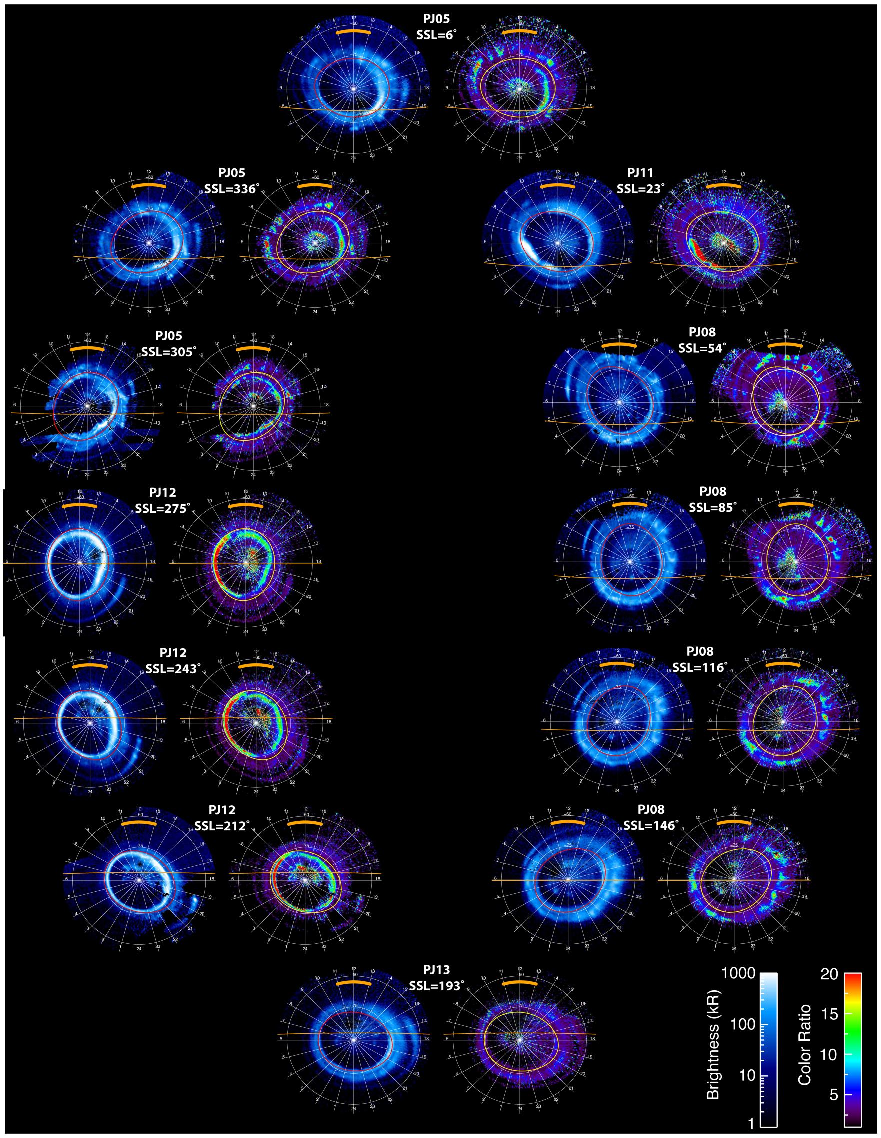
PJ05
SSL=6°
PJ05
SSL=336°
PJ11
SSL=23°
PJ05
SSL=305°
PJ08
SSL=54°
PJ12
SSL=275°
PJ08
SSL=85°
PJ12
SSL=243°
PJ08
SSL=116°
PJ12
SSL=212°
PJ08
SSL=146°
PJ13
SSL=193°
Brightness (kR)
1000
100
10
1
Color Ratio
20
15
10
5

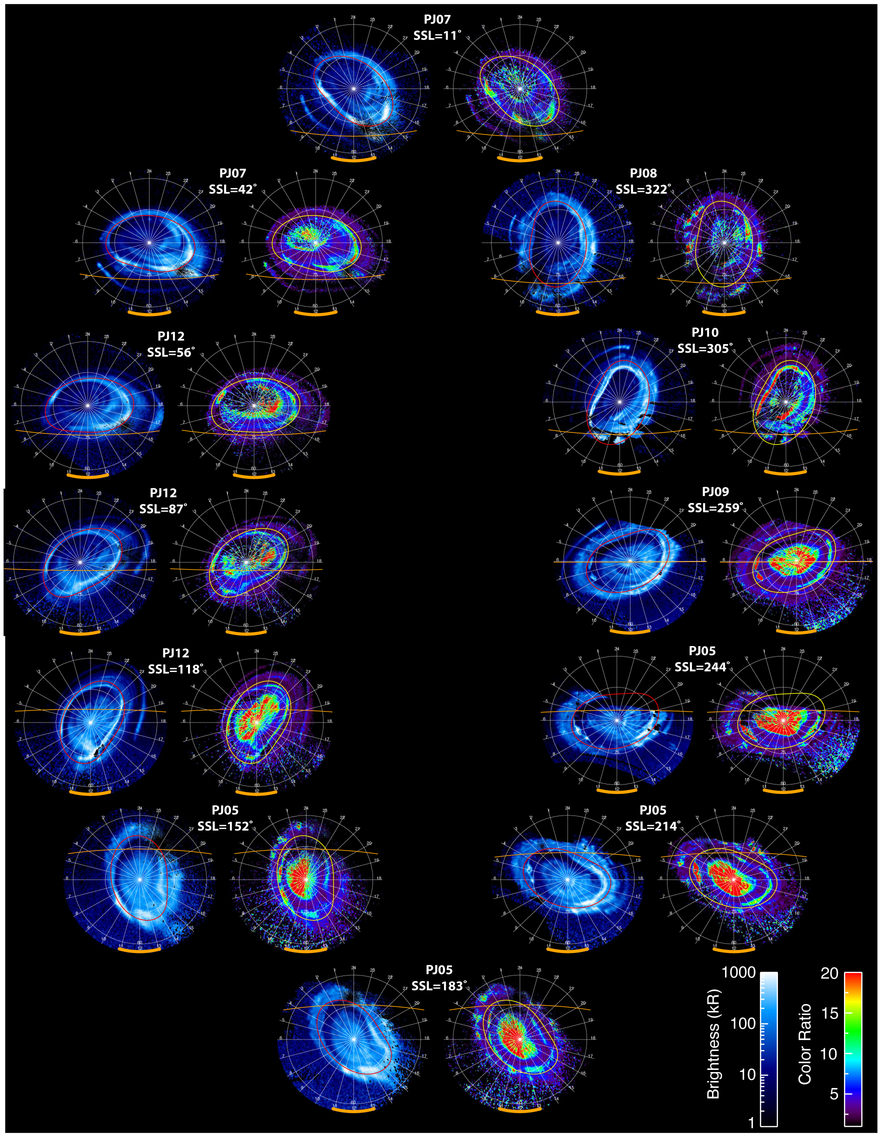
PJ07
SSL=11°
PJ07
SSL=42°
PJ08
SSL=322°
PJ12
SSL=56°
PJ10
SSL=305°
PJ12
SSL=87°
PJ09
SSL=259°
PJ12
SSL=118°
PJ05
SSL=244°
PJ05
SSL=152°
PJ05
SSL=214°
PJ05
SSL=183°
Brightness (kR)
1000
100
10
1
Color Ratio
20
15
10
5

Local Time Dependence of Jupiter's Polar Auroral Emissions Observed by Juno UVS

Thomas Greathouse[1], Randy Gladstone[1,2], Maarten Versteeg[1], Vincent Hue[1], Joshua Kammer[1], Rohini Giles[1], Michael Davis[1], Scott Bolton[1], Steven Levin[3], John Connerney[4], Jean-Claude Gérard[5], Denis Grodent[5], Bertrand Bonfond[5], Emma Bunce[6], and Marissa F. Vogt[7]

[1]Southwest Research Institute, San Antonio, TX, United States

[2]University of Texas at San Antonio, San Antonio, TX, United States

[3]Jet Propulsion Laboratory, Pasadena, CA, United States

[4]NASA Goddard Space Flight Center, Greenbelt, MD, United States

[5]Université de Liège, LPAP - STAR Institute, Liège, Belgium

[6]University Leicester, Leicester, United Kingdom

[7]Center for Space Physics, Boston University

Corresponding author: Thomas Greathouse (tgreathouse@swri.edu)

Key Points:

- Jupiter's bright and variable polar auroral swirl region emissions are observed to be weak/absent from 22 to 7 hours local solar time.
- Higher color ratios observed within the polar swirl region relative to the dark/active regions suggest differing physical mechanisms.
- Emissions from the newly defined polar collar (dark/active regions) correlate with magnetic local time regardless of local solar time.

Abstract

Auroral brightness and color ratio imagery, captured using the Juno mission's Ultraviolet Spectrograph, display intense emissions poleward of Jupiter's northern main emission, and these are split into two distinctly different spectral or "color ratio" regimes. The most poleward region, designated the "swirl region" by Grodent et al. (2003), exhibits a high color ratio, while low color ratio emissions are found within the collar around the swirl region but still poleward of the main emission. We confirm the apparent strong magnetospheric local time control within the polar collar (Grodent et al., 2003), with the dusk side bright "active region" emissions extending from ~11 to 22 hr of magnetospheric local time. These bright emissions dim by at least an order of magnitude between ~0 and 11 hr magnetospheric local time, in the midnight to dawn side "dark region". This magnetospheric local time structure holds true even when the entire northern oval is located on the night side of the planet (in ionospheric local time), a geometry unstudied prior to Juno, as it is unobservable from Earth. The swirl region brightens at ionospheric dawn (~5-7 ionospheric local time) and diminishes or completely disappears at ionospheric local times of ~20 to 22 hrs. Finally, the southern auroral polar emissions appear to share all of the local time dependencies of its northern counterpart, but at a reduced intensity.

Plain Language Summary

The Juno mission's unique observing geometry allows imaging of Jupiter's auroral polar emissions at all viewing orientations. The Juno-UVS dataset shows that emissions from the polar collar, a collar-shaped region located between the swirl region and the main auroral oval, are highly asymmetric, with strong emissions from near noon and dusk local times (~11-22 hours) and weak emissions from midnight to dawn local times (~22-11 hours). This local time mapping holds true regardless of viewing orientation, when the northern oval is completely in sunlight or completely in the dark, at ionospheric local times of noon and midnight, respectively. However, the high color ratio swirl region, poleward of the polar collar, appears to be more strongly controlled by ionospheric local time (local solar time), brightening at ionospheric dawn and dimming at ionospheric local times of 20-22 hrs. The difference in magnetospheric and ionospheric local time control of these two regions and their distinct difference in color ratio suggest they are governed by significantly different processes in the middle to outer magnetosphere. Possibly, the swirl region is connected to open or highly-twisted down-tail flux ropes while the polar collar is mapping to regions of closed magnetic flux in Jupiter's middle magnetosphere.

1. Introduction

Jupiter's ultraviolet aurorae provide a visual display of some of the complex interplay of Jupiter's strong magnetic field with the plasmas within the Jovian system. The Juno mission, with its highly elliptical polar orbit, was designed, in part, to bring a powerful package of in-situ and remote sensing instruments low over Jupiter's polar regions to probe the details of the high latitude magnetosphere (Bagenal et al., 2014; Bolton et al., 2017). The Juno Ultraviolet Spectrograph (UVS) (Gladstone et al., 2017) is an imaging spectrograph covering 68-210 nm. The instrument is used to produce brightness and color ratio maps of Jupiter's ultraviolet auroral H_2 emissions, providing information about the total flux and the average energy of precipitating electrons (Yung et al., 1982), respectively. These maps can be directly compared to measurements made by Juno's in-situ instruments (Ebert et al., 2019; Gérard et al., 2019; Allegrini et al., 2020b; Mauk et al., 2020; Szalay et al., 2020).

In addition to providing context imaging for the in-situ instruments, UVS also provides unique views of Jupiter's aurorae unobtainable from the Hubble Space Telescope (HST) (Grodent et al., 2018) or from Earth orbit in general (XMM, Chandra, or Hisaki). Due to Juno's polar orbit, UVS obtains near nadir views of Jupiter's aurorae, unlike the high zenith angle observations available with HST. Observations from HST are also limited to the planet's dayside, while UVS is able to provide observations at all local times. This makes Juno UVS uniquely suited to study the local time dependence of Jupiter's auroral emissions.

In this study, we present Juno UVS brightness and color ratio maps covering the full 24 hour range of local times and displaying the complex morphologies and local time behavior of the polar-most auroral emissions, i.e., those emissions occurring poleward of Jupiter's main auroral ovals. Bright emissions from within the auroral ovals is rather unique to Jupiter; in contrast, the polar caps of Earth and Saturn are mostly dark. It is thus not surprising that the polar-most regions of the Jovian aurorae are also the most poorly understood. While quite variable, the total emitted power of the polar regions in the UV range usually accounts for 1/3 of the total emitted power from the whole aurora, and the power in this region is generally correlated with that of the main emission (Nichols et al., 2009b; Grodent et al., 2018). Three sub-regions of Jupiter's polar UV aurora have been identified from HST images (Grodent et al., 2003): 1) the dark region on the dawn and night flanks of the main emissions, mostly devoid of UV emissions (e.g., Swithenbank-Harris et al., 2019); 2) the active region, where arcs and filaments (Nichols et al., 2007; 2009a; 2017; Grodent et al., 2018), very bright flares (Waite et al., 2001) and quasi-periodic flares (Bonfond et al., 2011; 2016) are found; and 3) the swirl region in the center, peppered with dynamic and chaotic emissions that are strongly absorbed by methane (Bonfond et al., 2017). These complicated polar auroral emissions are magnetically linked to processes in the mid- to outer-magnetosphere well beyond ~20-30 Jovian radii, R_J, the expected equatorial distance to which the main auroral emission maps in the magnetosphere (e.g., Cowley and Bunce, 2001; Hill, 2001). Moreover, the size and location of the swirl region is compatible with the area open to the solar wind deduced from flux-equivalence magnetic mapping models (Vogt et al., 2011; 2015; Bonfond et al., 2017). We leave discussions of the main emission (another name for the auroral ovals) and equatorward emissions for future studies, while the satellite footprint aurora have already been addressed in several studies (Szalay et al., 2018; Hue et al., 2019b; Allegrini et al., 2020a; Szalay et al., 2020).

2. Juno UVS Observations

2.1 Juno UVS mapping

UVS is mounted on the spinning, 2-rpm, Juno spacecraft, nominally looking radially outward with an entrance slit oriented parallel to the spin axis. In this configuration, the slit sweeps across the sky, capturing a 7.2° (slit length) by 360° swath every 30 seconds. UVS has a "dog bone" shaped slit, with two wide segments on either side of a narrower segment. During each spin, a point source is observed for 17 ms if it falls within the wide slit and for 2 ms if it falls within the narrow slit. Using the scan mirror located at the telescope's entrance aperture allows for the adjustment of the field of view fore or aft of the Juno spin plane by up to ±30°, in increments of 0.74°, resulting in a field of regard of 67.2° x 360°, slightly more than half the sky. We create images of Jupiter's auroral regions by adding together multiple spins of data taken with differing scan mirror positions. The exact number of spins needed to create a full image depends on the range of the spacecraft to Jupiter and the scan mirror pointing plan defined by the UVS team uniquely for each perijove (PJ), a close pass of Juno to Jupiter in its highly elliptical orbit. In general, it takes ~40 spins worth of data when observing from a range of 1.6 R_J (an altitude of 0.6 R_J). Given the 2-rpm spin rate of Juno, this equates to ~20 minutes to build composite images of the aurora. This type of data acquisition has several important repercussions for UVS imagery. The first is that even if UVS targets a given location within Jupiter's aurora, the absolute best temporal sampling achievable by UVS is 30 seconds, with each look corresponding to a 17 ms integration time. The second is that our composite images of the aurora include observations obtained at significantly different times. One side of the image may be observed 10-20 minutes before the other side of the image. An example of the production of such images is included in the supporting material S5 as multiple-spin animated GIF showing the addition of one spin at a time to produce a final image.

Brightness images presented here and in the supplementary material are calculated by integrating the observed H_2 emissions between 155 and 162 nm and multiplying by 8.1 to scale the them to all H_2 Werner and Lyman emissions (e.g., Figure 1). This process capitalizes on the transparency of Jupiter's atmosphere between 155 and 162 nm and then leverages models of H_2 emissions caused by electron impact to derive the total amount of energy emitted from H_2 due to electron precipitation (Gérard et al., 2019). Since the UVS instrument is a spectrograph, we simultaneously capture the UV emissions at all wavelengths between 68 and 210 nm (Hue et al., 2019a) with spectral resolution of ~1.3 nm within the narrow slit and 2-3 nm in the wide slits (Greathouse et al., 2013). This allows us to create accurate color ratio maps (e.g., Figure 2), where the color ratio is defined as the ratio of the radiance at 155-162 nm to the radiance at 125-130 nm (e.g., Bonfond et al., 2017). The wavelengths chosen for the color ratio are driven by methane's absorption spectrum, which has a long wavelength cutoff near 140 nm. The color ratio has long been used to infer the energy of the impacting electrons (e.g., Yung et al., 1982), with a higher color ratio implying higher energy electrons. The link between the color ratio and the particle energy follows the reasonable expectation that higher energy particles will plunge further into Jupiter's atmosphere. At these greater depths, the H_2 emissions are absorbed by the overlying CH_4 in Jupiter's atmosphere, preferentially removing flux from the 125-130 nm region relative to that at 155-162 nm, causing an increase in the color ratio (Yung et al., 1982). The energy dependence inferred from the color ratio assumes that the vertical structure of Jupiter's atmosphere is uniform across the polar region. This assumption has recently come under scrutiny (Gérard et al., 2014; Clark et al., 2018; Sinclair et al., 2020).

2.2 Image Rotation from System III Coordinates to a Magnetospheric Local Time Projection

In this study, we are primarily interested in changes in auroral emission as a function of local time, something not easily explored from Earth. There are two local times that are of potential interest here: the ionospheric local time (solar local time derived for an auroral position as its System III longitude compared to the System III subsolar longitude) and the magnetospheric local time (the approximate local time of the point where a magnetic field line from a given auroral position crosses the jovigraphic equator). Since we expect the auroral emissions to be primarily controlled by magnetospheric local time, we make a change of coordinate system due to the offset of Jupiter's magnetic dipole relative to Jupiter's rotational axis, which is the axis of the System III coordinate system. In producing our images, we first integrate 101 spins (50.5 minutes = 2 hours of local time for Jupiter) of UVS observations into a cylindrical map projection using Jupiter's System III coordinate frame. The relatively long integrations were used to guarantee good areal coverage and high signal to noise for the images. However, a drawback is that any local time variations will be blurred by 1/12th of a Jovian rotation period. Following this, we perform a rotation to replace the System III coordinate axis by the centroid of the 30 R_J mapping of the JRM09 model of Connerney et al. (2018) for the north and south pole independently. The location of the northern centroid is 71.2° latitude and 178.1° longitude System III, while the southern centroid is -82.5° latitude and 30.4° longitude. These positions require Z- and Y-axis rotations for the northern auroral maps of -178.1° and 18.8°, respectively, about the IAU_Jupiter coordinate frame (Acton, 1996). The corresponding rotations for the southern map are -30.4° and -7.5°, respectively. We then project the maps into orthographic projections orienting them such that they appear fixed in magnetospheric local time to aid the eye in looking for the expected magnetospheric local time effects. Figure 1 shows the result of this change in coordinate frame for an image of Jupiter's northern aurora. Figure 1a shows a System III orthographic projection, and Figure 1b shows the same data after recentering on the northern 30 R_J centroid and rotating such that the subsolar longitude is towards the bottom of the page. This remapping leads to the main auroral oval approximately centered in the image. If we observe brightness variations organized in magnetospheric local time poleward of the main emission in this new coordinate frame, then these variations are likely controlled by what is happening at similar local times in the middle to outer magnetosphere.

Although the coordinates in Figure 1b relate to the magnetospheric local time, the image still contains information about the ionospheric local time. The thick orange line shows the location of the sun over the integration period and the thin orange line shows the terminator at the midpoint of the image integration. Regions of the image between the terminator and the new pole are on the dayside (ionospheric daytime), even if they map to a night side magnetospheric local time. For example, in Figure 1b, there are little to no emissions seen in the sunlit region on the midnight side of the pole within the polar collar. This region experiences a daytime ionospheric local time (it is sunlit), while simultaneously being connected to the night side magnetosphere.

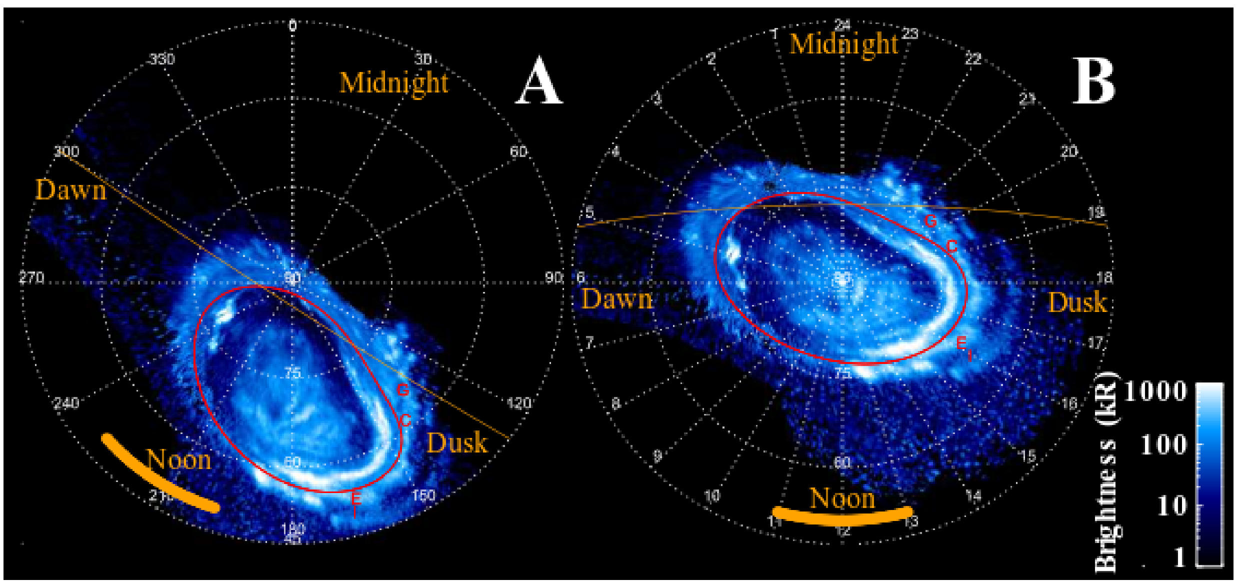

Figure 1: Panel A shows a brightness map of PJ5 data in System III coordinates. Panel B displays the same data in the magnetic dipole local time projection discussed in Section 2.2. The image was produced by integrating 101 spins of data, equivalent to an integration time period of 50.5 min. The local time map (B) is oriented such that noon at the midpoint of the integration time is directed down (towards the Sun), with dawn to the left and dusk to the right. The SIII longitudes in panel B have been replaced with magnetic local time values in hours. The terminator at 400 km altitude (orange thin line) is shown for the midpoint time while the thick orange line at the bottom shows the evolution of the Sun position over the integration time of the image (2 hours local time for Jupiter). The red ellipse in each panel demarcates the predicted Callisto footprint path, a representation of the mapping between the ionosphere and equatorial magnetosphere at ~26 R_J, using the JRM09 model.

2.3 Juno UVS' views of the poles

Using the magnetospheric local time projections of the data, we present observations of

Jupiter's northern aurora (tilted over as it is towards ~180° System III longitude) at approximately midnight (PJ8), dawn (PJ7), noon (PJ6), and dusk (PJ9) ionospheric local time (Fig. 2). The ionospheric local times can best be tracked looking at the terminator lines shown in Figure 2. For PJ6, when the aurora (180° longitude) is oriented most closely to ionospheric noon, the majority of the auroral oval is illuminated by the sun, while for PJ8, when the aurora is oriented most closely to ionospheric midnight (subsolar longitude ~0°), the majority of the oval is in darkness. While similar geometries to the ionospheric noon and dusk orientations in Figure 2 have been captured by HST many times in the past, only Juno could capture the midnight and dawn views shown in Figure 2. To compare images of Jupiter's aurora with distinctly different local time geometries, we must use images from multiple perijoves because the observation window for a given perijove is limited to a few hours. As Juno's orbit evolves over the course of the mission, the observation window for the northern polar region has been shrinking, decreasing coverage. However, the precession of the orbit is also positioning Juno at lower altitude over the north pole on each consecutive perijove, improving the spatial resolution of the maps over time. The situation is reversed in the south with viewing times increasing along with increasing spacecraft altitudes giving correspondingly lower spatial resolution maps. We present four south polar images in Figure 3 showing the local time variations in the south.

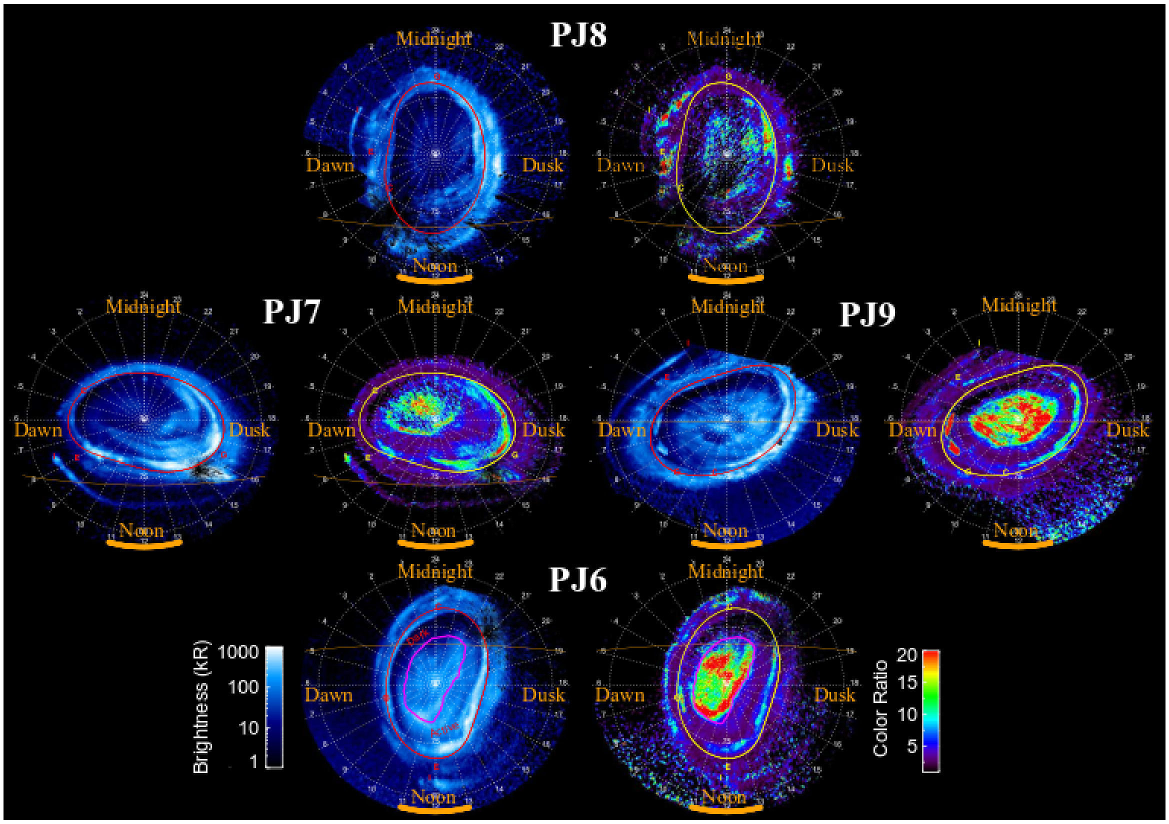

Figure 2: Maps of the northern auroral emissions with midnight, dawn, noon, and dusk (magnetic local time) labeled in orange, in both brightness on the left and color ratio on the right. Terminator, Sun direction, integration time, etc. are all as described in Fig 1. The path of the Callisto footprint is shown by the red curve in the brightness plots and the yellow curve within the color ratio plots for clarity. The PJ pass number from which the data were collected are listed in the figure between the brightness and color ratio maps. The approximate demarcation between the swirl region and polar collar is outlined in magenta in the PJ6 data at the bottom of the figure, and the dark and active regions within the polar collar are labeled in the PJ6 brightness map.

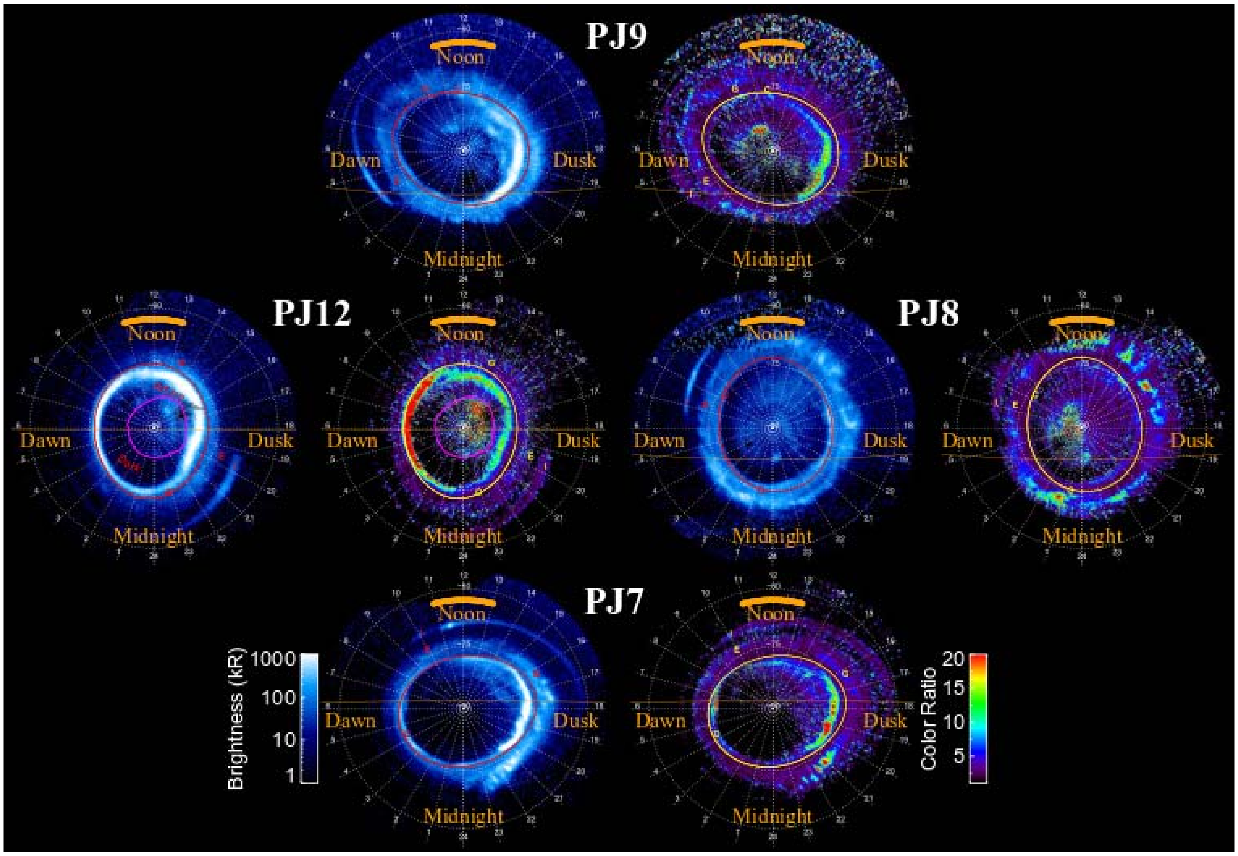

Figure 3: In these maps of the southern aurora, we have kept dawn on the left and dusk on the right, but have flipped noon and midnight relative to the plots of the northern aurora (Figure 2) with noon now pointed toward the top of the page. These maps are as would be seen from the spacecraft looking up at Jupiter's south pole. All the additional information (terminator, Callisto footprint path, local time, etc.) are the same as described in Figures 1 and 2. The approximate demarcation between swirl region and polar collar is outlined in magenta in the PJ12 data at the left of the figure, and the dark and active regions making up the polar collar are labeled in the PJ12 brightness map.

3. Results

3.1 The Polar Regions Redefined

When most of the auroral oval is sunlit, the color ratio maps of the northern aurora (PJ6, Figure 2) display a striking dichotomy between the "swirl region" and the "polar collar". The swirl region exhibits a high color ratio of ≥12, approximately encircled by the magenta line in the PJ6 images in Figure 2. The polar collar, outside of the swirl region but still within the main auroral oval, exhibits a low color ratio, ≤4 (Cf. Bonfond et al., 2017). While most obvious in the ionospheric noon-dusk view of the northern aurora where the swirl region emissions are brightest (PJ6 and PJ9, Fig. 2), this pattern is still evident at other ionospheric local times (see supplementary material). In this paper we consider the previously defined dark polar region and active region (see labels in PJ6 data, Fig. 2) (Grodent, 2015) to be part of a single region that we call the "polar collar", as we expect these two regions map to roughly similar radial distances in the magnetosphere and they exhibit the same color ratio emissions. The prime difference between the dark and active regions is a magnetospheric local time dependence, which we will discuss in the next section. The boundary between the swirl region and the polar collar is usually sharp and well defined in the color ratio maps, but is unremarkable in the brightness maps. This is especially noticeable on the dusk side where the polar collar emissions are similar in brightness to the dusk swirl-region emissions (PJ6 and PJ9, Fig. 2).

3.2 Polar Collar

Focusing now on the brightness maps of Figure 2 and the extra images in the supplementary material, it is striking that the polar collar emission shows strong (order of magnitude) magnetic local time dependence at all ionospheric local times (all subsolar longitudes). The Juno UVS map from PJ6 looks much like earlier observations taken from HST showing little to no emission on the dawn side of the polar collar (Swithenbank-Harris et al., 2019) until mid-morning where the polar collar emissions increase and can become as bright as the main emission. These emissions remain enhanced until late evening, ~21 hr magnetospheric local time, where they turn off. This local time variation gave rise to the dark and active region designations (Grodent et al., 2003). However, it could not be conclusively shown from HST observations alone if the polar collar always responds to magnetospheric local time drivers or if there is also a dependence on ionospheric local time. For the first time, the Juno UVS observations show that this polar collar emission structure is retained throughout all auroral ionospheric local times, even when the entire auroral oval is on the night side of Jupiter (i.e. PJ7 and PJ8 in Fig. 2), strongly supporting a magnetospheric rather than ionospheric local time driver for the emissions within the polar collar (Cowley et al., 2003). Additionally, the bright dusk-side polar collar emissions often organize into what appear to be concentric arcs alternating between higher and lower brightness, though all at relatively low color ratio. This behavior has been discussed at length in the literature, sometimes referred to as transient "inner ovals" (Nichols et al., 2009b). The Juno UVS observations show this behavior is independent of System III longitude and ionospheric local time, and appears to be purely a magnetospheric dusk-side phenomenon, as shown in Figure 4 at two very different ionospheric local times. Short dusk arcs are also observed from noon to early evening on the dusk side of some southern auroral maps such as the one from PJ7 in Figure 3.

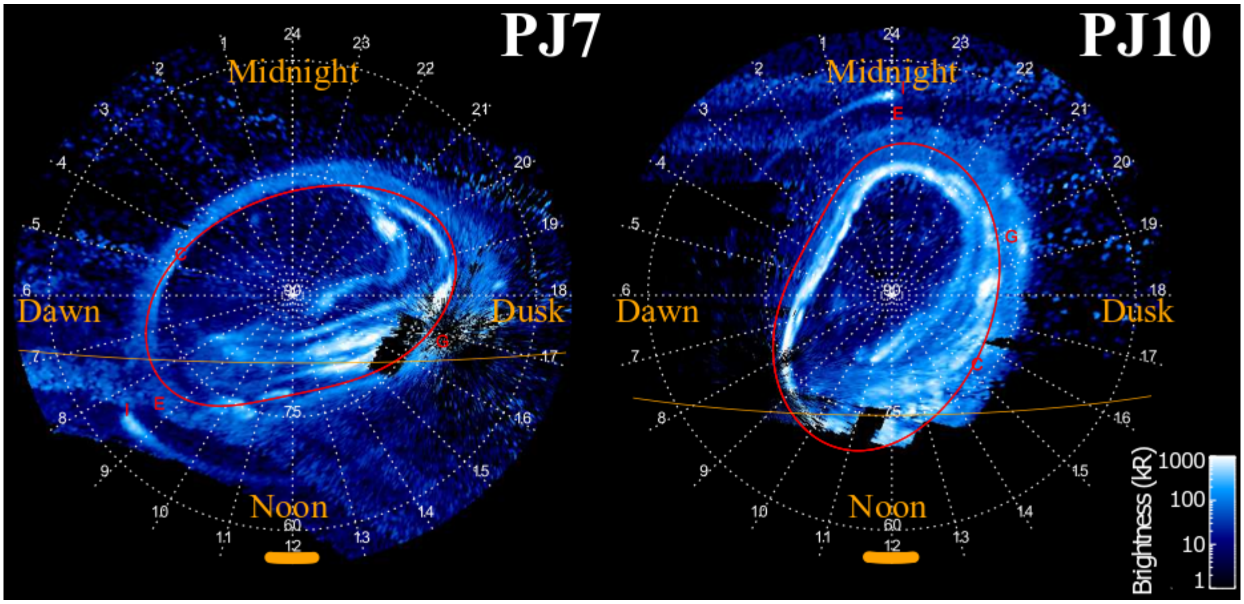

Figure 4: UV brightness maps from 31 spin (15.5 min) integrations of PJ7 and PJ10 observations. The dusk side concentric arcs within the polar collar are obvious in both, even though the System III longitudes and ionospheric local times are completely different.

3.3 Swirl Region

Surprisingly, the brightness of the swirl region appears to be primarily correlated with subsolar longitude, unlike the polar collar emissions. Looking at Figure 5 and data in the supplementary material S1 and S2, the initial brightening of the swirl region occurs very close to the dawn terminator. The terminator shown in the figures is calculated at 400 km above the 1-bar level, about the altitude of the auroral emissions. The swirl region remains bright throughout the time it is sunlit and for several hours after sunset (Figure 2) when the emissions then fade to a low level background state. This suggests that the swirl region brightness is affected by the amount of sunlight incident on the upper atmosphere, perhaps through photoionization-induced conductivity. It does not appear to be under magnetospheric local time control, as evidenced by the fact that the entire swirl region is bright at the bottom of Figure 2, with swirl region emissions bright even when mapped on the magnetospheric night side. The opposite is true when the swirl region is completely in the dark (top of Figure 2), showing the entire swirl region is dark including the area mapping to midday magnetospheric time. Interestingly, even though the brightness of the swirl region emissions is significantly reduced between midnight and dawn, most of the faint emissions observed during this time period are still of high color ratio.

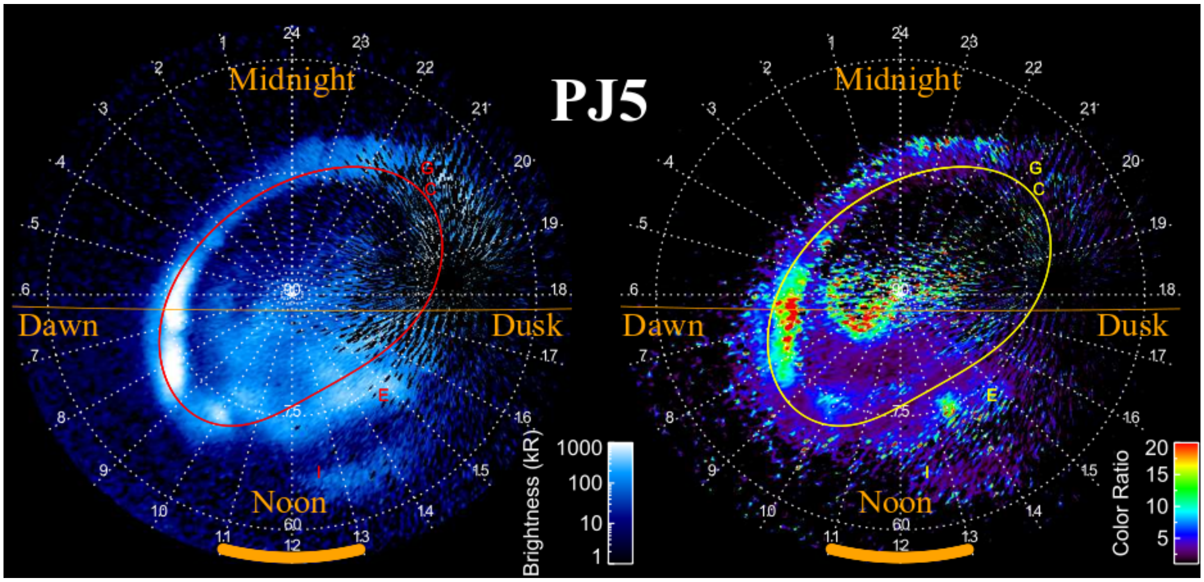

Figure 5: One of the best maps showing a portion of the swirl region brightening just as it crosses into sunlight. The majority of the swirl region is still in darkness exhibiting low emission brightness values.

3.4 Southern Polar Emissions Compared to the North

Though the south polar emissions shown in Figure 3 behave similarly to the north emissions described in the previous two sections, there are several differences worth noting. First is that the south polar emissions are generally much weaker than those in the north, as described by Grodent et al. (2018), and this is evident in the difference in emission strength and area between the northern and southern auroras shown in Figure 2Figure 3. The center of the south polar oval is much closer to Jupiter's south-pole rotational axis as compared to the north reducing the strength of the modulation of solar flux over a Jovian rotation within the south-polar swirl region. Given the weaker fluxes in the south-polar region, it is more difficult to make clear statements on the turn-on and -off times for the southern swirl and polar collar emission, but in general our observations suggest similar timing as those viewed in the north.

4. Discussion

Given the low color ratio and magnetospheric local time control of the polar collar in comparison to the high color ratio and ionospheric local time control of the swirl region, it seems likely that the physical phenomena responsible for producing the emissions in the polar collar and swirl region are different. Is the color ratio boundary tracing a distinct transition in the outer magnetosphere? In an attempt to address this question we employ the Vogt magnetic flux mapping model (Vogt et al., 2011; Vogt et al., 2015), updated to include the Jupiter JRM09 magnetic field model (Connerney et al., 2018). In Figure 6 we overlay the resultant local time and radial contours on top of brightness and color ratio maps from PJ5. We find that the red swirl region falls within the model contours suggesting it maps to beyond 150 R_J or would map beyond the magnetopause on the dayside in that model, which could be interpreted as mapping to a region of open flux. Whether this region is truly open flux or just highly twisted flux ropes extending to extreme distances down the magnetotail (Isbell et al., 1984; McComas and Bagenal, 2007; Zhang et al., 2021) cannot be discerned here. Possibly future magnetospheric models will be able to resolve this boundary and explain the different dynamics on either side leading to the clear auroral color ratio dichotomy.

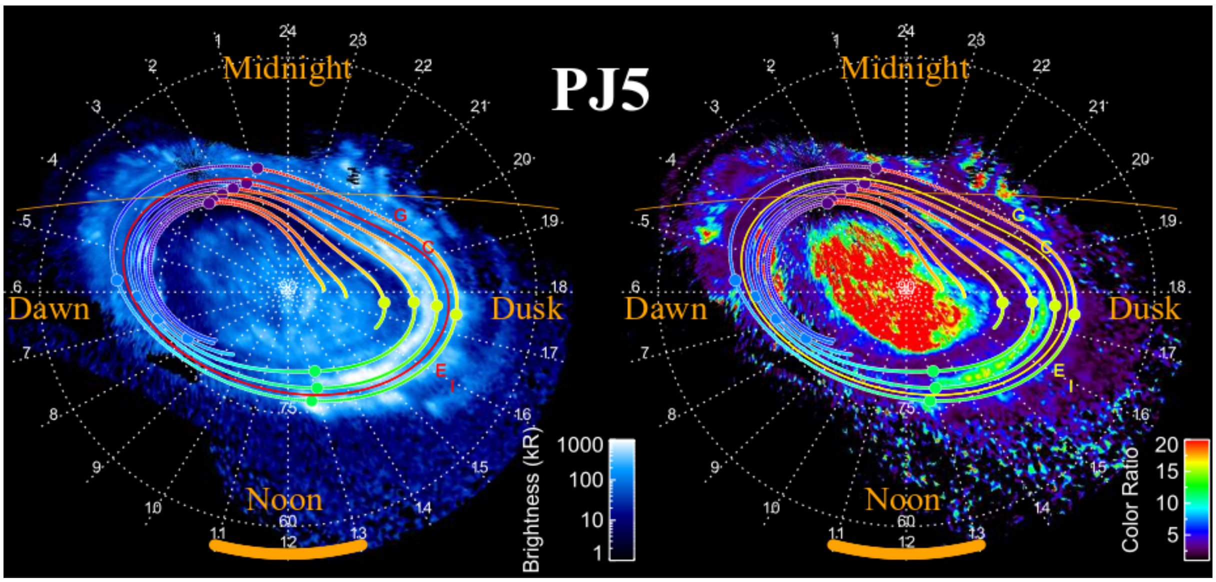

Figure 6: Observation of the north polar aurora taken during PJ5 similar in local time to that from PJ9 shown in Figure 2. Here we overplot Vogt et al.'s 2015 model contours corresponding to 15, 45, 75, 105, 135, and 150 R_J from outermost to innermost on the figure. Each contour is color coded in rainbow fashion to denote local time in the magnetosphere (purple = 0 hr, green = 12 hr, and red = 24 hr). The purple, blue, green and yellow dots on the contour indicate midnight, dawn, noon and dusk in the magnetosphere, respectively.

Several possibilities exist for producing the higher color ratio emissions within the swirl region. The first is that for some reason the downward going magnetospheric electrons within this region are of higher energy than those observed over the polar collar. Higher energy electrons will travel deeper into Jupiter's atmosphere and excite the H_2 emissions at greater depth. These H_2 emissions would then exhibit a higher color ratio due to the absorption of CH_4 in the overlying atmosphere. While this is quite likely the simplest and most plausible reasoning, Juno to date has only rarely observed such a high-energy downward propagating electron population over the swirl region. To the contrary, Juno has primarily measured high energy,

>1MeV, electrons directed up from Jupiter's swirl region, but not a strong downward component (Clark et al., 2017; Mauk et al., 2020). It is possible that Juno has not yet gotten low enough over the northern swirl region to get below the acceleration region. If this is the case, Juno should be able to resolve the issue during the extended mission where the altitude of the northern auroral passes will continue to shrink. A second possibility is that the swirl region has a significantly different CH_4 vertical profile as compared to regions outside the swirl region. Several lines of evidence support the idea of a different CH_4 vertical structure associated with the auroral region (Moriconi et al., 2017; Clark et al., 2018; Sinclair et al., 2020). A sudden increase in the altitude of the CH_4 homopause relative to regions outside the swirl region would create a higher color ratio within the swirl region even for a uniform electron downward energy flux. However, as already stated, downward electrons have only rarely been found over the swirl region in amounts capable of reproducing the emissions observed in the UV (Ebert et al., 2019; Gérard et al., 2019). A third possibility is that sunlight would initiate/enhance photoionization of the upper atmosphere and in particular methane and other light hydrocarbons at the top of the neutral atmosphere. Ionization of the hydrocarbons would increase the ionospheric density at the base of the ionosphere, pushing the ionosphere deeper into Jupiter's upper atmosphere. This extension to greater depths coupled with aurorally driven Pedersen currents crossing the swirl region may be the cause of the high color ratio emissions if the collisions causing the H_2 emissions observed by UVS in the polar region are in fact coming from near the base of the ionosphere. However, this Pedersen current requires that ambient ionospheric ions carrying the current are accelerated to a few 10s of eV, in order to excite the H_2 emissions, which is difficult to do. Whatever the cause of the emissions, we observe that they brighten near sunrise and remain strong several hours of local time past sunset. It could be that the deeper ionospheric layer created during the day can exist well into the night due to a time lag in the recombination of the electrons and molecular hydrocarbon ions, or because some underlying current exists which would help support the extra ionization instigated by the sunlight during the daylight hours. Further evaluation of this and other possible explanations for the swirl region emissions goes beyond the scope of this observational paper. We leave it to future works to disentangle the exact mechanisms.

The description in section 3.3 of the local time variability in the swirl region is true for most of the observations made by Juno UVS. However, there are a few observations where some unique emissions appear in the swirl region when it is positioned on the night side in the dark (midnight to dawn ionospheric local time). We show two such examples in Figure 7. Between the hours of ~2 and 6 magnetic local time, we have observed localized, high brightness, and lower color ratio (<8) emissions coming from discrete locations in the swirl region (examples circled in green in Figure 7). These observations sometimes show single spots of emission, as shown at the bottom of Figure 7, while other features have been seen to evolve over time to trace out swirls (top of Figure 7). Given their inconsistency (not seen in all instances, e.g. PJ7 and PJ8 in Figure 2) and their distinctive lower color ratio in the swirl region, which at most other times show emissions of high color ratio, we suspect these emissions are due to a distinct phenomenon occurring in the midnight to dawn sector of the magnetosphere and mapping to great radial distances, >150 R_J from comparisons with the Vogt JRM09 flux mapping results. The emission circled in PJ3 in Figure 7 has been characterized as a polar auroral bright spot by Haewsantati et al. (2021). As the Juno mission continues, we hope to observe such events while the spacecraft is connected to their magnetic field lines in order to sample the particles forming these emissions to help trace their origin and the reason for their different UV emission characteristics.

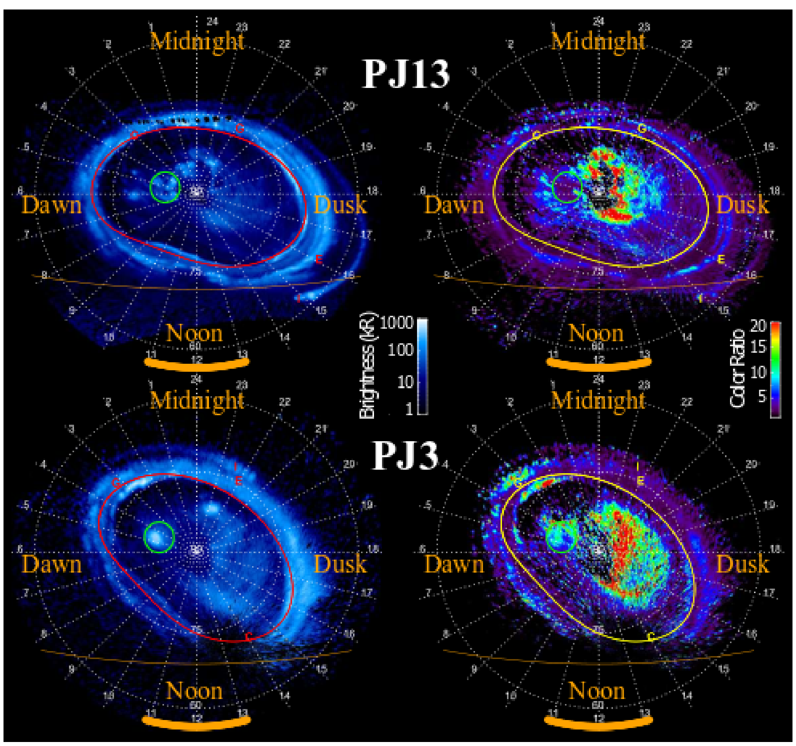

Figure 7: UV brightness and color ratio maps of the northern aurora from PJ3 (bottom) and PJ13 (top). The green circles enclose brightness anomalies, in what would generally be a low brightness period in the swirl region. The color ratio maps show that the emissions, though occurring in the swirl region, are of low to modest color ratio, quite different from the usual high color ratio emissions found there. While the green circles in a single pair of brightness and color ratio plots are in exactly the same place, there was no attempt to place them in the same position between PJ13 and PJ3. The fact that the circles in the two different observations are so close may be chance or may hint that both events have similar source regions in the outer magnetosphere, preferentially manifesting themselves at similar magnetospheric local time.

5. Conclusions

The imagery of Jupiter's northern and southern auroral zones captured from the unique vantage point of Juno UVS has produced an unbiased dataset with which to probe possible local time effects in Jupiter's magnetosphere. The global views of Jupiter's UV polar auroral emissions on the night side, at resolutions equal to or better than those captured on the dayside by HST, show the following key results:

1) The high color ratio of the polar swirl region makes it easily recognizable in UVS color ratio imagery in the middle of the northern auroral oval, and slightly offset in the southern auroral oval. The emissions in the polar swirl region are generally bright from about 5-7 am until 20-22 hours ionospheric local time. The rest of the time, the emissions are an order of magnitude weaker or non-existent. It is interesting that the local time variation of these emissions are anti-correlated with the intense upward moving electron beams discussed by Bonfond et al. (2018) measured over the polar swirl region.

2) The polar collar, between the main emission and swirl region, shows magnetospheric local time control, with faint emissions observed from ~22 hours until mid-morning or noon, and bright emissions from noon until ~22 hours. Additionally, the region of bright emissions in the polar collar (previously called the active region) can exhibit arcs of emission concentric to or forking from the main emission (Nichols et al., 2009b). These concentric arcs may form at any System III longitude, but only on the dusk side of the polar collar (Fig. 4). Similarly, we sometimes find concentric arcs of emission on the dusk side of the southern auroral polar collar like those in the north.

3) For brief periods, and only during some perijove passes, we observe intense, localized emissions from the polar swirl region between about 2 and 6 am magnetic local time while

the swirl region is positioned in darkness (ionospheric local time). Interestingly, these emissions can be of low color ratio. Given the low color ratio and local time of generation, it seems likely that they are produced by a separate phenomenon at large radial distances (>150 R_J) unrelated to the usual high-color-ratio emissions seen in the swirl regions when sunlit.

4) We observe that the intensity of the polar auroral emissions in the south are much reduced compared to those in the north in agreement with Grodent et al. (2018). This fact and the more poleward orientation of the southern aurora makes disentangling ionospheric and magnetospheric local time drivers difficult from southern hemisphere maps. However, the southern polar auroral emissions exhibit similar structures as the north with both a polar collar and swirl region. The local time control of these regions appears to agree with that in the north with the polar collar showing magnetospheric local time control and the swirl region exhibiting ionospheric local time control.

Acknowledgments, Samples, and Data

This work was funded by NASA's New Frontiers Program for Juno via contract with the Southwest Research Institute. M.V. was supported by the Juno Participating Scientist program (grant number 80NSSC19K1263) and by NASA grant 80NSSC17K0777. B.B. is a Research Associate of the Fonds de la Recherche Scientifique - FNRS. The Juno data used in this study can be obtained from the Planetary Data System (PDS) at https://pds-atmospheres.nmsu.edu/data_and_services/atmospheres_data/JUNO/uvs.html . Images supporting the assertions made in this paper were produced by T.G. using the Juno UVS observations from perijoves 1, 3-13. All the 101 spin integrated images from these orbits can be found in the supporting materials to this article (S1 and S3). Any further detailed questions about the production of the UVS images presented here should be directed to T.G.

References

Acton, C. H. (1996), Ancillary data services of NASA's Navigation and Ancillary Information Facility, *Planetary and Space Science*, *44*(1), 65-70.

Allegrini, F., et al. (2020a), First Report of Electron Measurements During a Europa Footprint Tail Crossing by Juno, *Geophysical Research Letters*, *47*, e89732, doi:10.1029/2020gl089732.

Allegrini, F., et al. (2020b), Energy Flux and Characteristic Energy of Electrons Over Jupiter's Main Auroral Emission, *Journal of Geophysical Research (Space Physics)*, *125*, e27693.

Bagenal, F., et al. (2014), Magnetospheric Science Objectives of the Juno Mission, *Space Science Reviews*, doi:10.1007/s11214-014-0036-8.

Bolton, S. J., et al. (2017), The Juno Mission, *Space Science Reviews*, *213*(1), 5-37, doi:10.1007/s11214-017-0429-6.

Bonfond, B., et al. (2018), Bar Code Events in the Juno-UVS Data: Signature ~10 MeV Electron Microbursts at Jupiter, *Geophysical Research Letters*, *45*, 12,108, doi:10.1029/2018gl080490.

Bonfond, B., et al. (2017), Morphology of the UV aurorae Jupiter during Juno's first perijove observations, *Geophysical Research Letters*, *44*(10), 4463-4471, doi:10.1002/2017GL073114.

Bonfond, B., D. Grodent, S. V. Badman, J. C. Gérard, and A. Radioti (2016), Dynamics of the flares in the active polar region of Jupiter, *Geophysical Research Letters*, *43*(23), 11,963-911,970, doi:10.1002/2016GL071757.

Bonfond, B., M. F. Vogt, J. C. Gérard, D. Grodent, A. Radioti, and V. Coumans (2011), Quasi-periodic polar flares at Jupiter: A signature of pulsed dayside reconnections?, *Geophysical Research Letters*, *38*(2), doi:10.1029/2010gl045981.

Clark, G., et al. (2017), Observation and interpretation of energetic ion conics in Jupiter's polar magnetosphere, *Geophysical Research Letters*, *44*(10), 4419-4425, doi:10.1002/2016GL072325.

Clark, G., et al. (2018), Precipitating Electron Energy Flux and Characteristic Energies in Jupiter's Main Auroral Region as Measured by Juno/JEDI, *Journal of Geophysical Research (Space Physics)*, *123*, 7554.

Connerney, J. E. P., et al. (2018), A New Model of Jupiter's Magnetic Field From Juno's First Nine Orbits, *Geophysical Research Letters*, *45*, 2590-2596.

Cowley, S. W. H., and E. J. Bunce (2001), Origin of the main auroral oval in Jupiter's coupled magnetosphere-ionosphere system, *Planetary and Space Science*, *49*, 1067-1088.

Cowley, S. W. H., E. J. Bunce, T. S. Stallard, and S. Miller (2003), Jupiter's polar ionospheric flows: Theoretical interpretation, *Geophysical Research Letters*, *30*, 24-21.

Ebert, R. W., et al. (2019), Comparing Electron Energetics and UV Brightness in Jupiter's Northern Polar Region During Juno Perijove 5, *Geophysical Research Letters*, *46*, 19-27.

Gérard, J.-C., B. Bonfond, D. Grodent, A. Radioti, J. T. Clarke, G. R. Gladstone, J. H. Waite, D. Bisikalo, and V. I. Shematovich (2014), Mapping the electron energy in Jupiter's aurora: Hubble spectral observations, *Journal of Geophysical Research (Space Physics)*, *119*, 9072-9088.

Gérard, J.-C., et al. (2019), Contemporaneous Observations of Jovian Energetic Auroral Electrons and Ultraviolet Emissions by the Juno Spacecraft, *Journal of Geophysical Research: Space Physics*, *124*(11), 8298-8317, doi:10.1029/2019ja026862.

Gladstone, G. R., et al. (2017), The Ultraviolet Spectrograph on NASA's Juno Mission, *Space Science Reviews*, *213*, 447-473.

Greathouse, T. K., G. R. Gladstone, M. W. Davis, D. C. Slater, M. H. Versteeg, K. B. Persson, B. C. Walther, G. S. Winters, S. C. Persyn, and J. S. Eterno (2013), Performance results from in-flight commissioning of the Juno Ultraviolet Spectrograph (Juno-UVS).

Grodent, D. (2015), A Brief Review of Ultraviolet Auroral Emissions on Giant Planets, *Space Science Reviews*, *187*(1), 23-50, doi:10.1007/s11214-014-0052-8.

Grodent, D., et al. (2018), Jupiter's Aurora Observed With HST During Juno Orbits 3 to 7, *Journal of Geophysical Research (Space Physics)*, *123*, 3299-3319.

Grodent, D., J. T. Clarke, J. H. Waite, S. W. H. Cowley, J.-C. GéRard, and J. Kim (2003), Jupiter's polar auroral emissions, *Journal of Geophysical Research (Space Physics)*, *108*.

Haewsantati, K., et al. (2021), Morphology of Jupiter's Polar Auroral Bright Spot Emissions via Juno-UVS Observations, *Journal of Geophysical Research: Space Physics*, *126*(2), e2020JA028586, doi:https://doi.org/10.1029/2020JA028586.

Hill, T. W. (2001), The Jovian auroral oval, *Journal of Geophysical Research*, *106*, 8101, doi:10.1029/2000ja000302.

Hue, V., et al. (2019a), In-flight Characterization and Calibration of the Juno-ultraviolet Spectrograph (Juno-UVS), *The Astronomical Journal*, *157*.

Hue, V., et al. (2019b), Juno-UVS Observation of the Io Footprint During Solar Eclipse, *Journal of Geophysical Research (Space Physics)*, *124*, 5184.

Isbell, J., A. J. Dessler, and J. H. Waite, Jr. (1984), Magnetospheric energization by interaction between planetary spin and the solar wind, *Journal of Geophysical Research*, *89*, 10716.

Mauk, B. H., et al. (2020), Energetic Particles and Acceleration Regions Over Jupiter's Polar Cap and Main Aurora: A Broad Overview, *Journal of Geophysical Research (Space Physics)*, *125*, e27699, doi:10.1029/2019ja027699.

McComas, D. J., and F. Bagenal (2007), Jupiter: A fundamentally different magnetospheric interaction with the solar wind, *Geophysical Research Letters*, *34*, L20106.

Moriconi, M. L., et al. (2017), Preliminary JIRAM results from Juno polar observations: 3. Evidence of diffuse methane presence in the Jupiter auroral regions, *Geophysical Research Letters*, *44*(10), 4641-4648, doi:https://doi.org/10.1002/2017GL073592.

Nichols, J. D., et al. (2017), Response of Jupiter's auroras to conditions in the interplanetary medium as measured by the Hubble Space Telescope and Juno, *Geophysical Research Letters*, n/a-n/a, doi:10.1002/2017GL073029.

Nichols, J. D., E. J. Bunce, J. T. Clarke, S. W. H. Cowley, J.-C. Gérard, D. Grodent, and W. R. Pryor (2007), Response of Jupiter's UV auroras to interplanetary conditions as observed by the Hubble Space Telescope during the Cassini flyby campaign, *Journal of Geophysical Research (Space Physics)*, *112*, A02203.

Nichols, J. D., J. T. Clarke, J. C. Gérard, and D. Grodent (2009a), Observations of Jovian polar auroral filaments, *Geophysical Research Letters*, *36*(8), doi:10.1029/2009gl037578.

Nichols, J. D., J. T. Clarke, J. C. Gérard, D. Grodent, and K. C. Hansen (2009b), Variation of different components of Jupiter's auroral emission, *Journal of Geophysical Research: Space Physics*, *114*(A6), doi:10.1029/2009ja014051.

Sinclair, J. A., et al. (2020), Spatial Variations in the Altitude of the CH4 Homopause at Jupiter's Mid-to-high Latitudes, as Constrained from IRTF-TEXES Spectra, *The Planetary Science Journal*, *1*(3), 85, doi:10.3847/psj/abc887.

Swithenbank-Harris, B. G., J. D. Nichols, and E. J. Bunce (2019), Jupiter's Dark Polar Region as Observed by the Hubble Space Telescope During the Juno Approach Phase, *Journal of Geophysical Research (Space Physics)*, *124*, 9094.

Szalay, J. R., et al. (2020), Alfvénic Acceleration Sustains Ganymede's Footprint Tail Aurora, *Geophysical Research Letters*, *47*, e86527.

Szalay, J. R., et al. (2018), In Situ Observations Connected to the Io Footprint Tail Aurora, *Journal of Geophysical Research (Planets)*, *123*, 3061.

Vogt, M. F., E. J. Bunce, M. G. Kivelson, K. K. Khurana, R. J. Walker, A. Radioti, B. Bonfond, and D. Grodent (2015), Magnetosphere-ionosphere mapping at Jupiter: Quantifying the effects of using different internal field models, *Journal of Geophysical Research (Space Physics)*, *120*, 2584-2599.

Vogt, M. F., M. G. Kivelson, K. K. Khurana, R. J. Walker, B. Bonfond, D. Grodent, and A. Radioti (2011), Improved mapping of Jupiter's auroral features to magnetospheric sources, *Journal of Geophysical Research (Space Physics)*, *116*, A03220.

Waite, J. H., et al. (2001), An auroral flare at Jupiter, *Nature*, *410*, 787.

Yung, Y. L., G. R. Gladstone, K. M. Chang, J. M. Ajello, and S. K. Srivastava (1982), H2 fluorescence spectrum from 1200 to 1700 A by electron impact - Laboratory study and application to Jovian aurora, *The Astrophysical Journal Letters*, *254*, L65-L69.

Zhang, B., et al. (2021), How Jupiter’s unusual magnetospheric topology structures its aurora, *Science Advances*, *7*(15), eabd1204, doi:10.1126/sciadv.abd1204.

Supporting Information for "Local Time Dependence of Jupiter's Polar Auroral Emissions Observed by Juno UVS"

Thomas Greathouse[1], Randy Gladstone[1,2], Maarten Versteeg[1], Vincent Hue[1], Joshua Kammer[1], Rohini Giles[1], Michael Davis[1], Scott Bolton[1], Steven Levin[3], John Connerney[4], Jean-Claude Gérard[5], Denis Grodent[5], Bertrand Bonfond[5], Emma Bunce[6], and Marissa F. Vogt[7]

[1]Southwest Research Institute, San Antonio, TX, United States

[2]University of Texas at San Antonio, San Antonio, TX, United States

[3]Jet Propulsion Laboratory, Pasadena, CA, United States

[4]NASA Goddard Space Flight Center, Greenbelt, MD, United States

[5]Université de Liège, LPAP - STAR Institute, Liège, Belgium

[6]University Leicester, Leicester, United Kingdom

[7]Center for Space Physics, Boston University

Contents of this file

S1: Northern auroral dataset

As described in the main text we have created 101-spin integrated brightness and color ratio maps of the northern aurora from all the calibrated Juno UVS observations from perijoves 1 and 3-13. Just prior to Juno's second perijove pass, a spacecraft anomaly caused all instruments to shut down. Thus, no UVS data was recorded during perijove 2. The full description of the figures and annotations are given in the caption of Figure 2 in the main text. The images in this appendix are ordered by their mid-point time sub-solar System III longitude, which is also printed on each page of the pdf.

S2: Northern auroral clock style image

Similar to figure 2 in the main text, this clock style image of the northern auroral emissions contains more maps, higher temporal sampling, at the cost of smaller map sizes and slightly less detail.

S3: Southern auroral dataset

The southern dataset is presented the same way as described in figure 3 of the main text and includes all the calibrated data from perijoves1 and 3-13.

S4: Southern auroral clock style image

Similar to figure 3 in the main text, this clock style image of the southern auroral emissions contains more maps, higher temporal sampling, at the cost of smaller map sizes and slightly less detail.

S5: PJ5 movie of map production

This movie depicts the integration of multiple spins of Juno UVS data in order to produce brightness and color ratio maps like those shown in the main paper in the supplements 1 and 2. The movie begins with the mapping of a single spin of data from only the wide slits and continues adding in consecutive scan data for 45 spins worth of data collection. The initial spin of data in this particular animation is taken 45 spins or 22.5 minutes prior to the last spin of data and thus the image is a composite image that presents portions of the aurora at a given time along with other portions of the aurora taken at a much different time. Areas in the map that contain multiple spins worth of emission data are averaged together. UVS can at best measure variability at a 30 second cadence given the 2 rpm spin rate of the spacecraft. However, given the scale of the auroral regions at low spacecraft/Jupiter ranges means that the time to capture two consecutive images of the same surface area can range from 30 seconds to tens of minutes depending on the perijove unique scan mirror pointing planned by the UVS team.

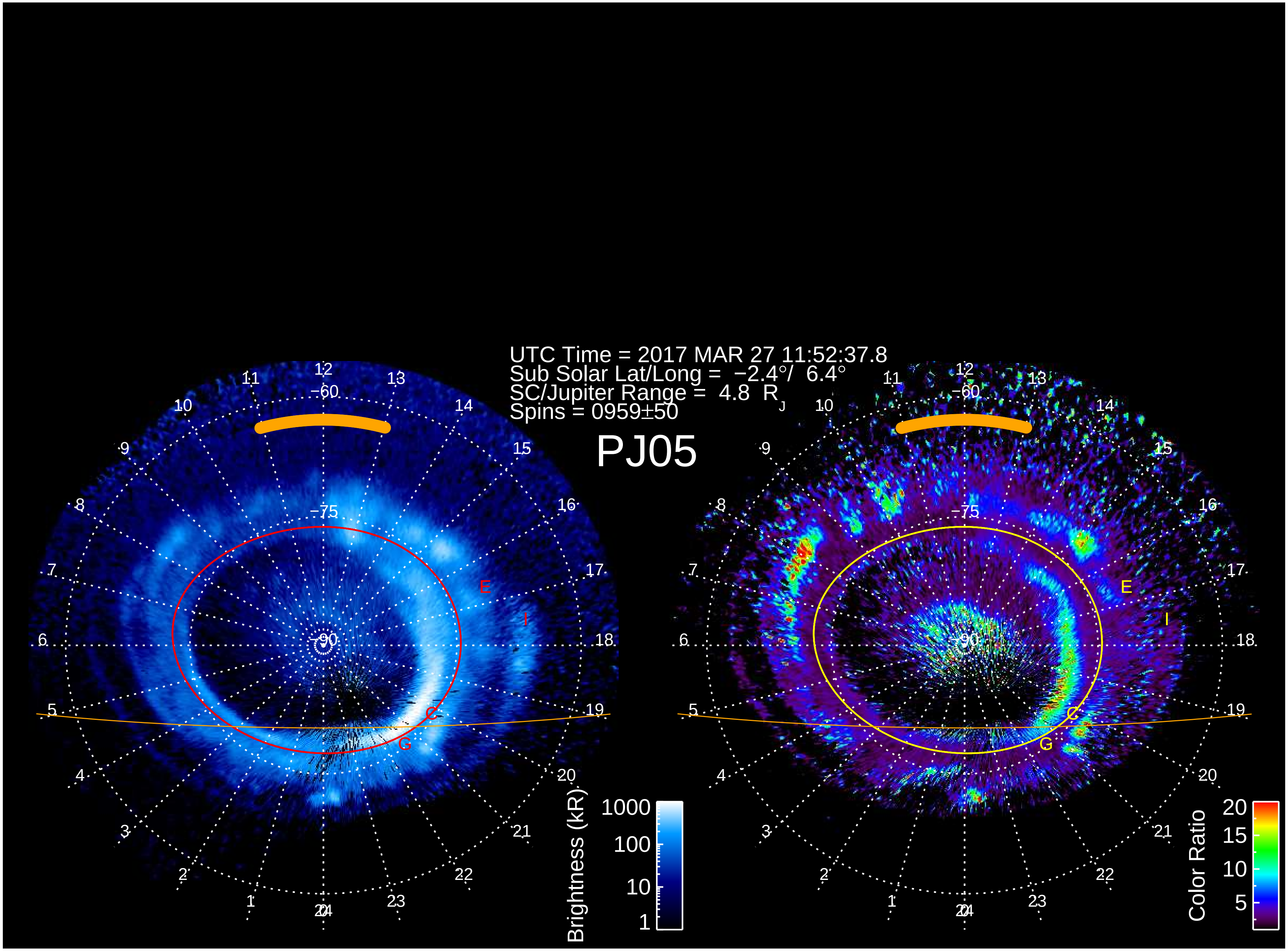
UTC Time = 2017 MAR 27 11:52:37.8
Sub Solar Lat/Long = −2.4°/ 6.4°
SC/Jupiter Range = 4.8 R_J
Spins = 0959±50
PJ05
Brightness (kR)
1000
100
10
1
Color Ratio
20
15
10
5
E
I
C
G

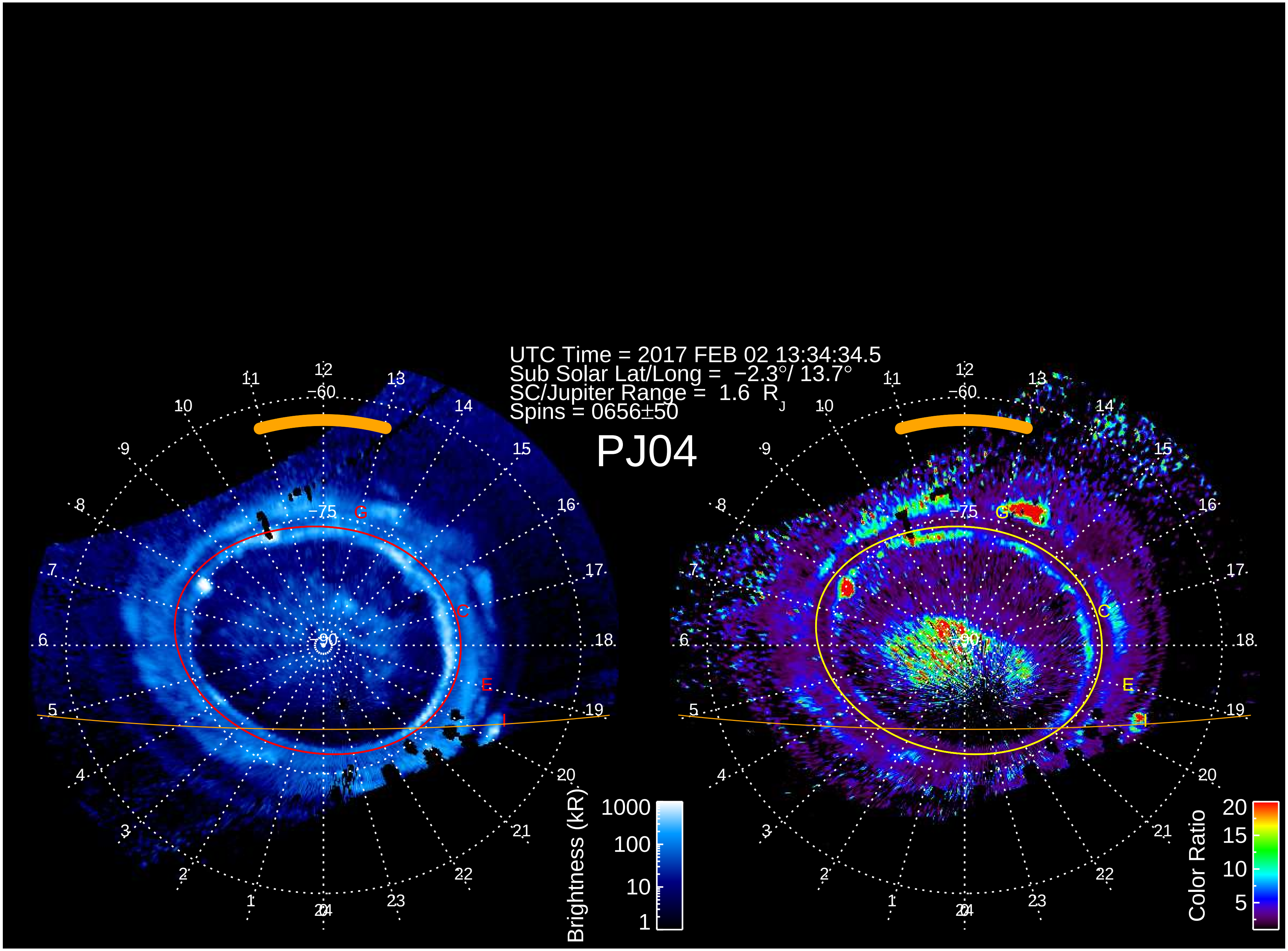
UTC Time = 2017 FEB 02 13:34:34.5
Sub Solar Lat/Long = −2.3°/ 13.7°
SC/Jupiter Range = 1.6 R_J
Spins = 0656±50
PJ04
Brightness (kR)
1000
100
10
1
Color Ratio
20
15
10
5

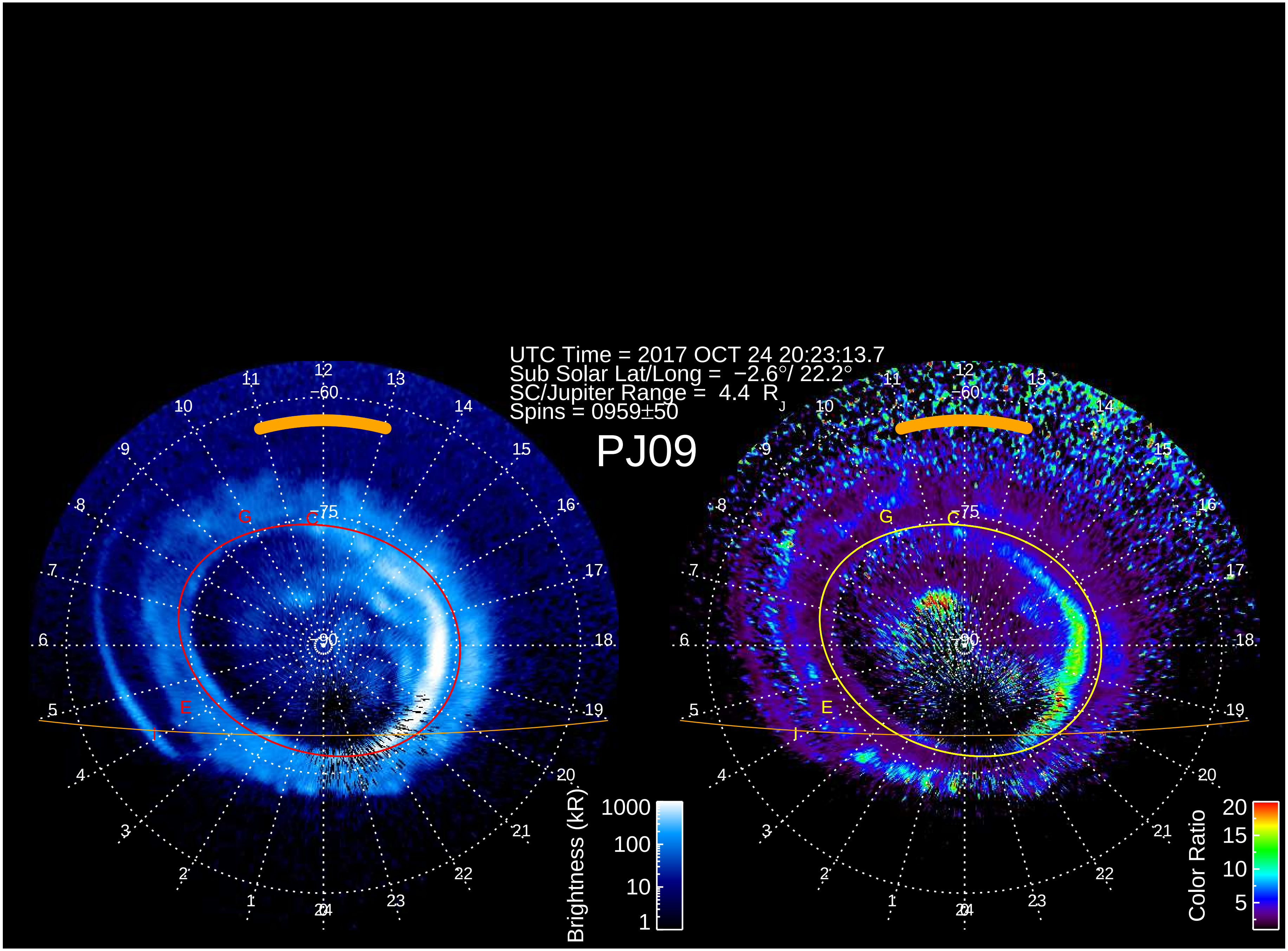

UTC Time = 2017 OCT 24 20:23:13.7
Sub Solar Lat/Long = −2.6°/ 22.2°
SC/Jupiter Range = 4.4 R_J
Spins = 0959±50
PJ09
Brightness (kR)
1000
100
10
1
Color Ratio
20
15
10
5

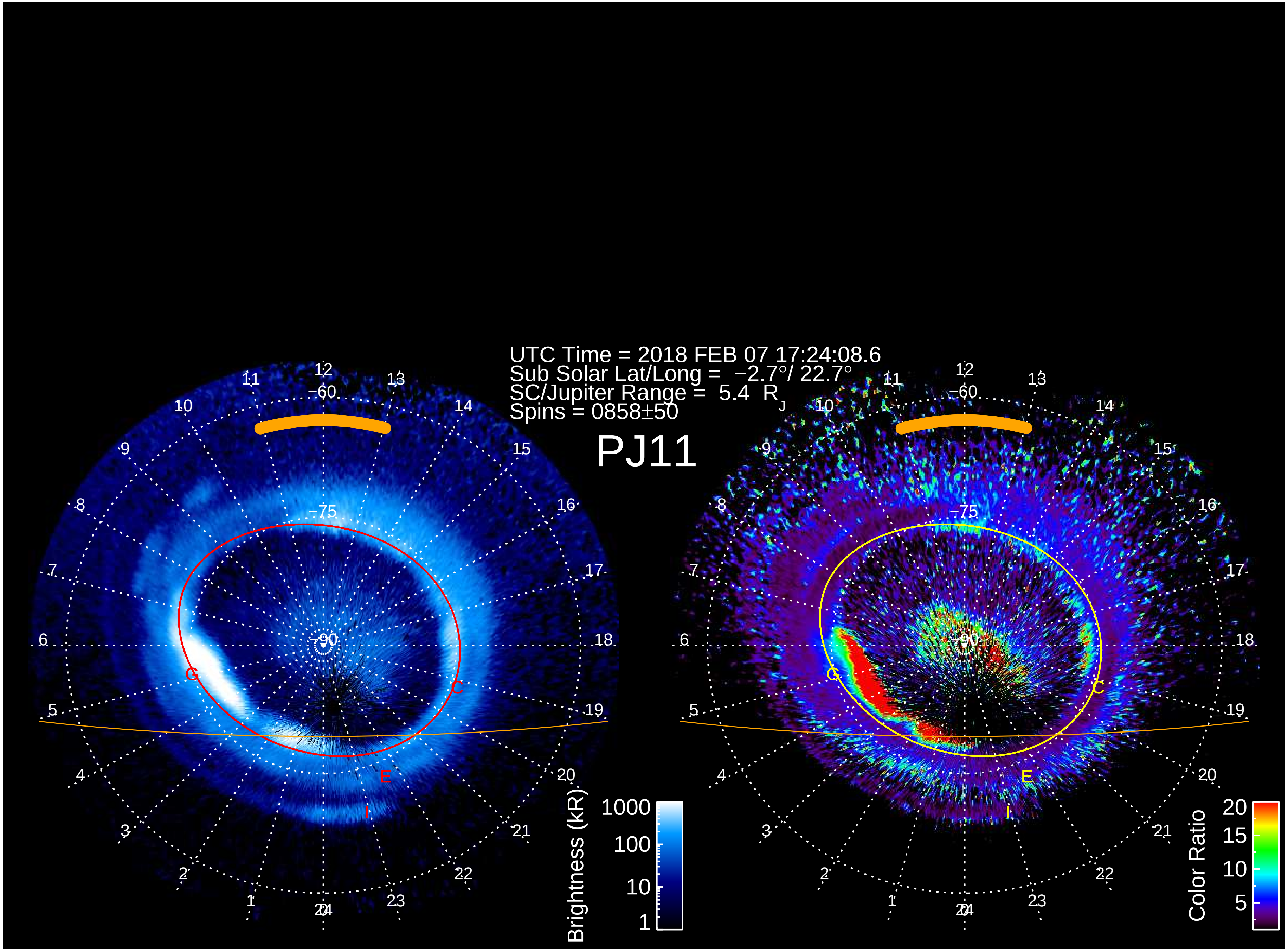
UTC Time = 2018 FEB 07 17:24:08.6
Sub Solar Lat/Long = −2.7°/ 22.7°
SC/Jupiter Range = 5.4 R_J
Spins = 0858±50
PJ11
Brightness (kR)
1000
100
10
1
Color Ratio
20
15
10
5

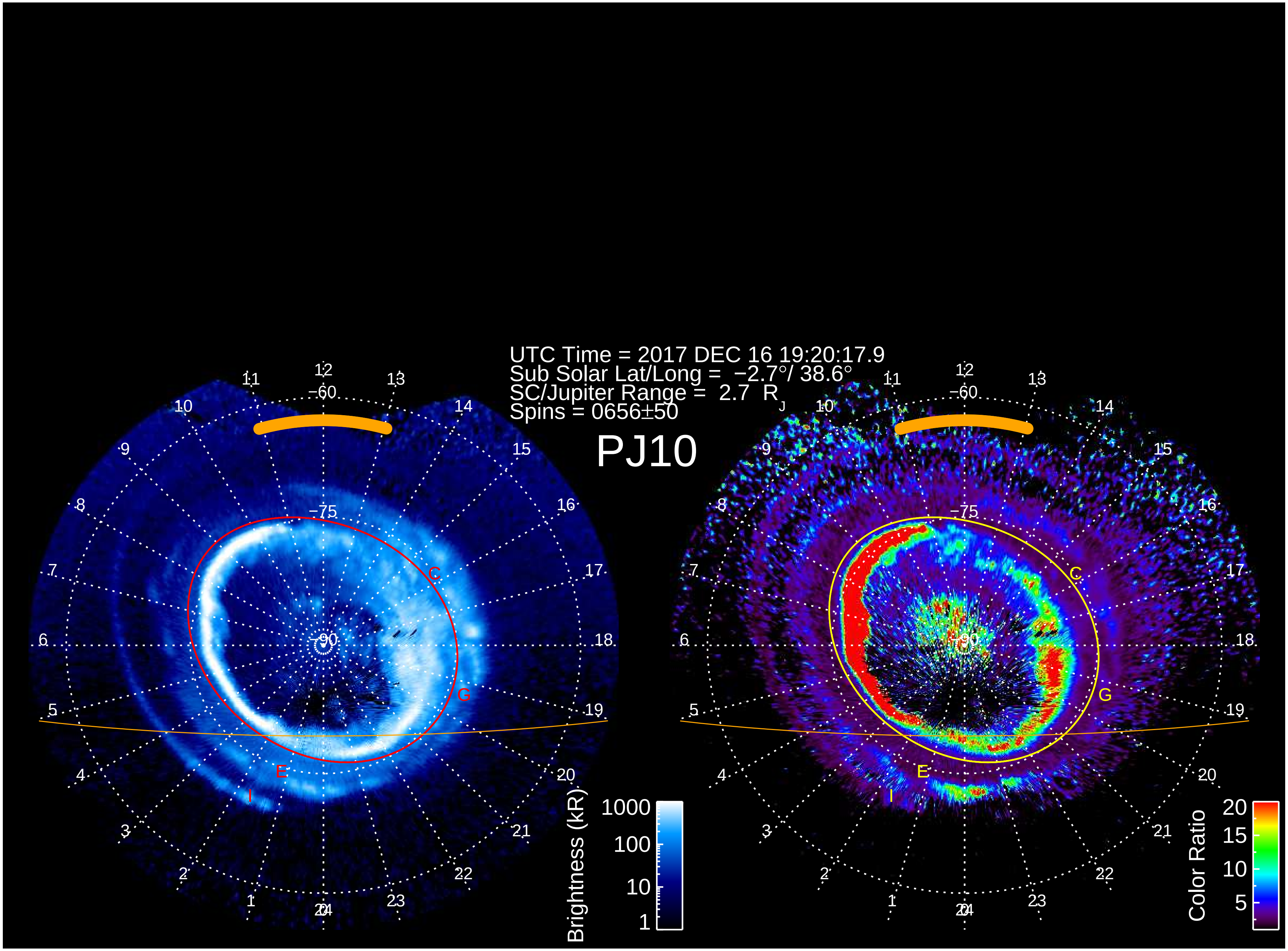
UTC Time = 2017 DEC 16 19:20:17.9
Sub Solar Lat/Long = −2.7°/ 38.6°
SC/Jupiter Range = 2.7 R J
Spins = 0656±50
PJ10
Brightness (kR)
1000
100
10
1
Color Ratio
20
15
10
5
C
G
E
I

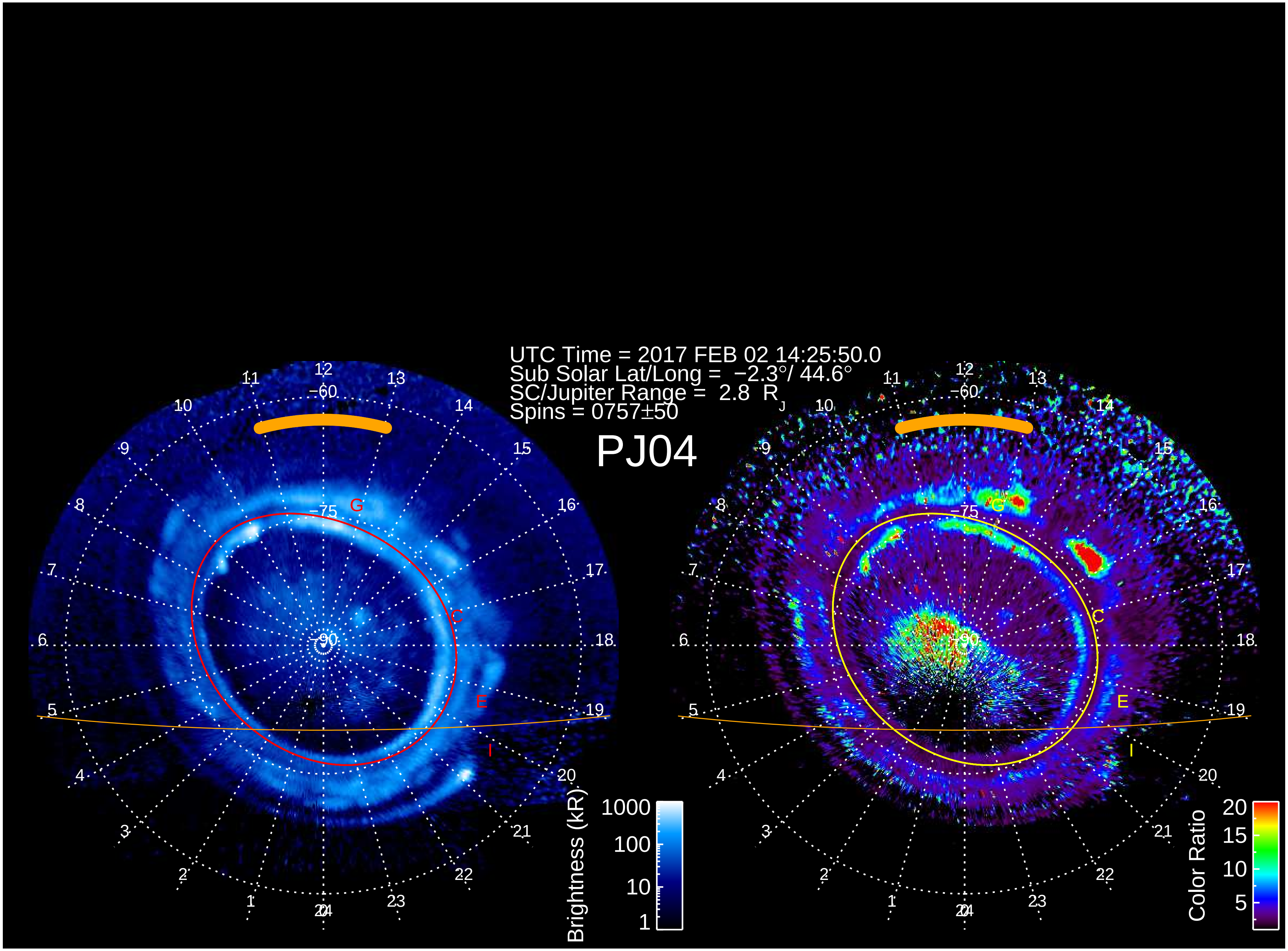

UTC Time = 2017 FEB 02 14:25:50.0
Sub Solar Lat/Long = −2.3°/ 44.6°
SC/Jupiter Range = 2.8 R J
Spins = 0757±50
PJ04
Brightness (kR)
1000
100
10
1
Color Ratio
20
15
10
5

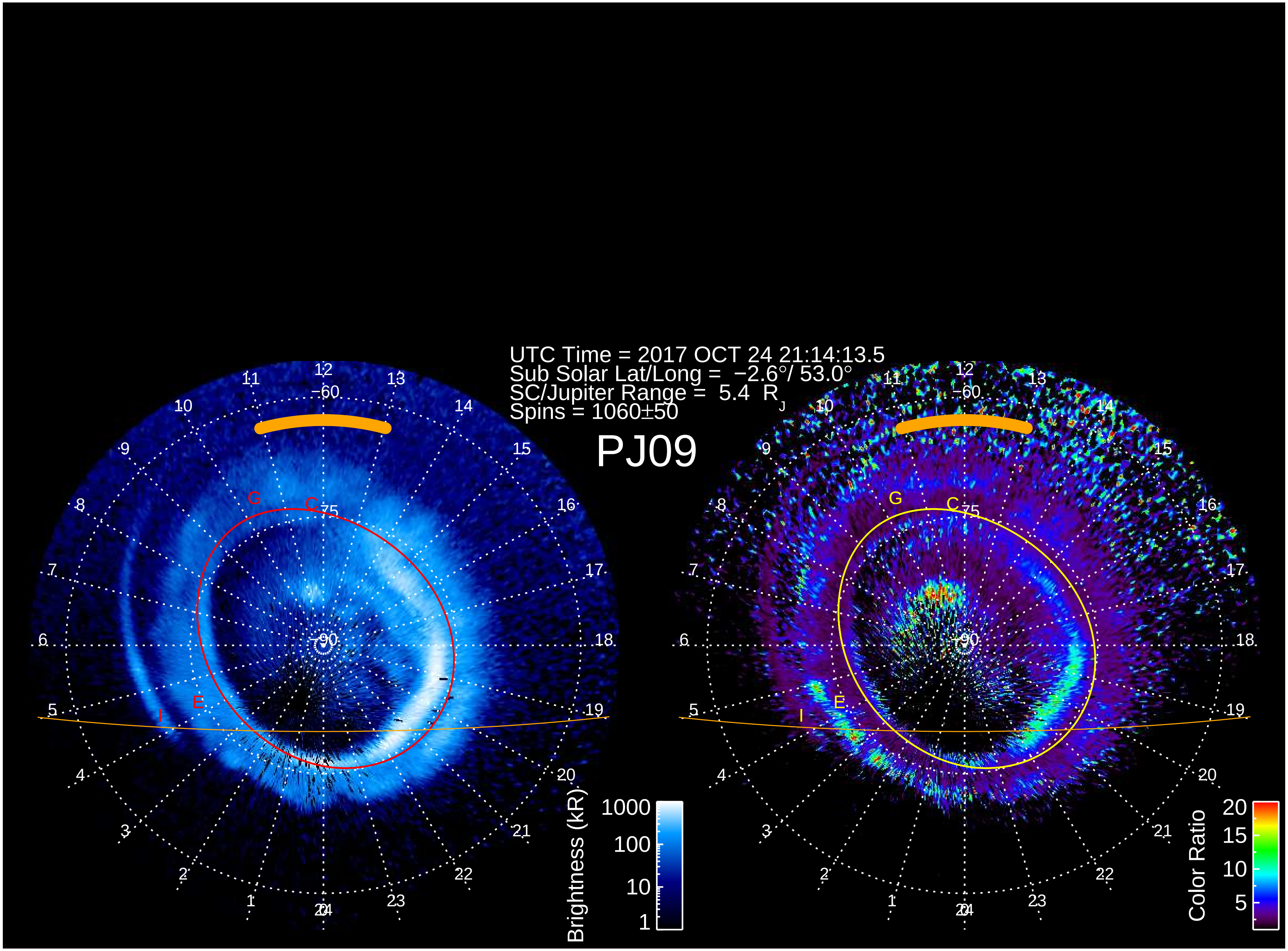
UTC Time = 2017 OCT 24 21:14:13.5
Sub Solar Lat/Long = −2.6°/ 53.0°
SC/Jupiter Range = 5.4 R_J
Spins = 1060±50
PJ09
Brightness (kR)
1000
100
10
1
Color Ratio
20
15
10
5

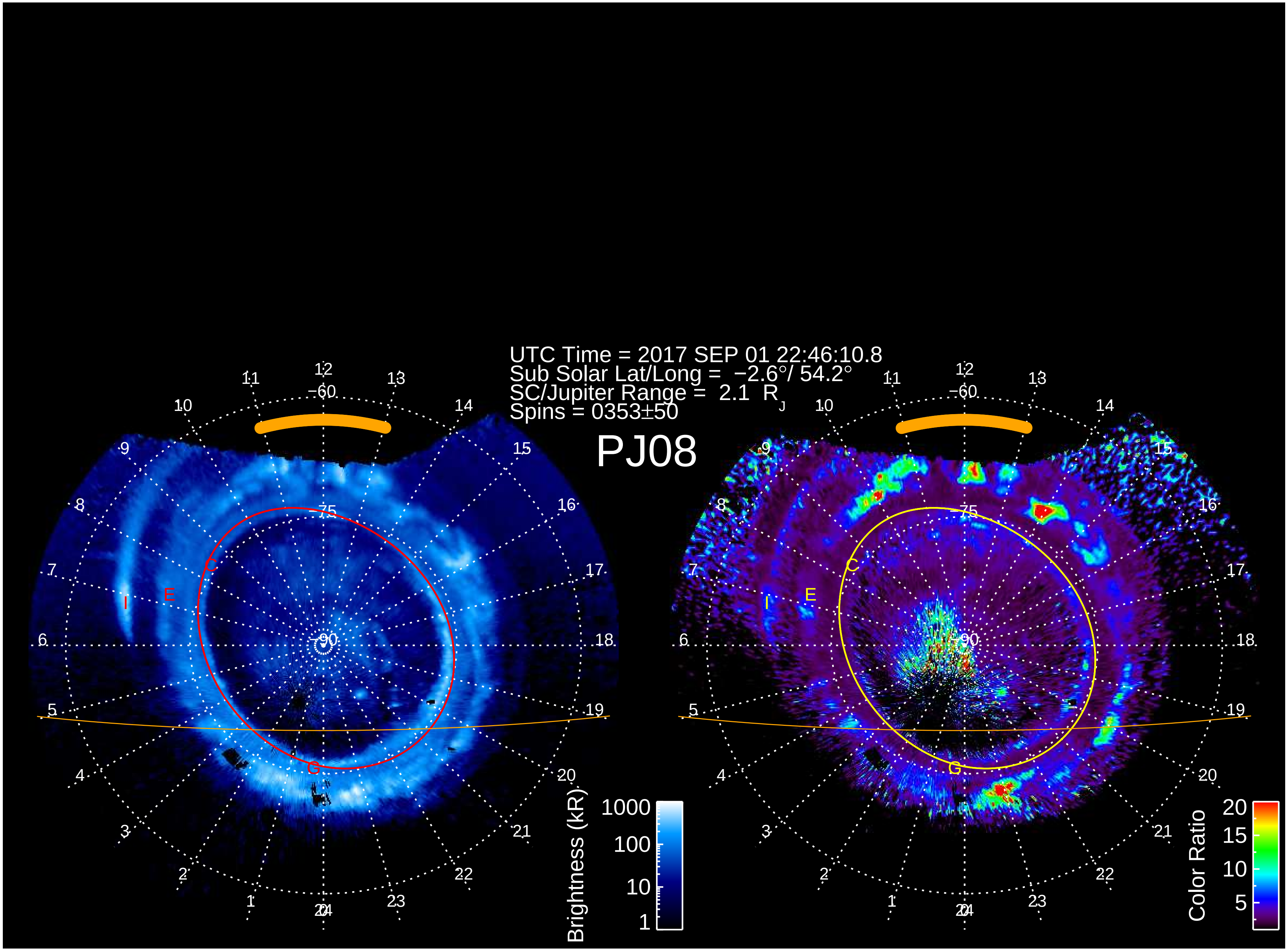

UTC Time = 2017 SEP 01 22:46:10.8
Sub Solar Lat/Long = −2.6°/ 54.2°
SC/Jupiter Range = 2.1 R$_J$
Spins = 0353±50
PJ08
Brightness (kR)
1000
100
10
1
Color Ratio
20
15
10
5

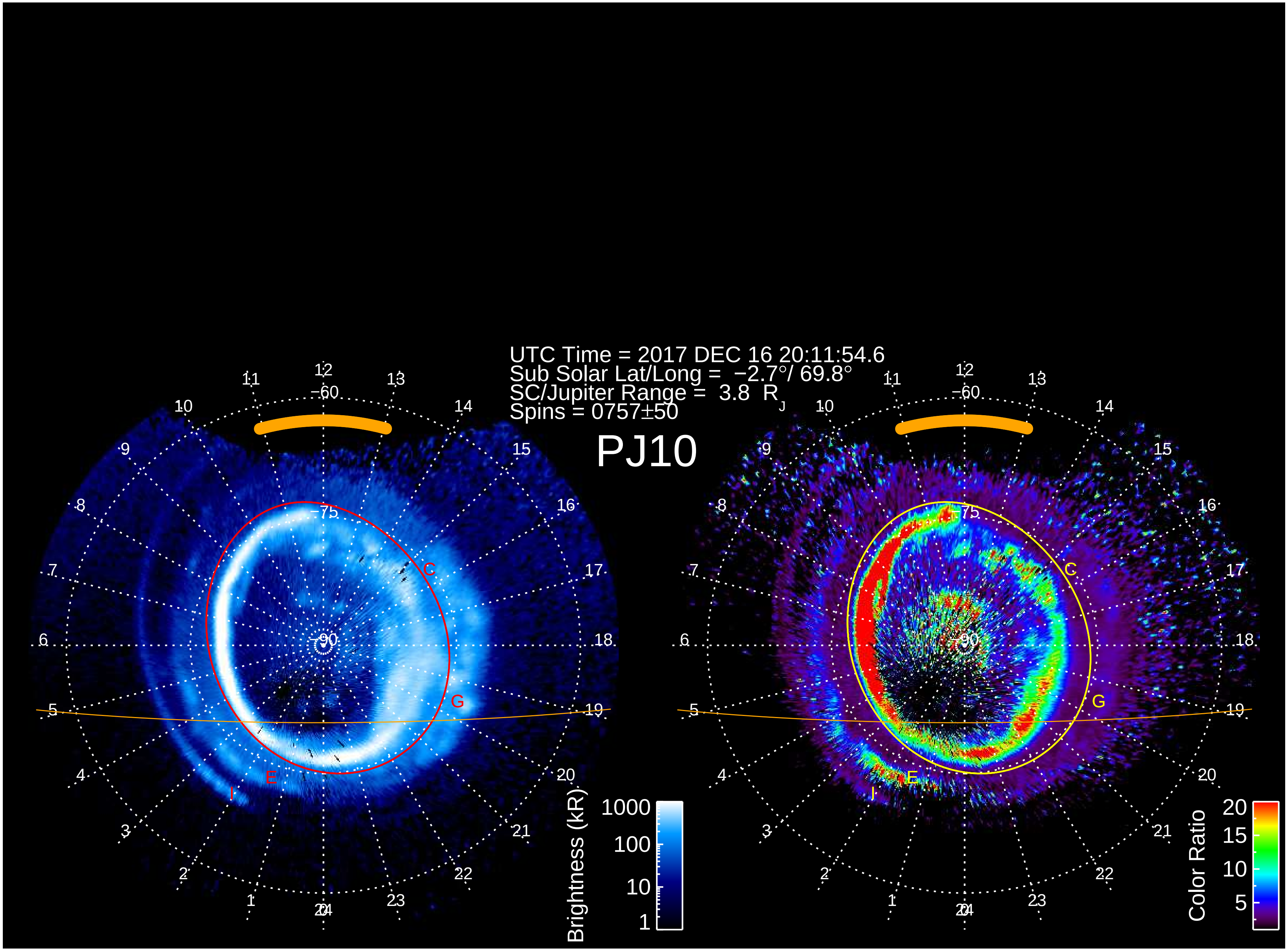

UTC Time = 2017 DEC 16 20:11:54.6
Sub Solar Lat/Long = −2.7°/ 69.8°
SC/Jupiter Range = 3.8 R_J
Spins = 0757±50
PJ10
Brightness (kR)
1000
100
10
1
Color Ratio
20
15
10
5
C
G
E
I

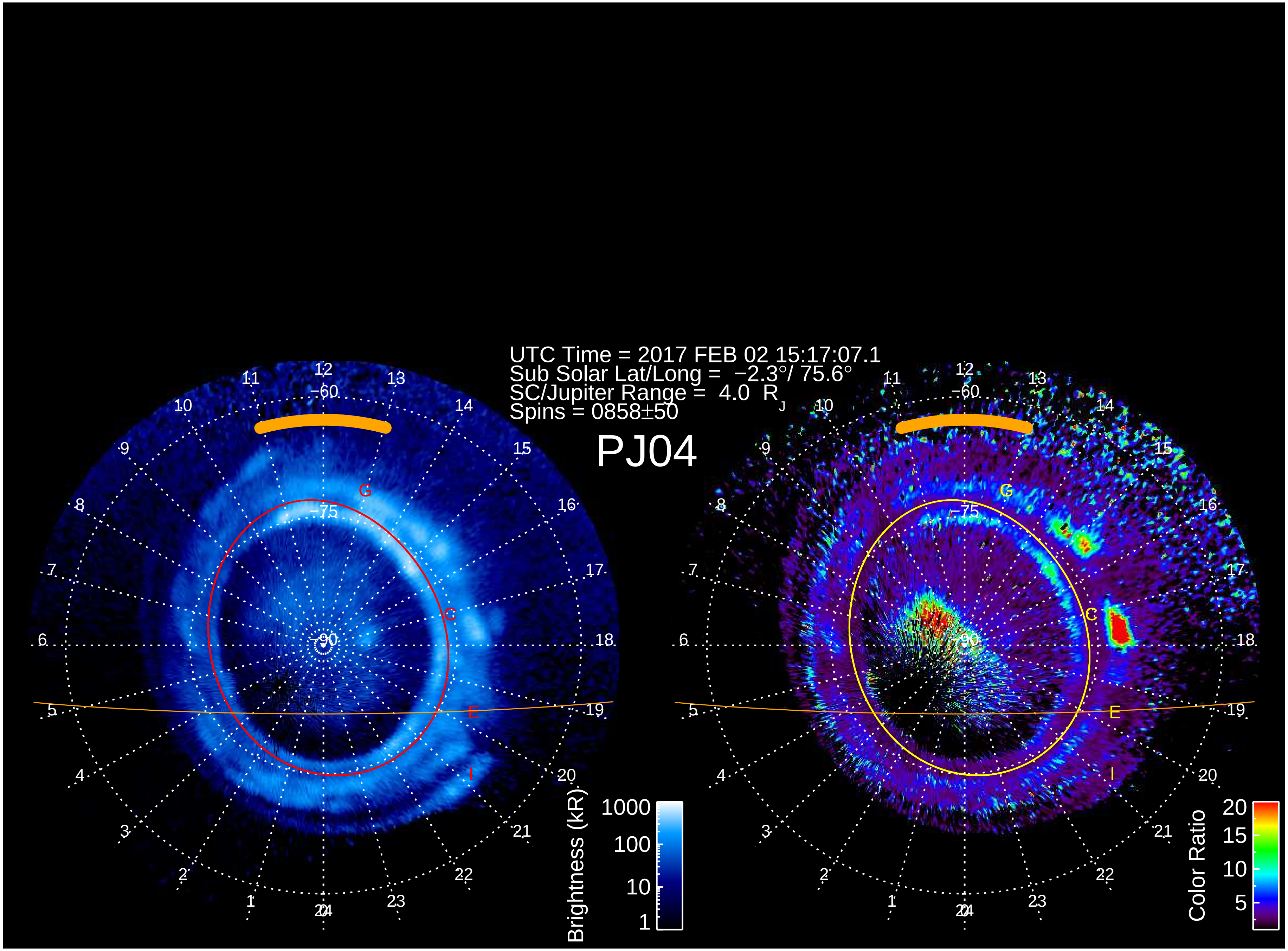

UTC Time = 2017 FEB 02 15:17:07.1
Sub Solar Lat/Long = −2.3°/ 75.6°
SC/Jupiter Range = 4.0 R_J
Spins = 0858±50
PJ04
Brightness (kR)
1000
100
10
1
Color Ratio
20
15
10
5

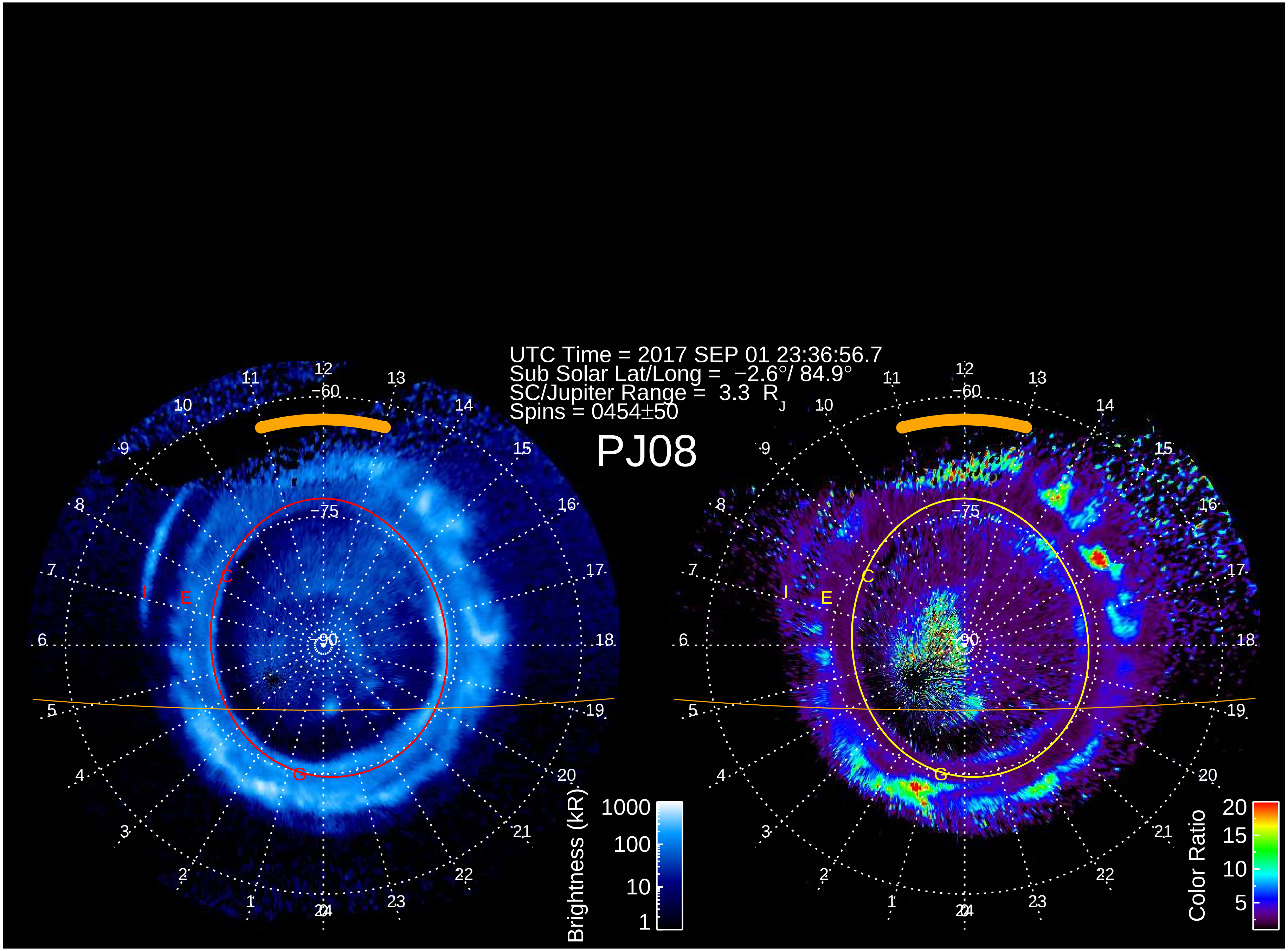

UTC Time = 2017 SEP 01 23:36:56.7
Sub Solar Lat/Long = −2.6°/ 84.9°
SC/Jupiter Range = 3.3 R_J
Spins = 0454±50
PJ08
Brightness (kR)
1000
100
10
1
Color Ratio
20
15
10
5

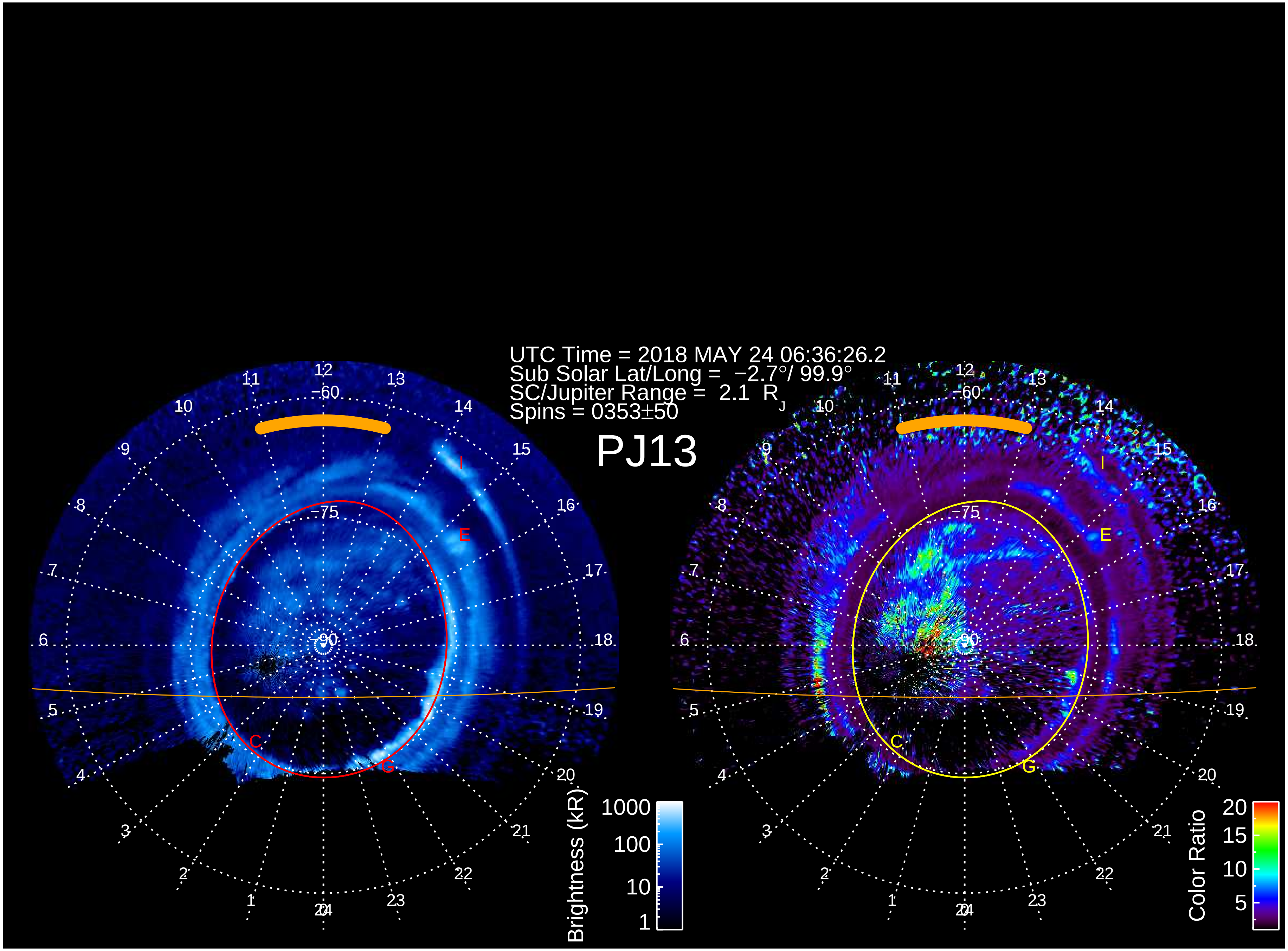

UTC Time = 2018 MAY 24 06:36:26.2
Sub Solar Lat/Long = −2.7°/ 99.9°
SC/Jupiter Range = 2.1 R_J
Spins = 0353±50
PJ13
Brightness (kR)
1000
100
10
1
Color Ratio
20
15
10
5

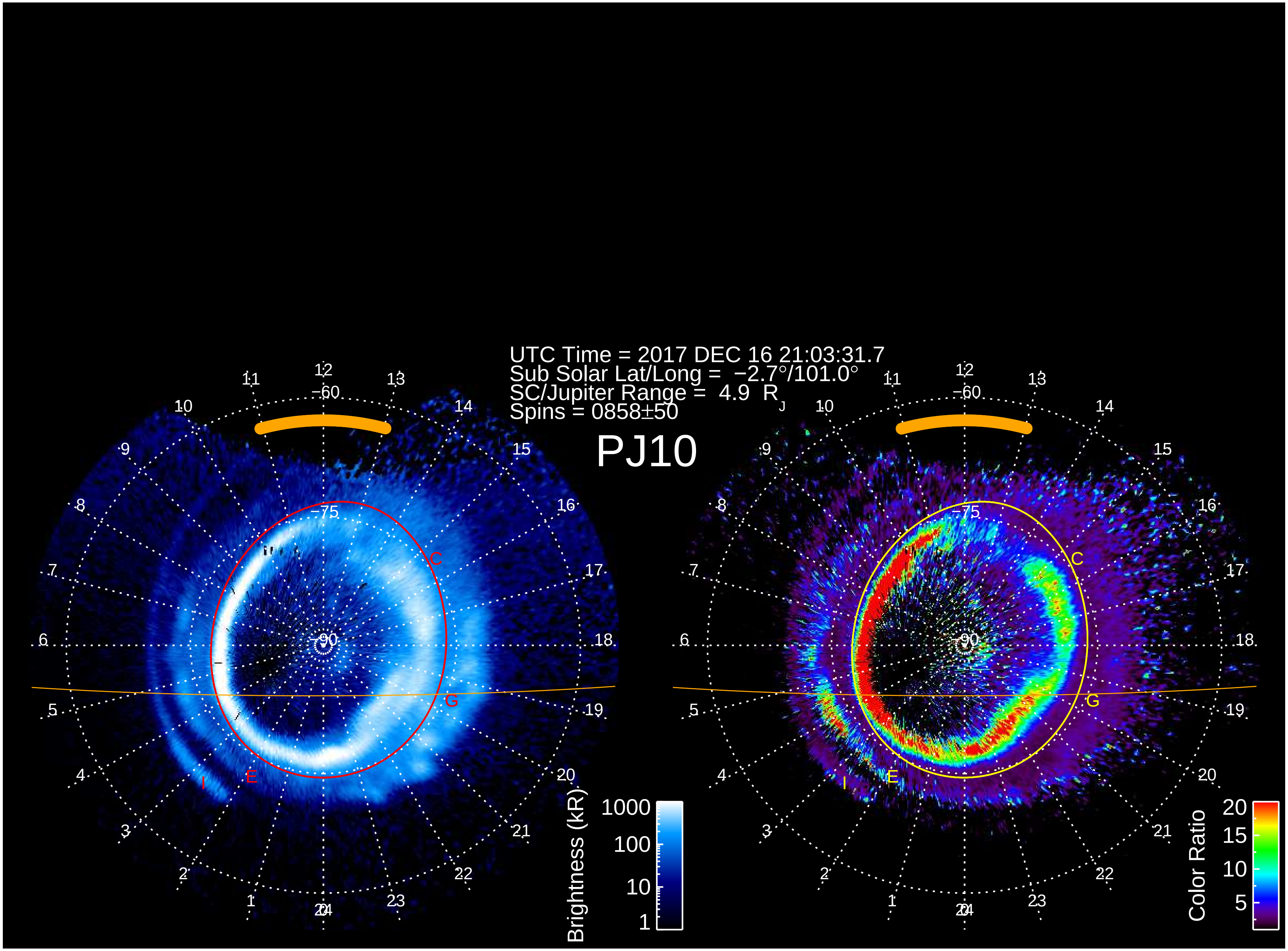
UTC Time = 2017 DEC 16 21:03:31.7
Sub Solar Lat/Long = −2.7°/101.0°
SC/Jupiter Range = 4.9 R_J
Spins = 0858±50
PJ10
Brightness (kR)
1000
100
10
1
Color Ratio
20
15
10
5
C
G
I
E
−60
−75
−90

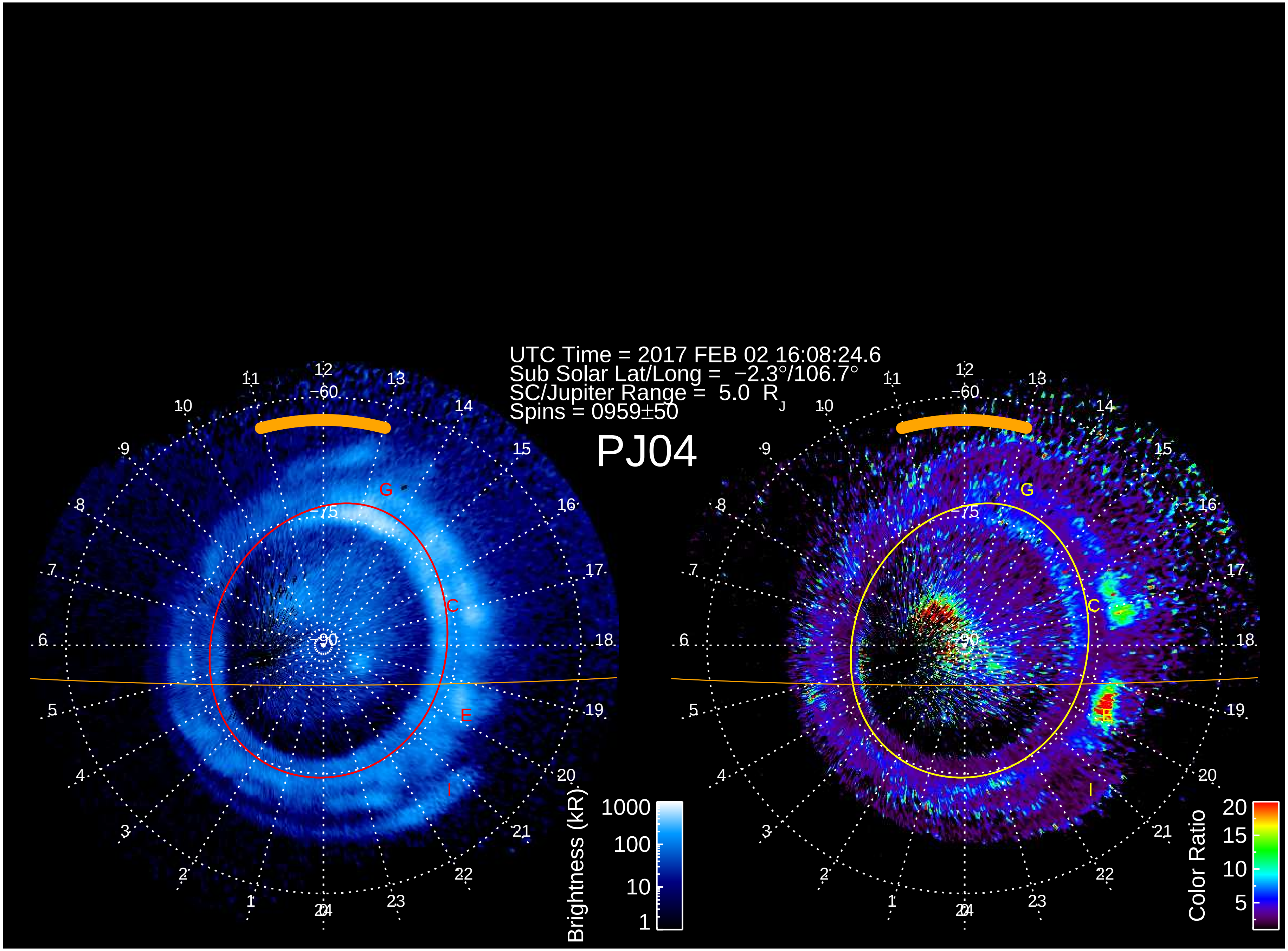

UTC Time = 2017 FEB 02 16:08:24.6
Sub Solar Lat/Long = −2.3°/106.7°
SC/Jupiter Range = 5.0 R_J
Spins = 0959±50
PJ04
G
C
E
I
Brightness (kR)
1000
100
10
1
Color Ratio
20
15
10
5

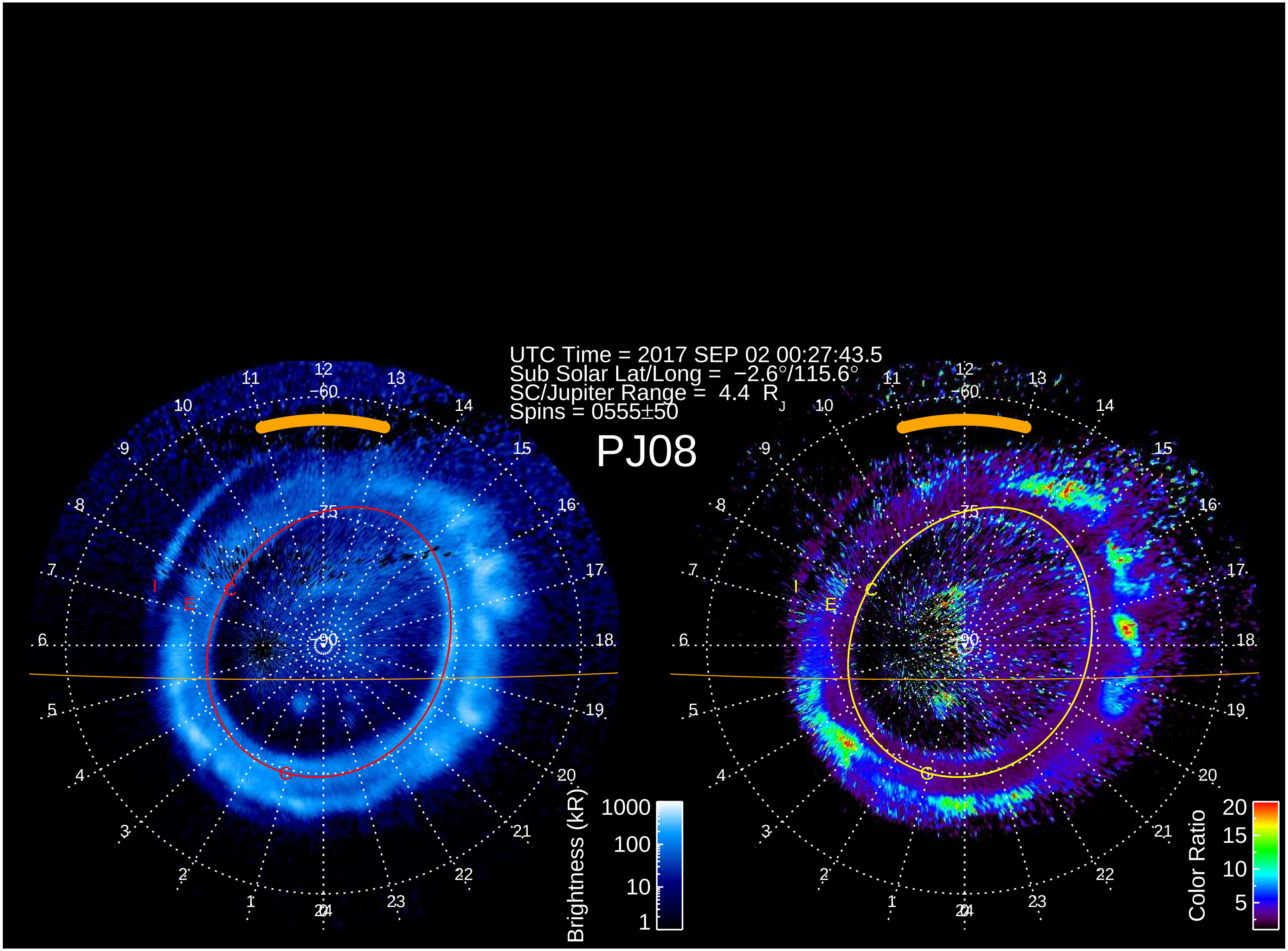

UTC Time = 2017 SEP 02 00:27:43.5
Sub Solar Lat/Long = −2.6°/115.6°
SC/Jupiter Range = 4.4 R
J
Spins = 0555±50
PJ08
Brightness (kR)
1000
100
10
1
Color Ratio
20
15
10
5

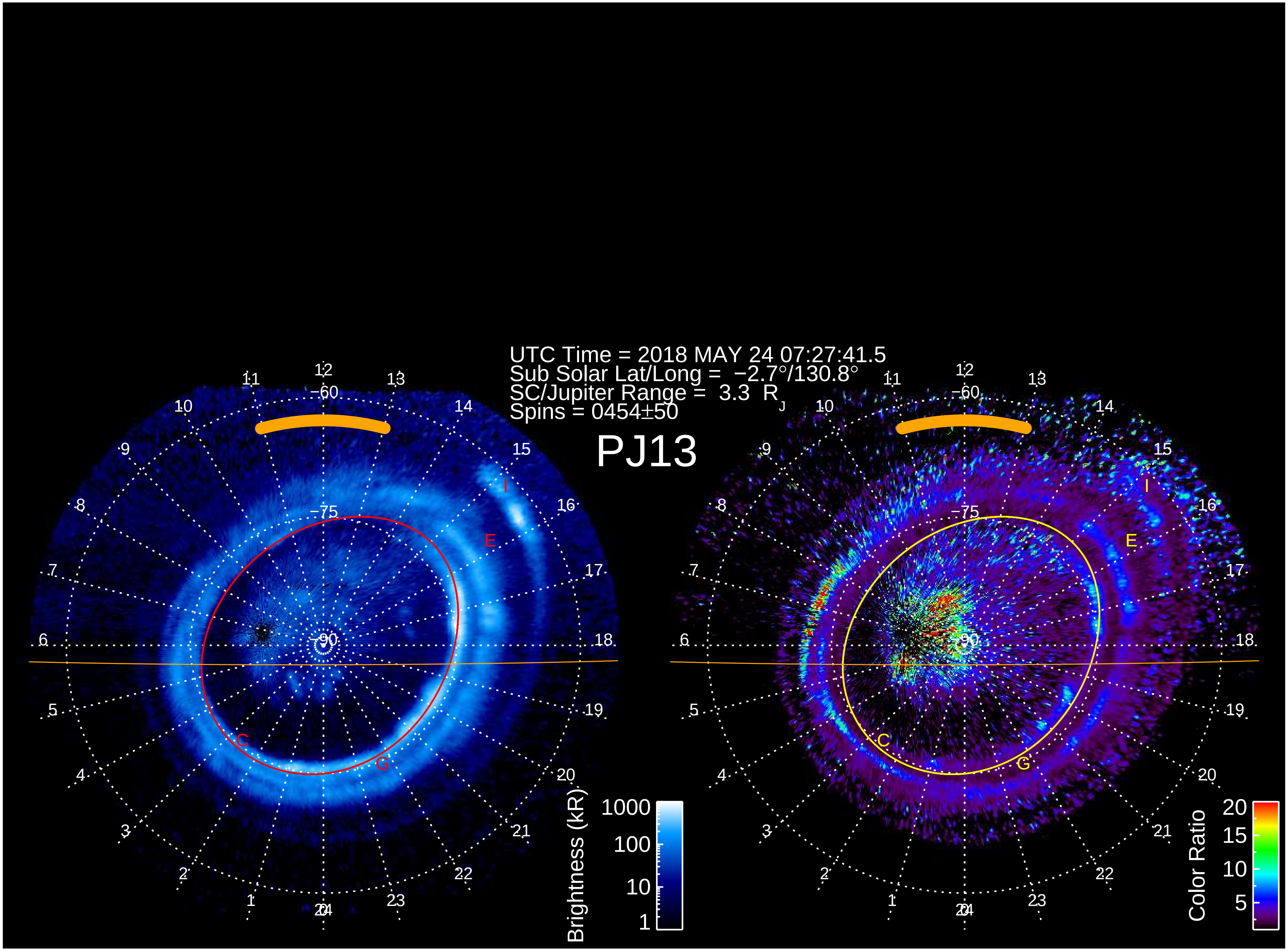

UTC Time = 2018 MAY 24 07:27:41.5
Sub Solar Lat/Long = −2.7°/130.8°
SC/Jupiter Range = 3.3 R$_J$
Spins = 0454±50
PJ13
Brightness (kR)
1000
100
10
1
Color Ratio
20
15
10
5

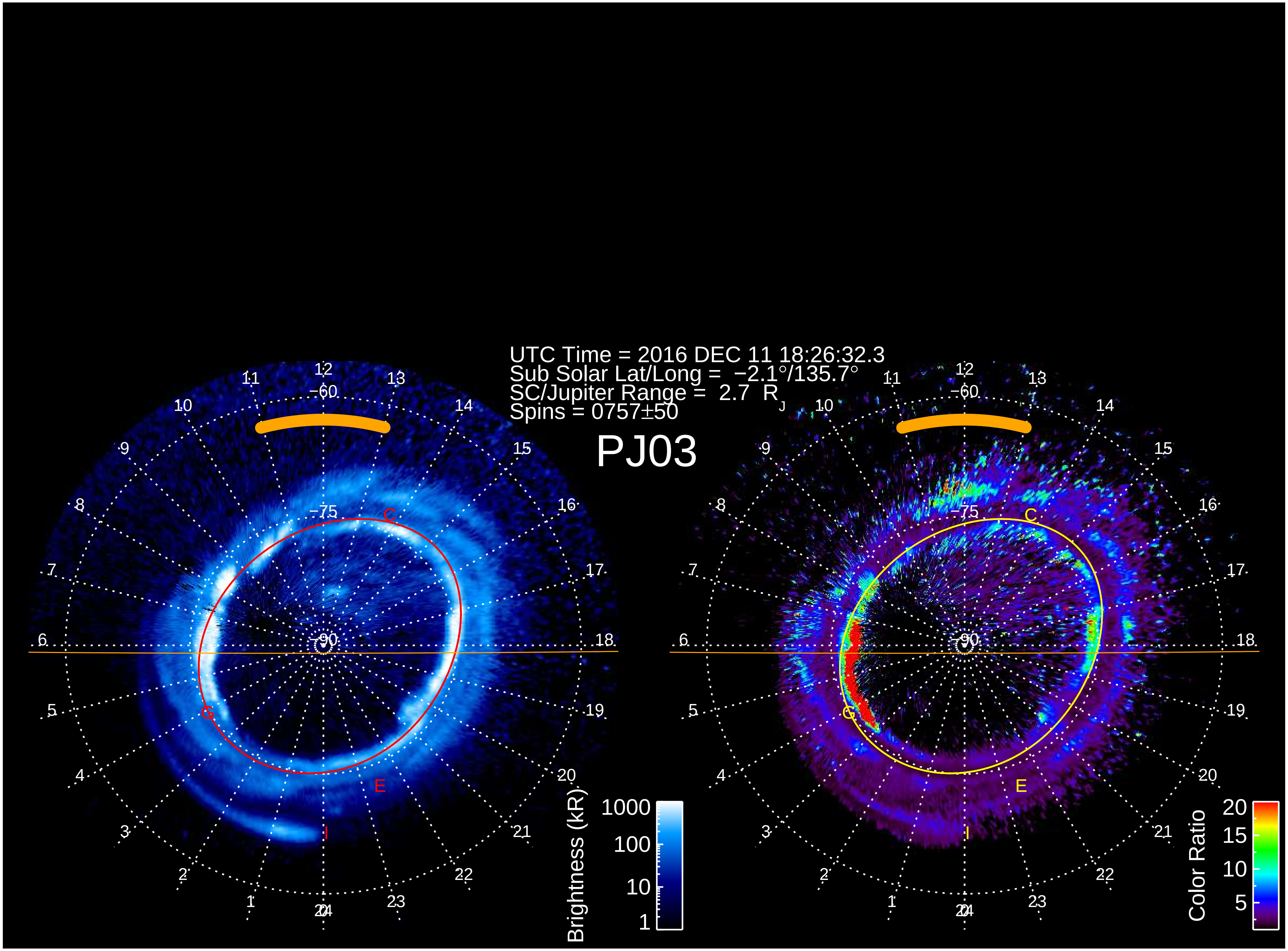

UTC Time = 2016 DEC 11 18:26:32.3
Sub Solar Lat/Long = −2.1°/135.7°
SC/Jupiter Range = 2.7 R$_J$
Spins = 0757±50
PJ03
Brightness (kR)
1000
100
10
1
Color Ratio
20
15
10
5

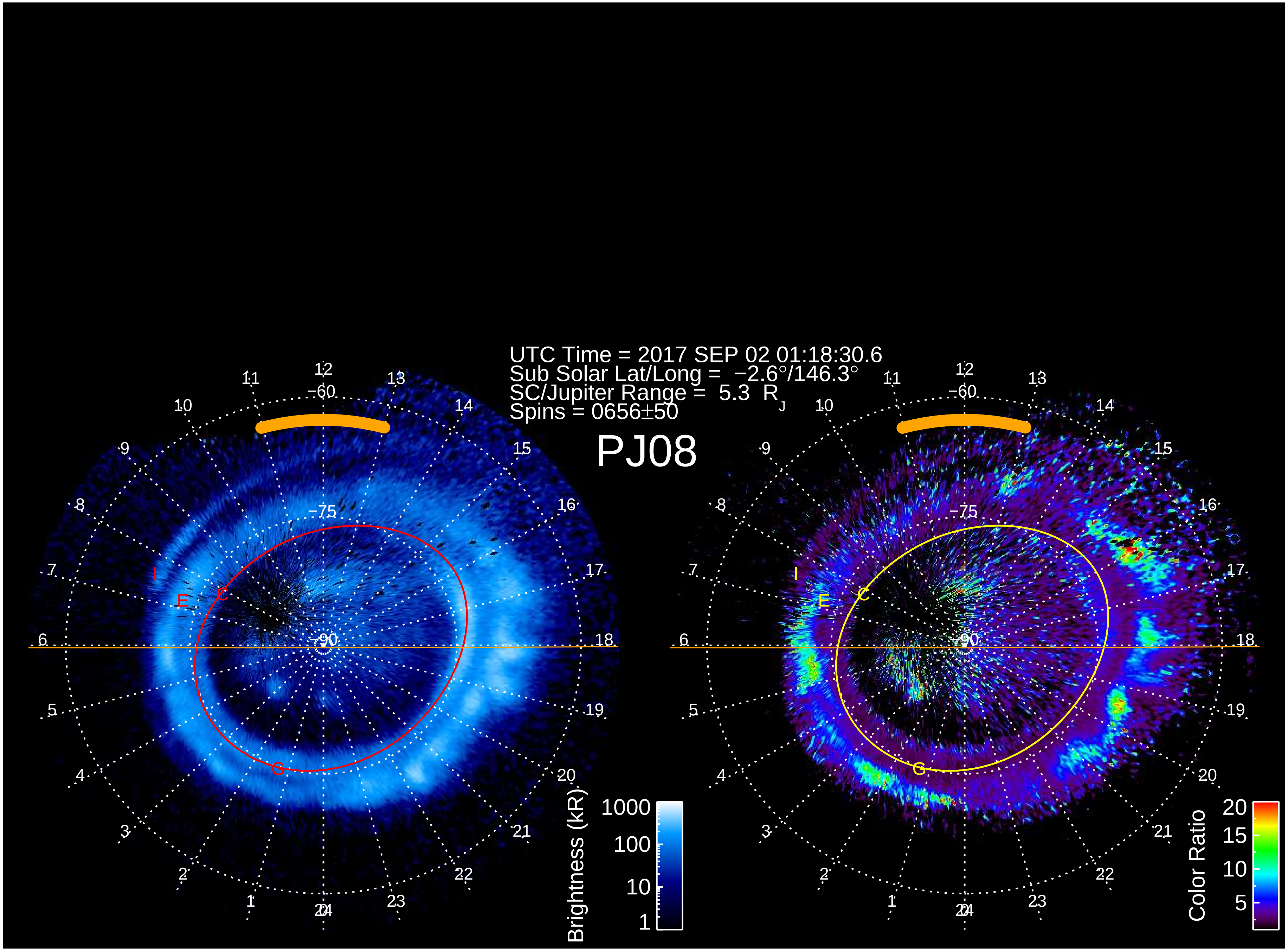

UTC Time = 2017 SEP 02 01:18:30.6
Sub Solar Lat/Long = −2.6°/146.3°
SC/Jupiter Range = 5.3 R_J
Spins = 0656±50
PJ08
Brightness (kR)
1000
100
10
1
Color Ratio
20
15
10
5

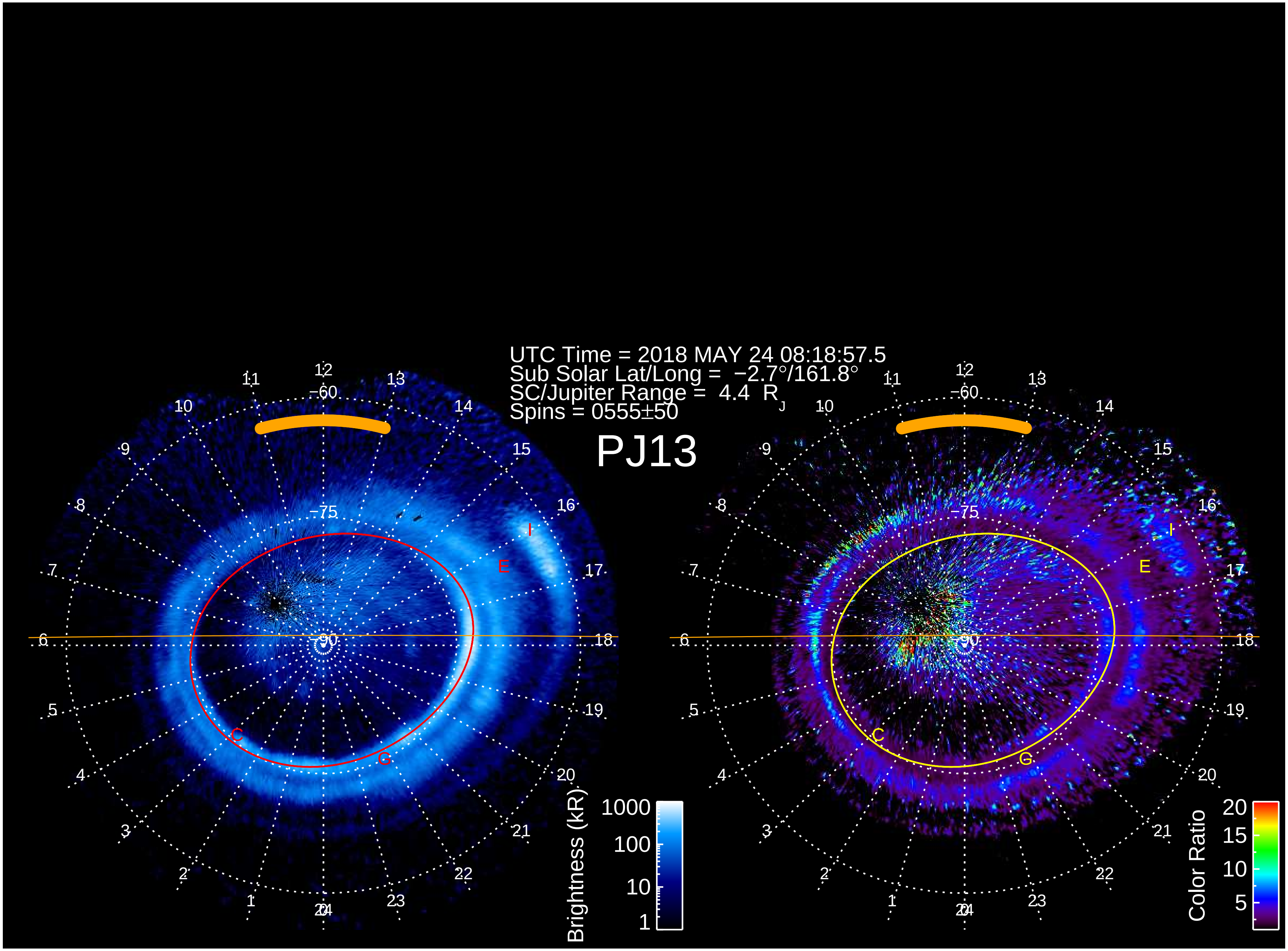
UTC Time = 2018 MAY 24 08:18:57.5
Sub Solar Lat/Long = −2.7°/161.8°
SC/Jupiter Range = 4.4 R_J
Spins = 0555±50
PJ13
Brightness (kR)
1000
100
10
1
Color Ratio
20
15
10
5

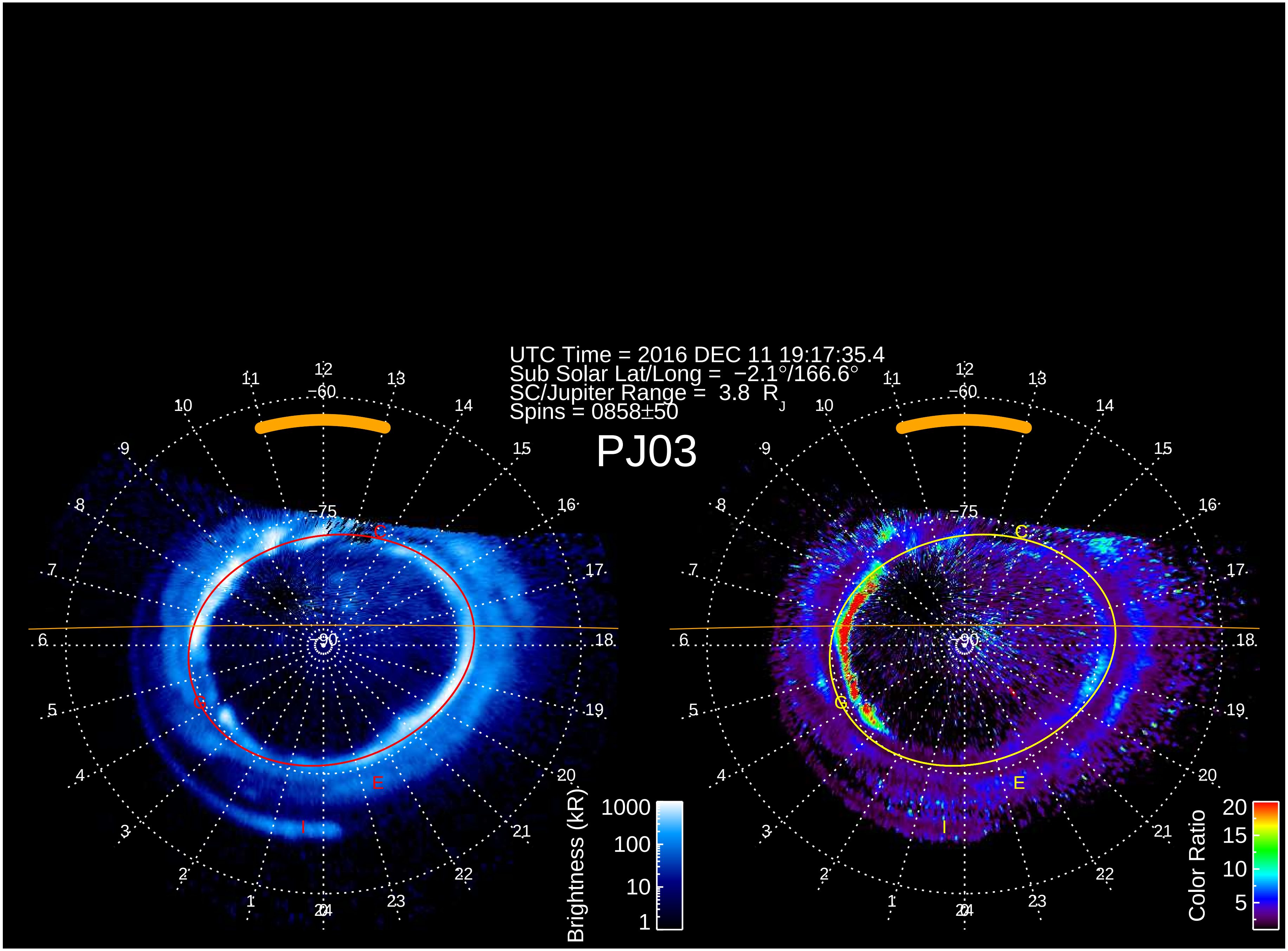

UTC Time = 2016 DEC 11 19:17:35.4
Sub Solar Lat/Long = −2.1°/166.6°
SC/Jupiter Range = 3.8 R_J
Spins = 0858±50
PJ03
Brightness (kR)
1000
100
10
1
Color Ratio
20
15
10
5

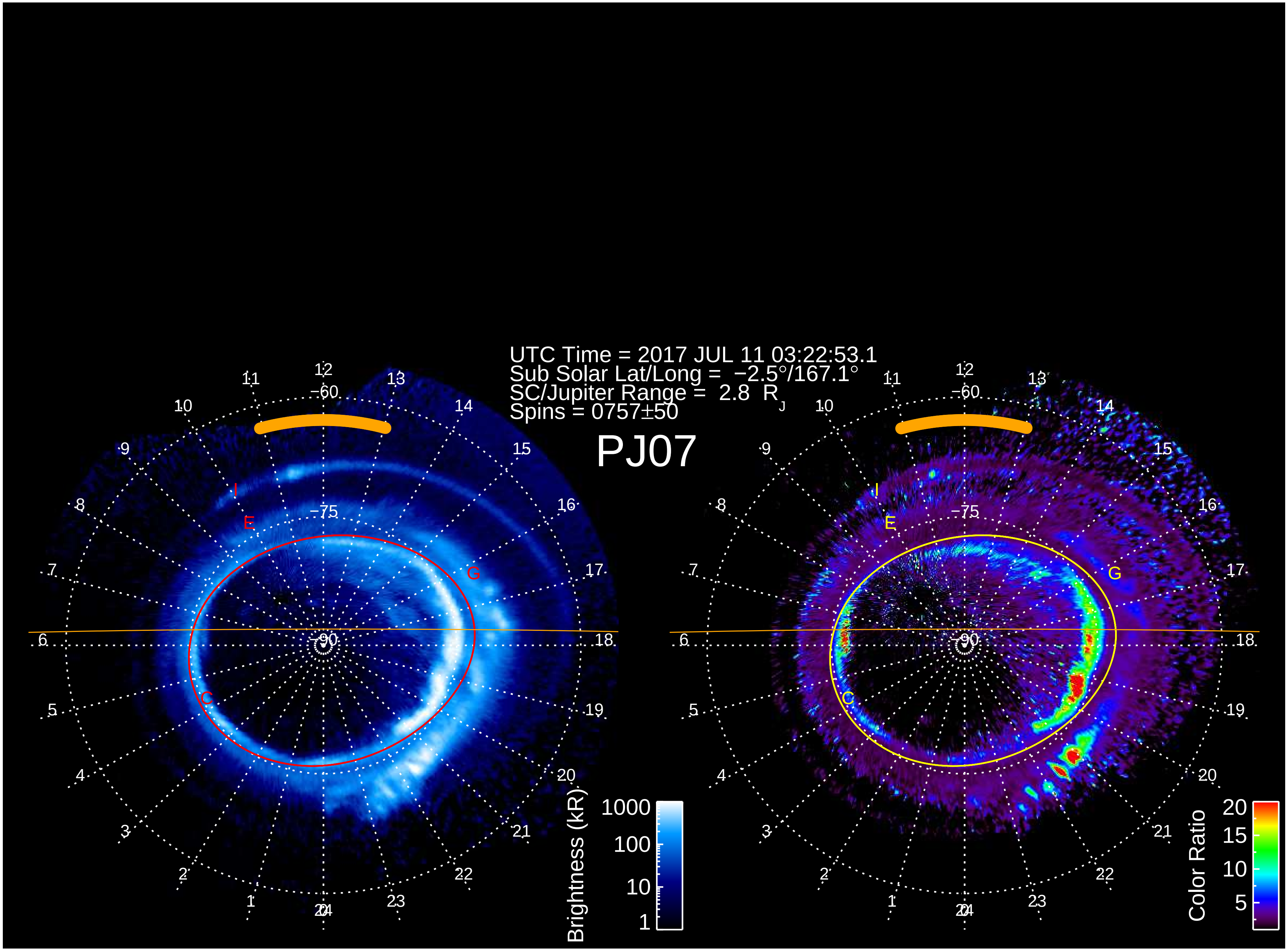

UTC Time = 2017 JUL 11 03:22:53.1
Sub Solar Lat/Long = −2.5°/167.1°
SC/Jupiter Range = 2.8 R_J
Spins = 0757±50
PJ07
Brightness (kR)
1000
100
10
1
Color Ratio
20
15
10
5

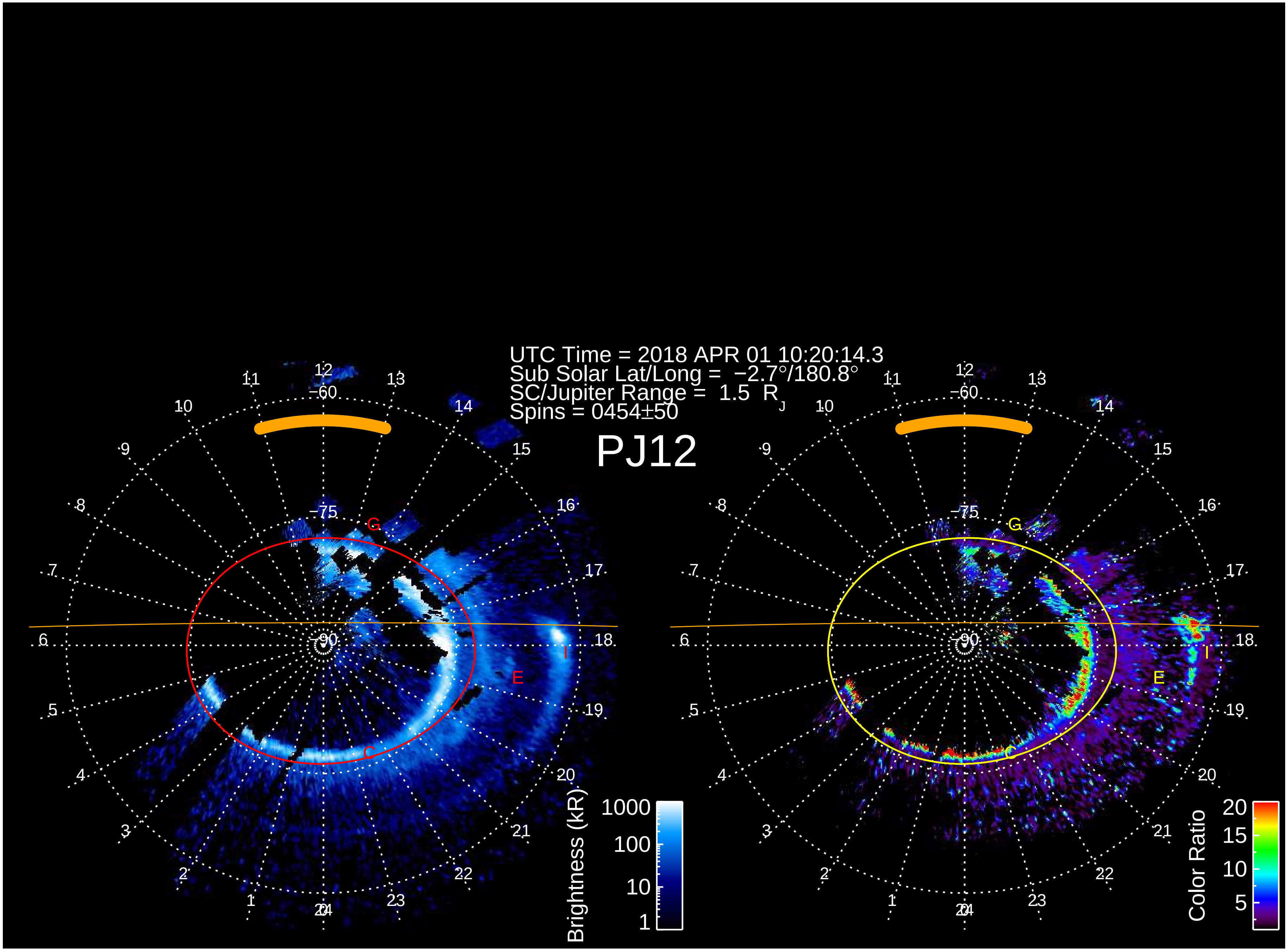

UTC Time = 2018 APR 01 10:20:14.3
Sub Solar Lat/Long = −2.7°/180.8°
SC/Jupiter Range = 1.5 R_J
Spins = 0454±50
PJ12
Brightness (kR)
1000
100
10
1
Color Ratio
20
15
10
5
−60
−75
−90
G
E
I
C

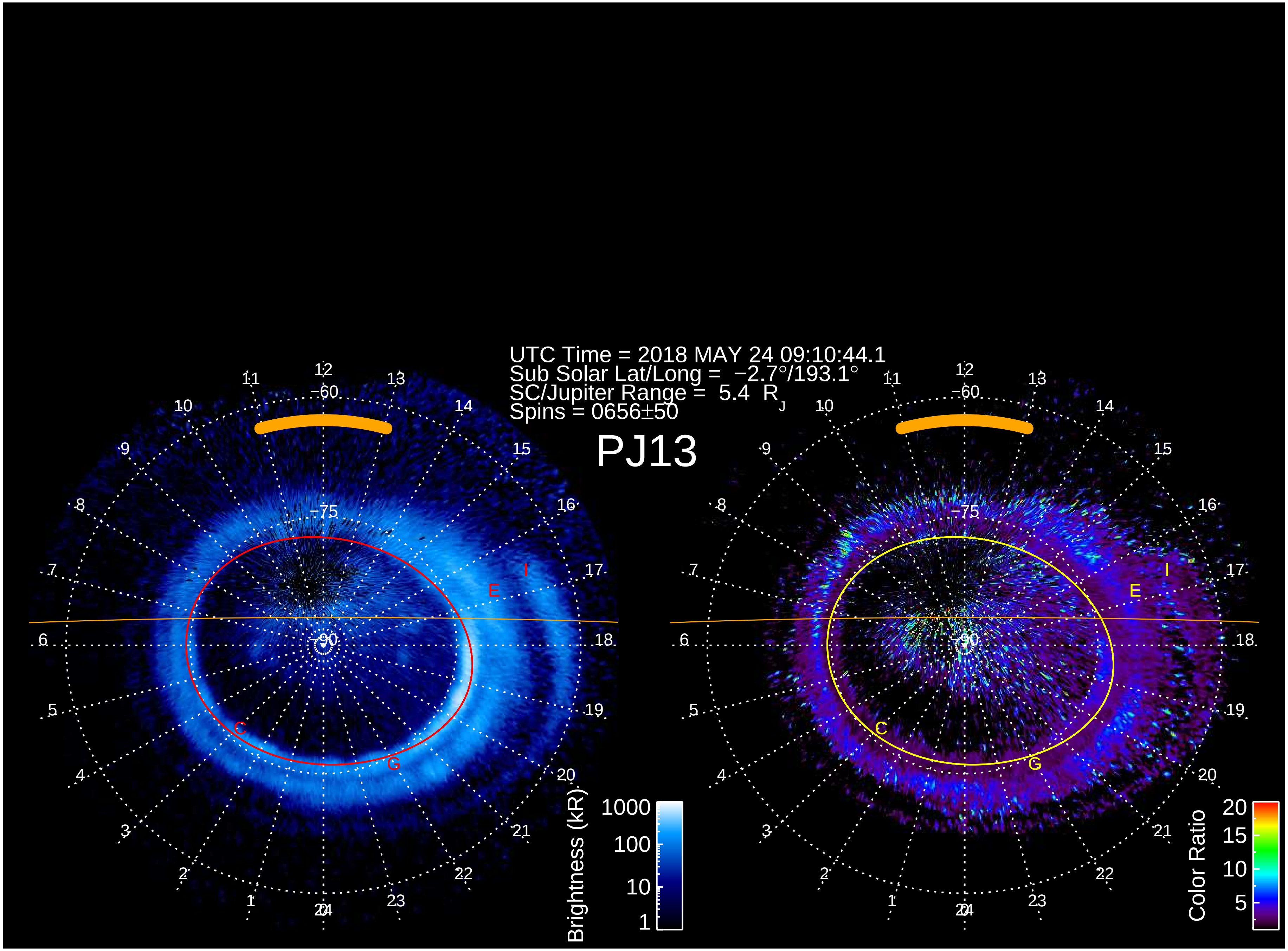

UTC Time = 2018 MAY 24 09:10:44.1
Sub Solar Lat/Long = −2.7°/193.1°
SC/Jupiter Range = 5.4 R$_J$
Spins = 0656±50
PJ13
Brightness (kR)
1000
100
10
1
Color Ratio
20
15
10
5

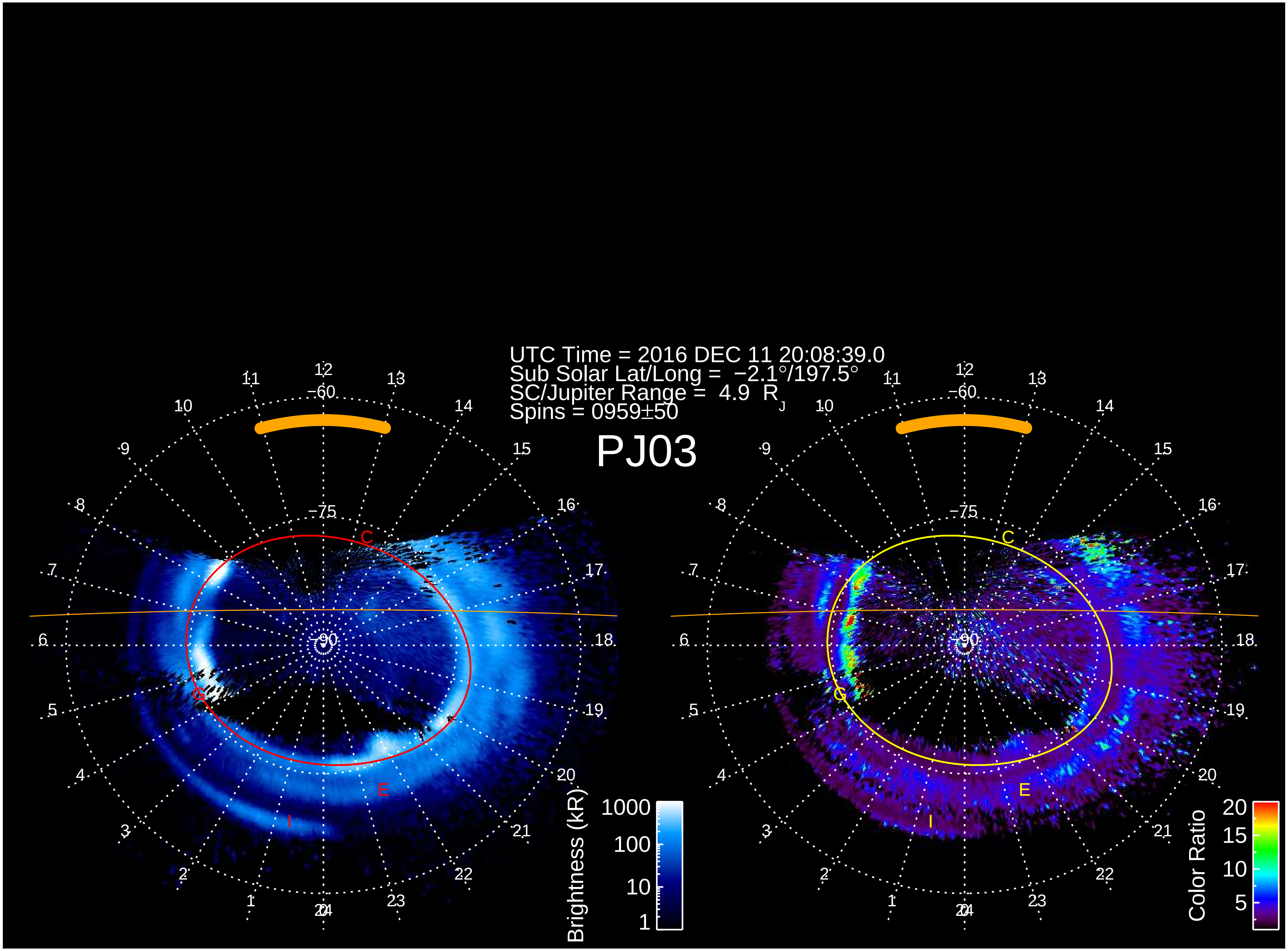
UTC Time = 2016 DEC 11 20:08:39.0
Sub Solar Lat/Long = −2.1°/197.5°
SC/Jupiter Range = 4.9 R_J
Spins = 0959±50
PJ03
Brightness (kR)
1000
100
10
1
Color Ratio
20
15
10
5

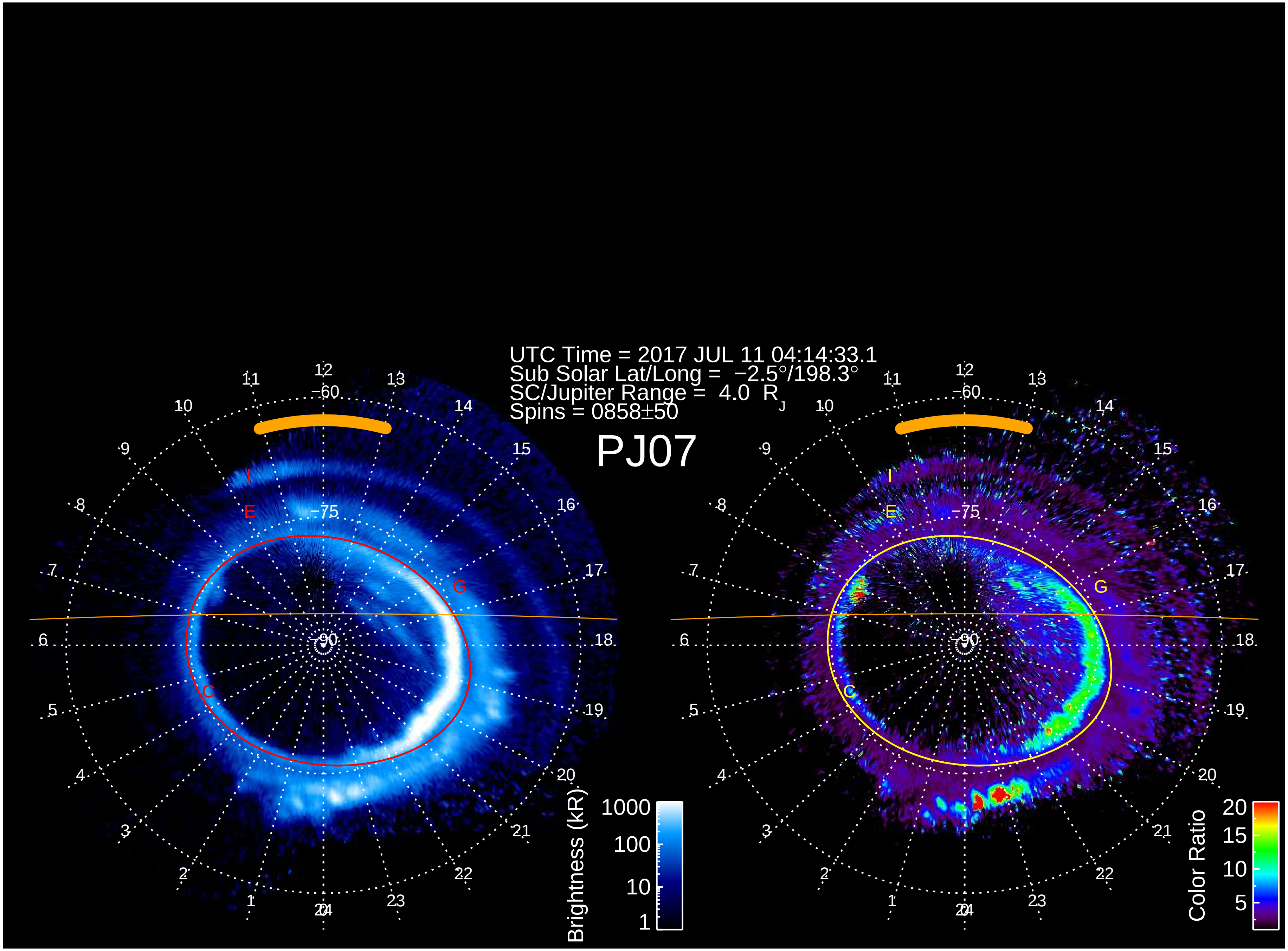

UTC Time = 2017 JUL 11 04:14:33.1
Sub Solar Lat/Long = −2.5°/198.3°
SC/Jupiter Range = 4.0 R
J
Spins = 0858±50
PJ07
Brightness (kR)
1000
100
10
1
Color Ratio
20
15
10
5
−60
−75
−90
I
E
G
C

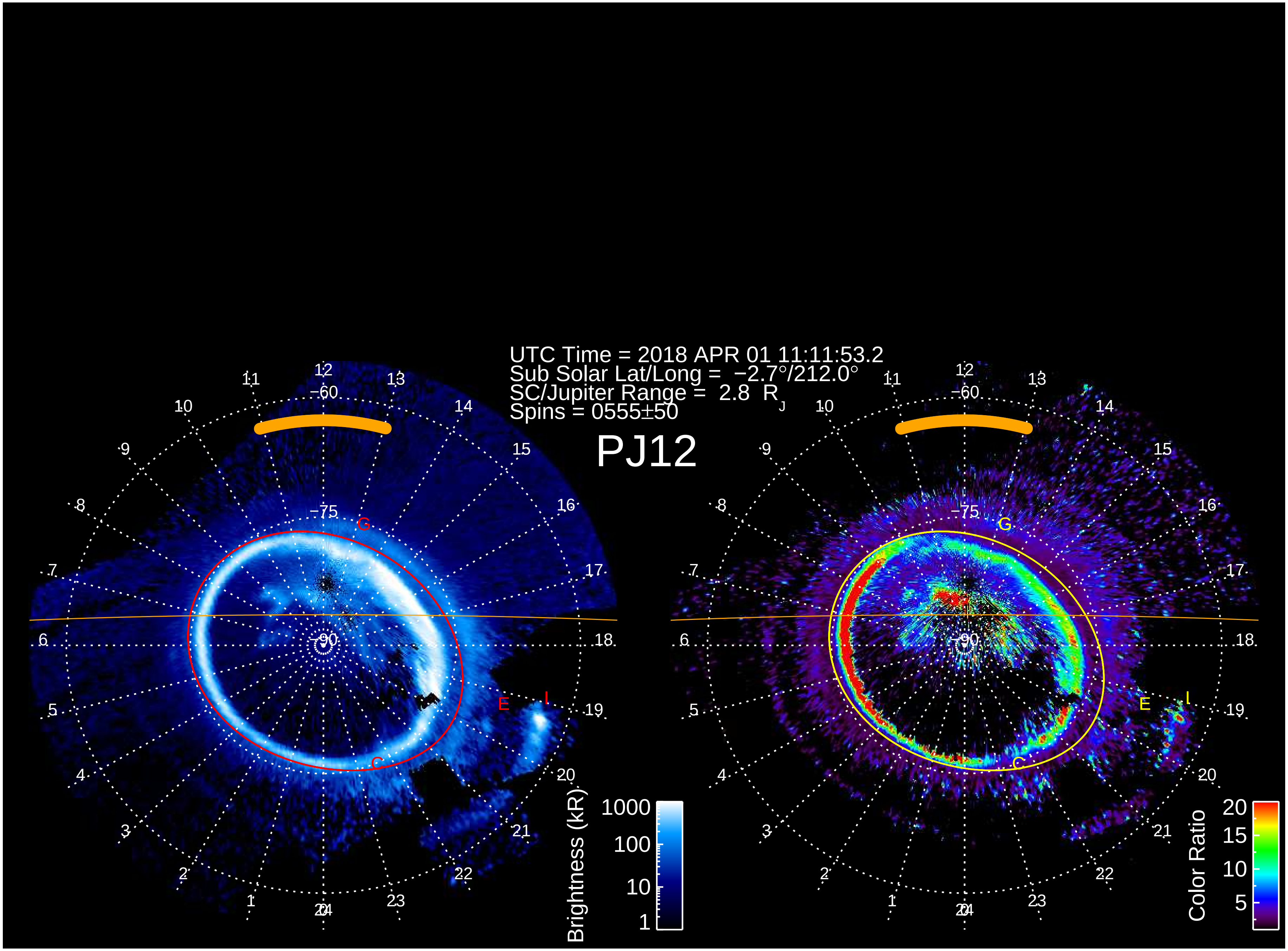
UTC Time = 2018 APR 01 11:11:53.2
Sub Solar Lat/Long = −2.7°/212.0°
SC/Jupiter Range = 2.8 R_J
Spins = 0555±50
PJ12
Brightness (kR)
1000
100
10
1
Color Ratio
20
15
10
5

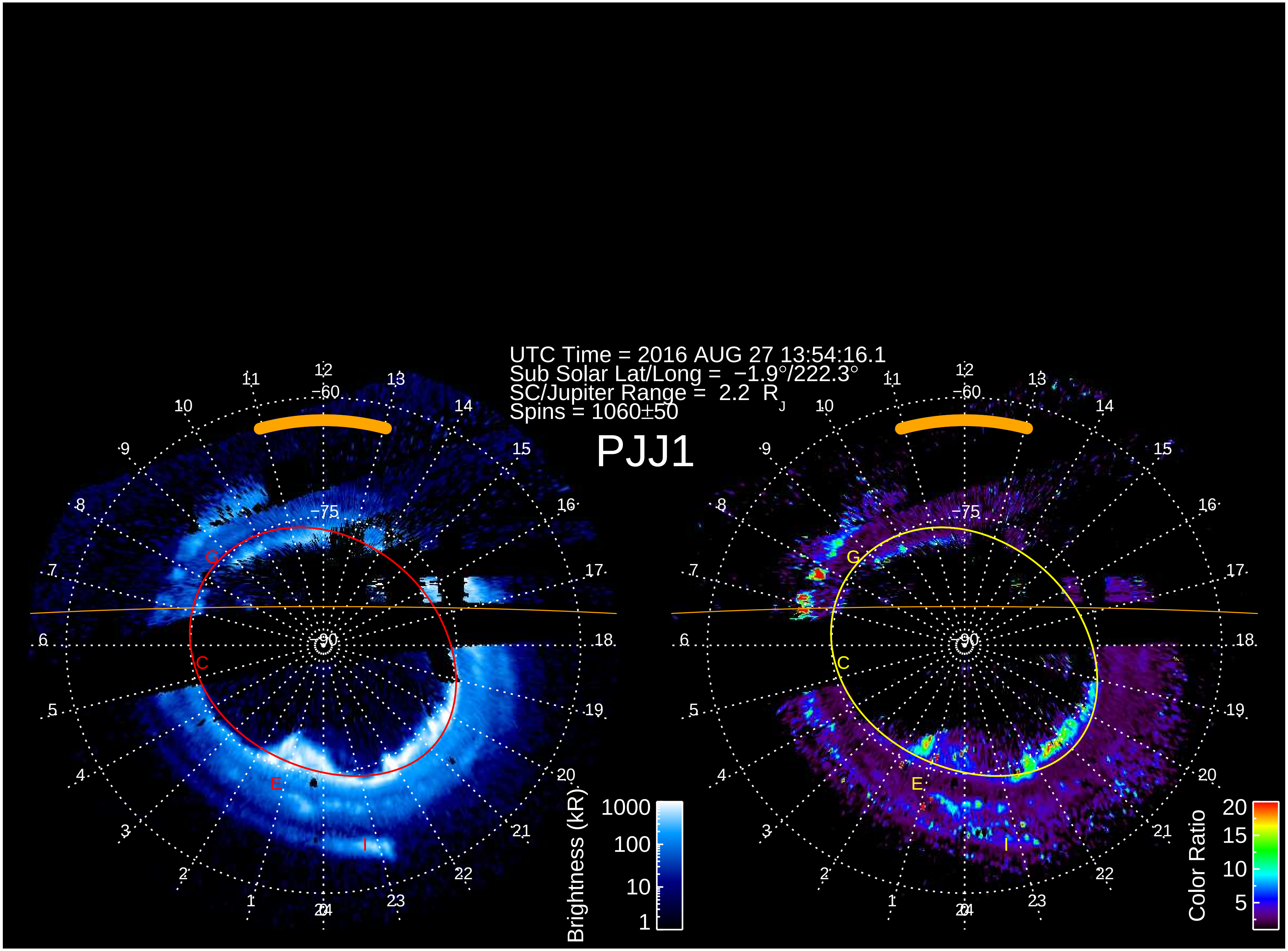
UTC Time = 2016 AUG 27 13:54:16.1
Sub Solar Lat/Long = −1.9°/222.3°
SC/Jupiter Range = 2.2 R$_J$
Spins = 1060±50
PJJ1
Brightness (kR)
1000
100
10
1
Color Ratio
20
15
10
5
G
C
E
I
−60
−75
−90

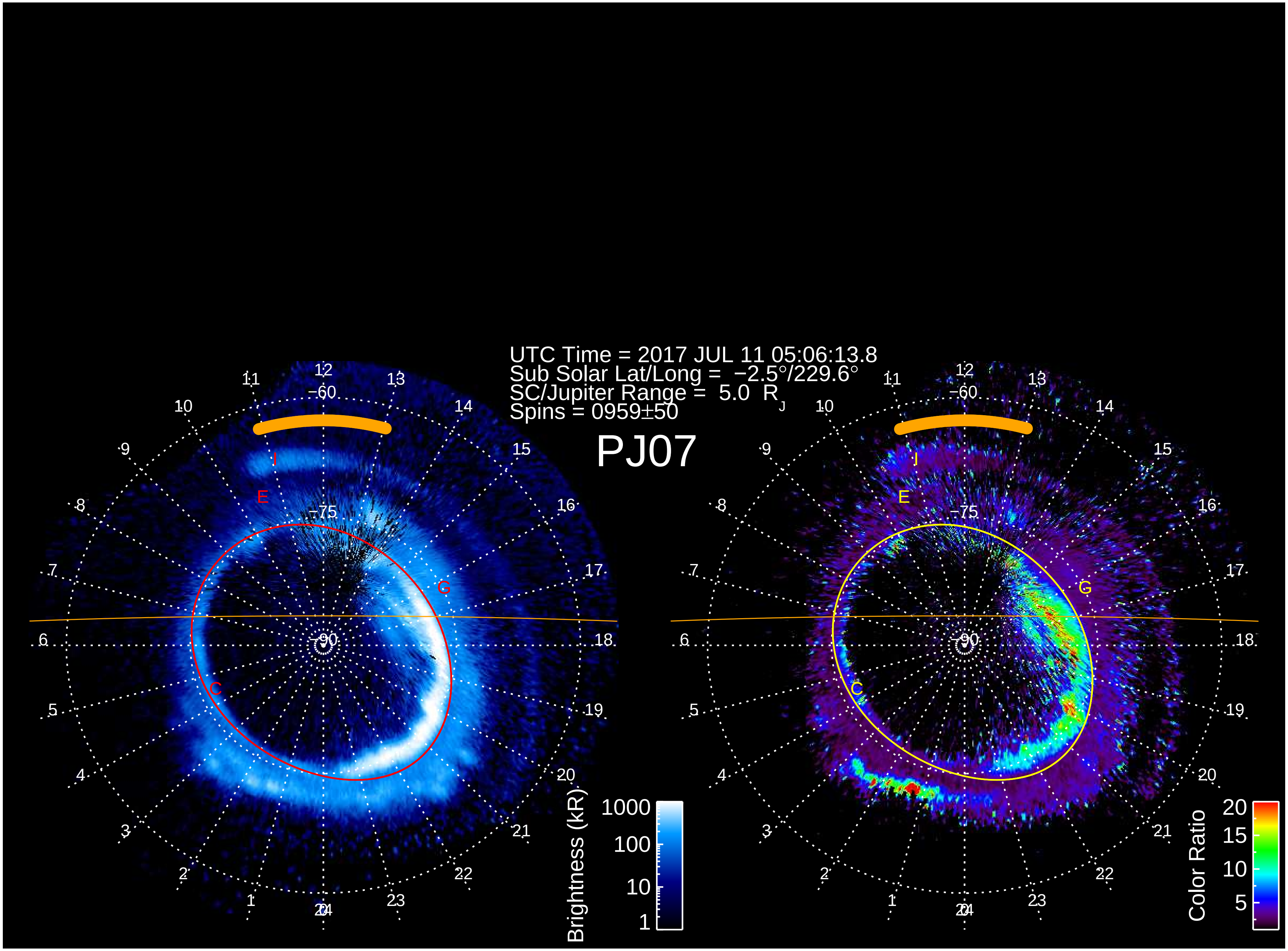

UTC Time = 2017 JUL 11 05:06:13.8
Sub Solar Lat/Long = −2.5°/229.6°
SC/Jupiter Range = 5.0 R_J
Spins = 0959±50
PJ07
Brightness (kR)
1000
100
10
1
Color Ratio
20
15
10
5

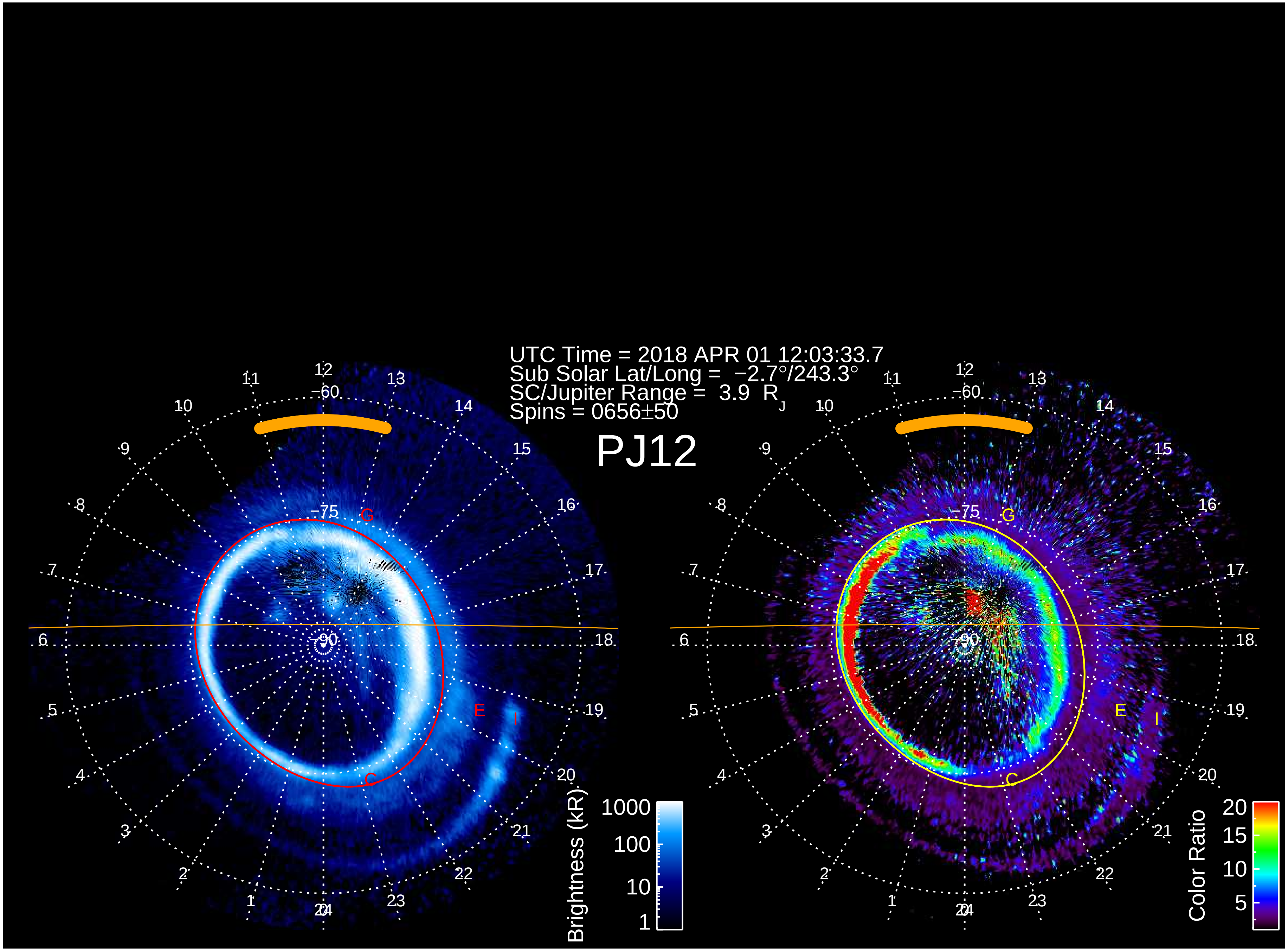

UTC Time = 2018 APR 01 12:03:33.7
Sub Solar Lat/Long = −2.7°/243.3°
SC/Jupiter Range = 3.9 R_J
Spins = 0656±50
PJ12
Brightness (kR)
1000
100
10
1
Color Ratio
20
15
10
5
G
E
I
C
−60
−75
−90

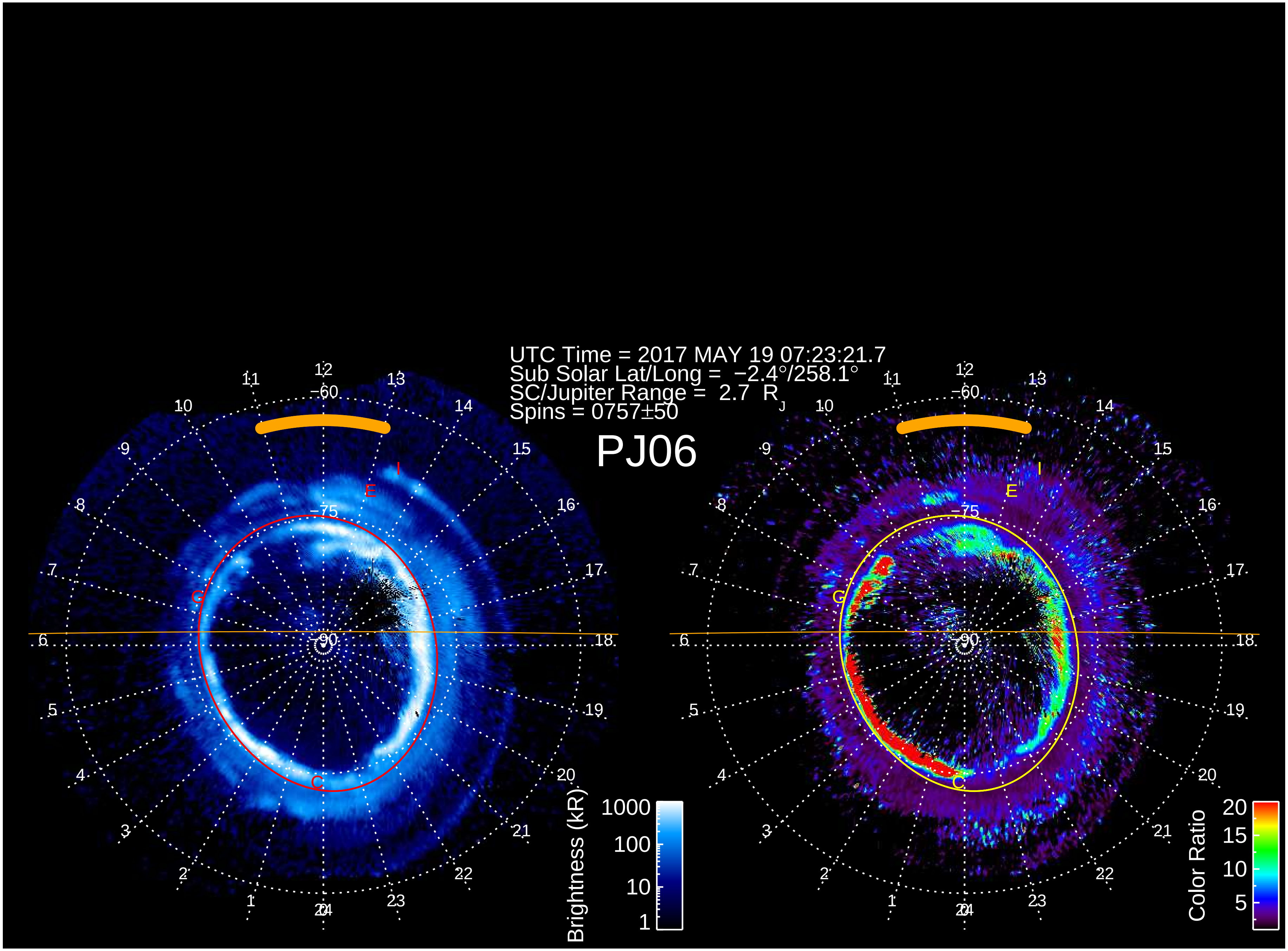
UTC Time = 2017 MAY 19 07:23:21.7
Sub Solar Lat/Long = −2.4°/258.1°
SC/Jupiter Range = 2.7 R J
Spins = 0757±50
PJ06
Brightness (kR)
1000
100
10
1
Color Ratio
20
15
10
5

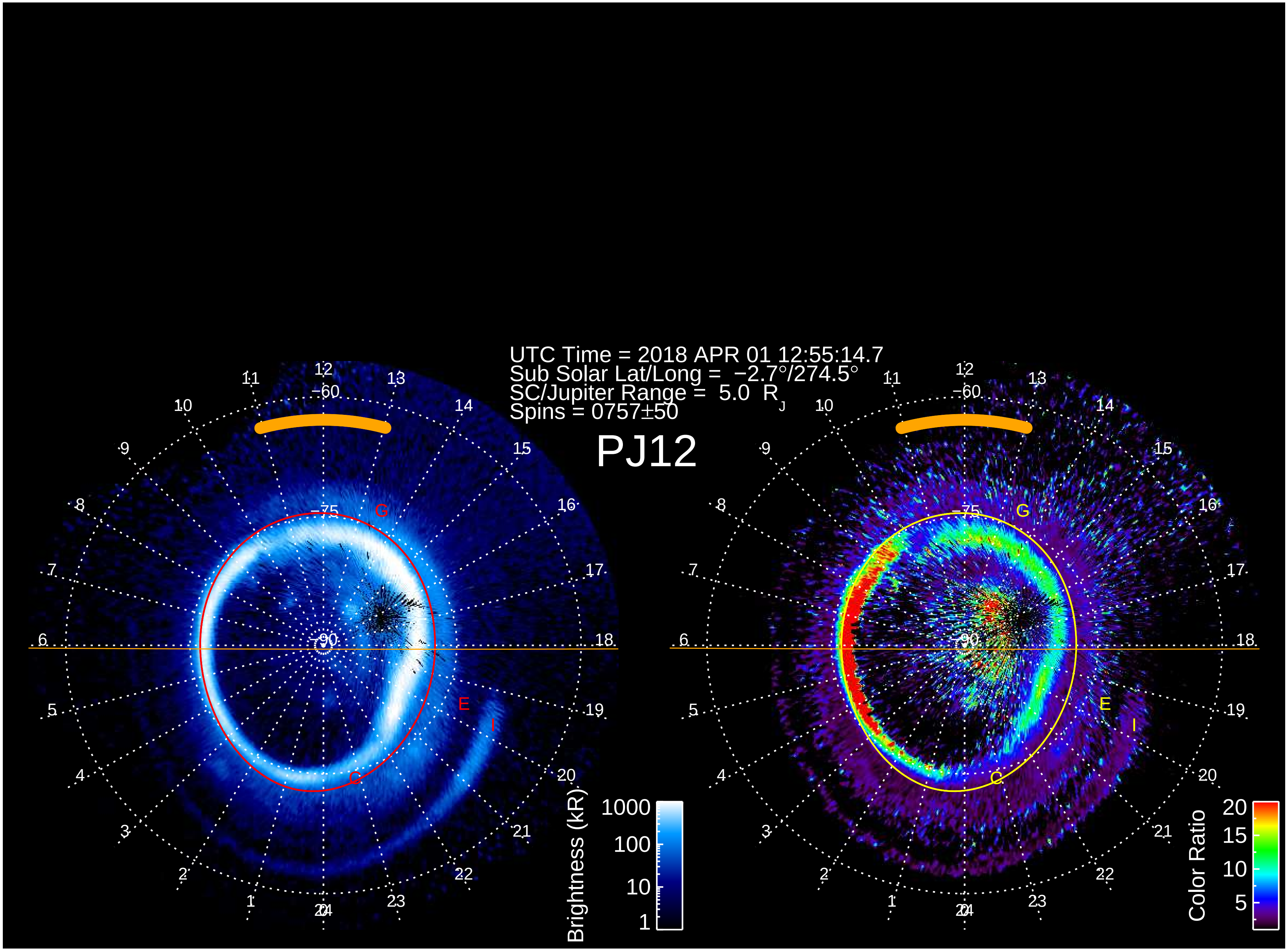

UTC Time = 2018 APR 01 12:55:14.7
Sub Solar Lat/Long = −2.7°/274.5°
SC/Jupiter Range = 5.0 R_J
Spins = 0757±50
PJ12
G
E
I
C
Brightness (kR)
1000
100
10
1
Color Ratio
20
15
10
5

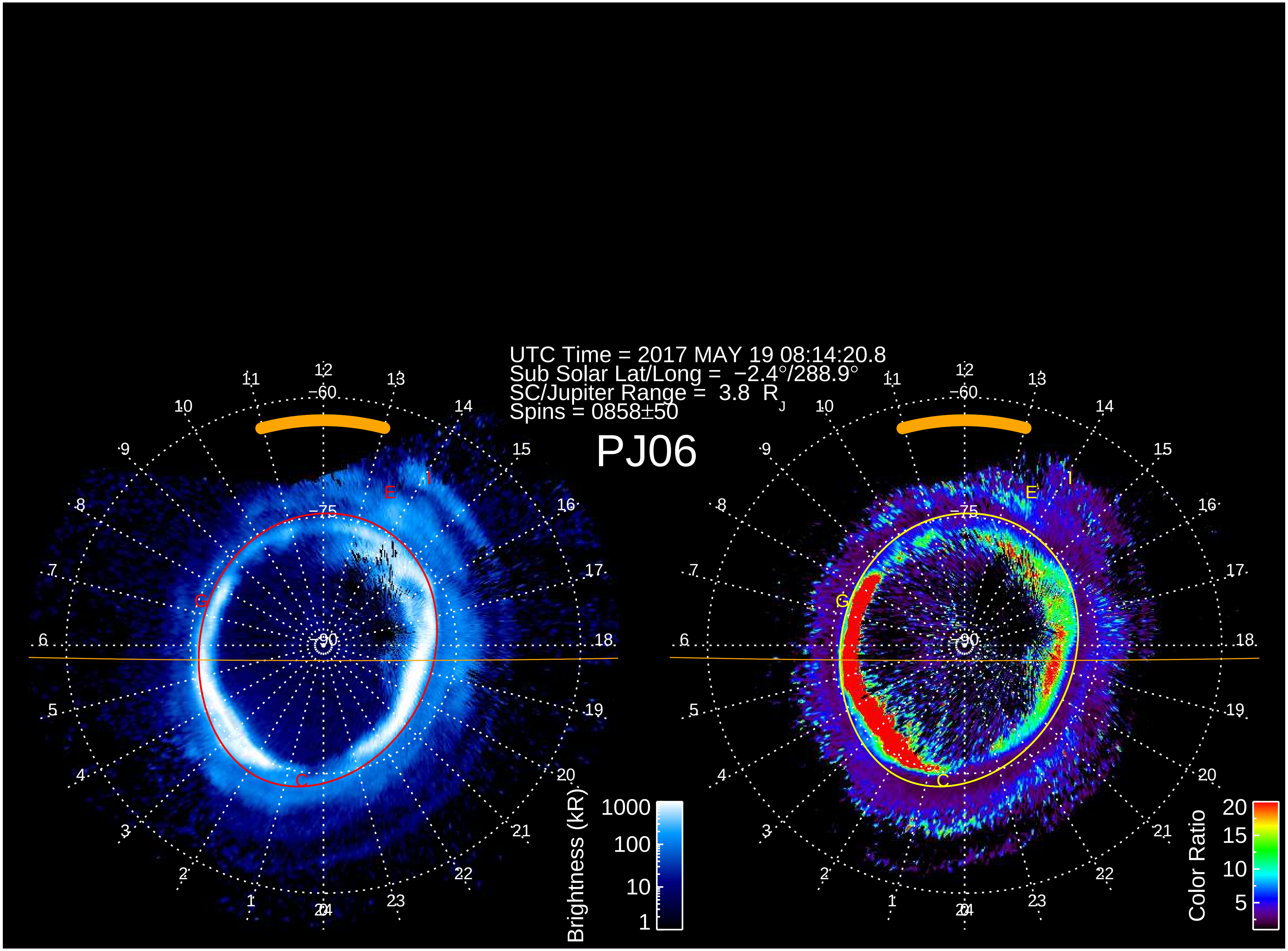
UTC Time = 2017 MAY 19 08:14:20.8
Sub Solar Lat/Long = −2.4°/288.9°
SC/Jupiter Range = 3.8 R_J
Spins = 0858±50
PJ06
Brightness (kR)
1000
100
10
1
Color Ratio
20
15
10
5

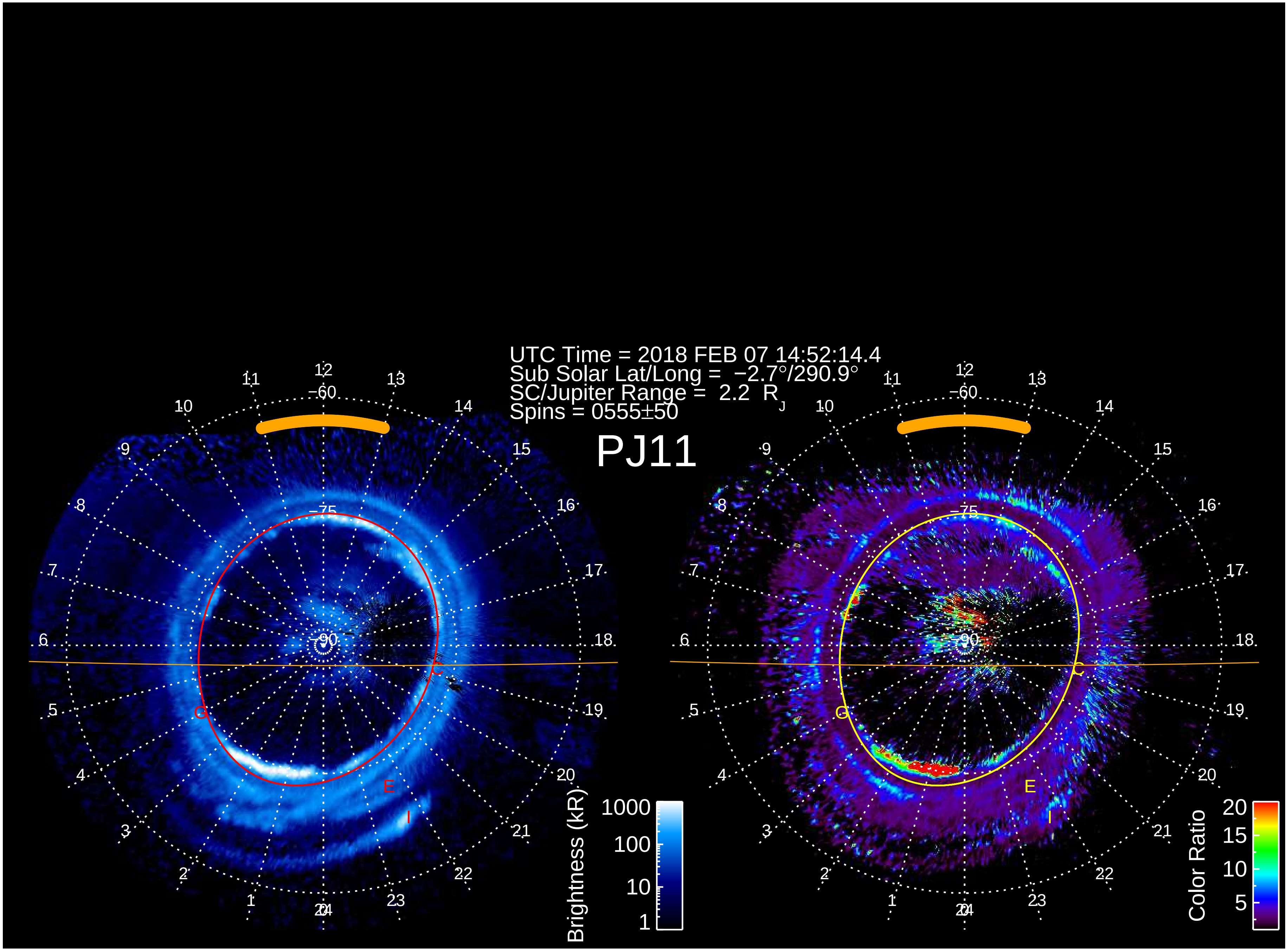

UTC Time = 2018 FEB 07 14:52:14.4
Sub Solar Lat/Long = −2.7°/290.9°
SC/Jupiter Range = 2.2 R_J
Spins = 0555±50
PJ11
Brightness (kR)
1000
100
10
1
Color Ratio
20
15
10
5

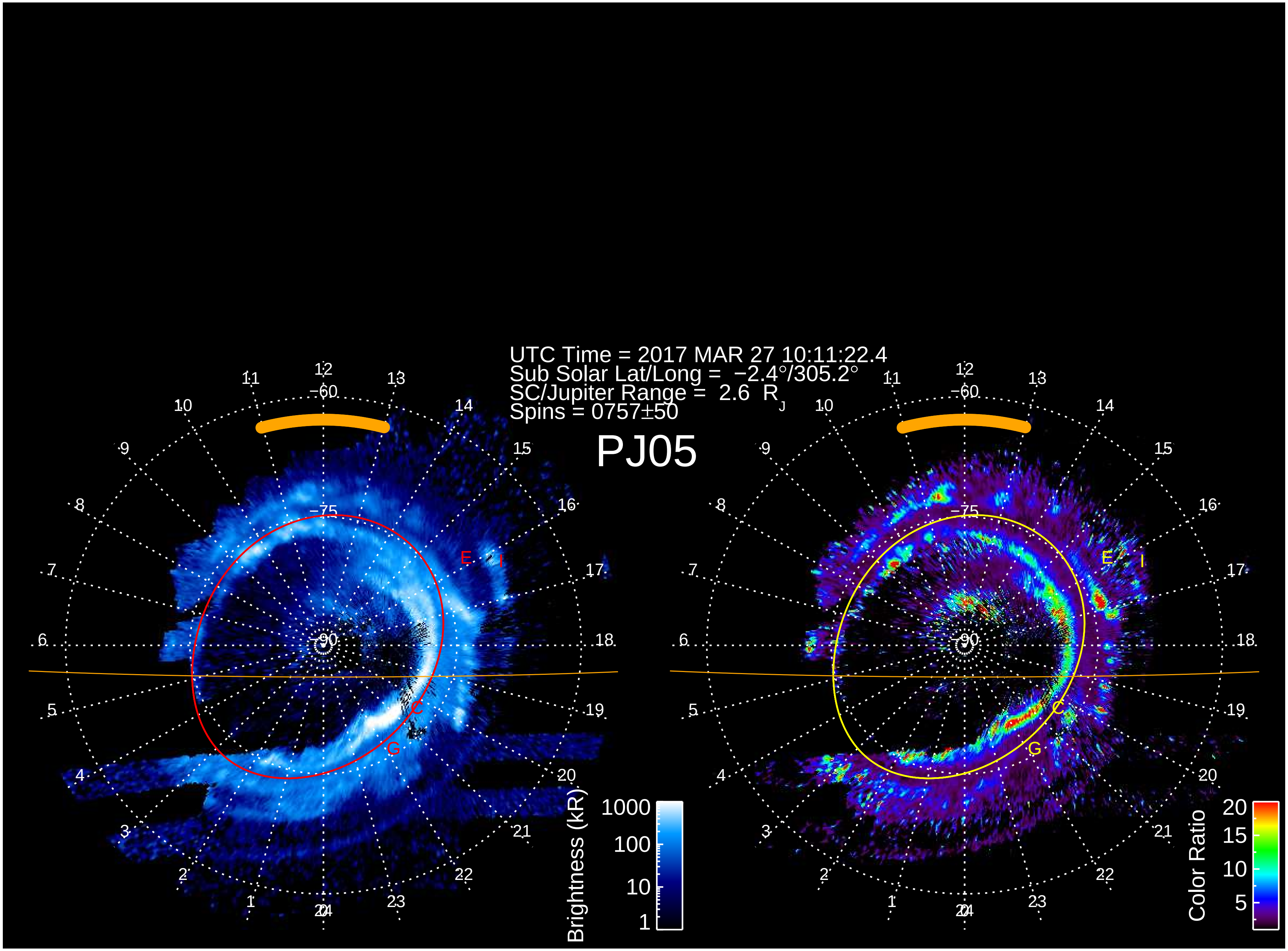

UTC Time = 2017 MAR 27 10:11:22.4
Sub Solar Lat/Long = −2.4°/305.2°
SC/Jupiter Range = 2.6 R$_J$
Spins = 0757±50
PJ05
Brightness (kR)
1000
100
10
1
Color Ratio
20
15
10
5
−60
−75
−90
E
I
C
G

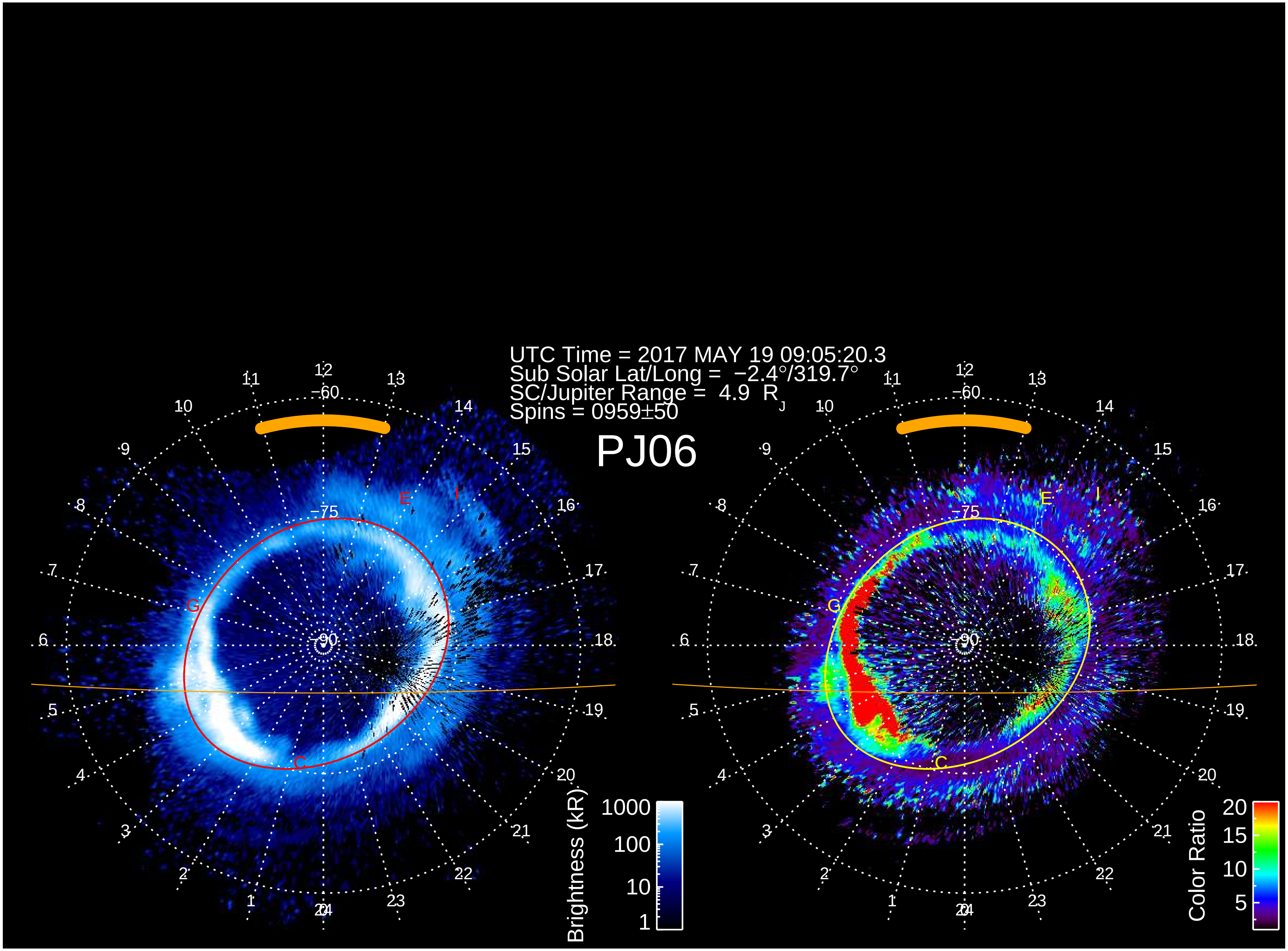

UTC Time = 2017 MAY 19 09:05:20.3
Sub Solar Lat/Long = −2.4°/319.7°
SC/Jupiter Range = 4.9 R$_J$
Spins = 0959±50
PJ06
Brightness (kR)
1000
100
10
1
Color Ratio
20
15
10
5

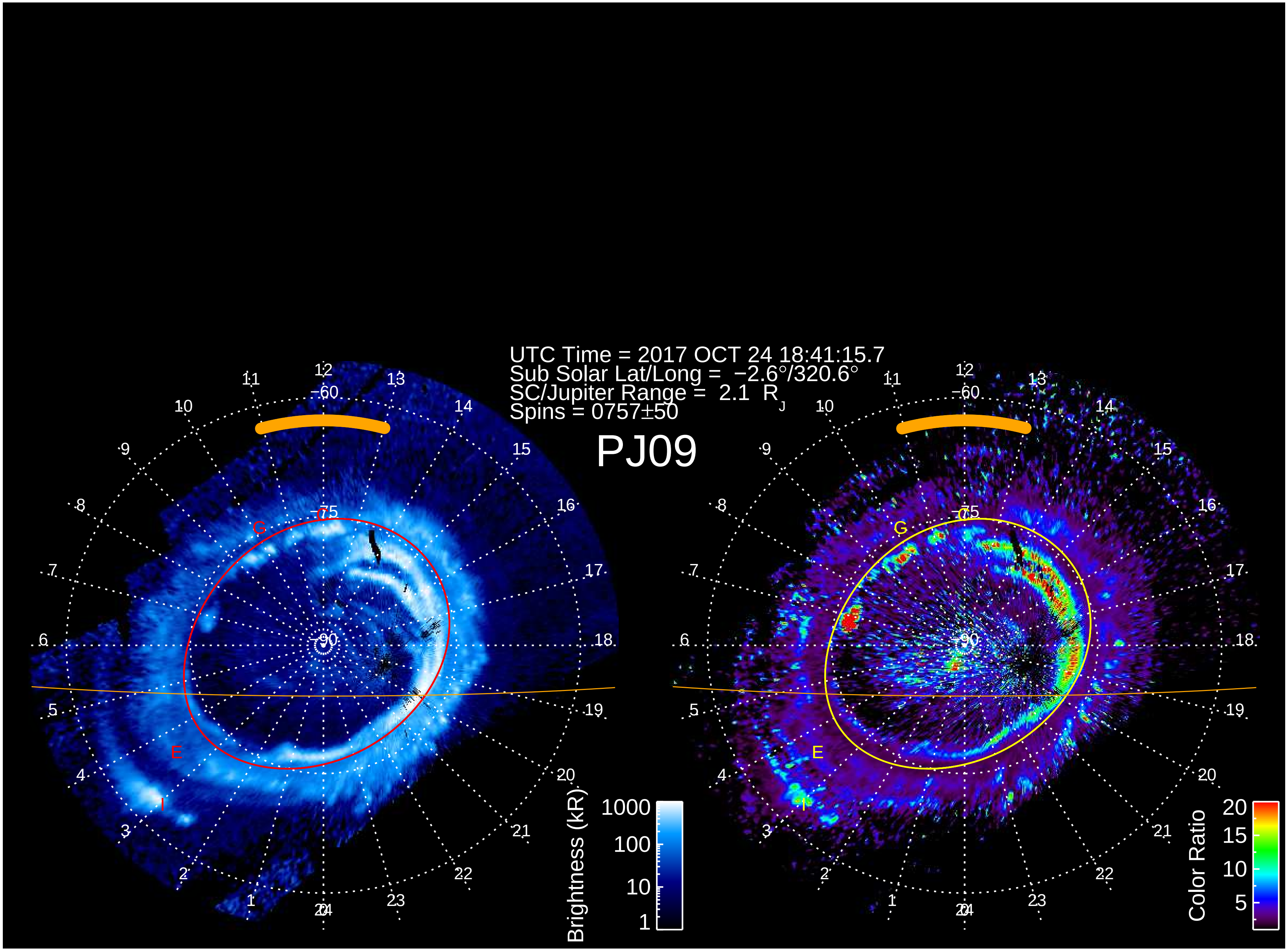

UTC Time = 2017 OCT 24 18:41:15.7
Sub Solar Lat/Long = −2.6°/320.6°
SC/Jupiter Range = 2.1 R_J
Spins = 0757±50
PJ09
Brightness (kR)
1000
100
10
1
Color Ratio
20
15
10
5

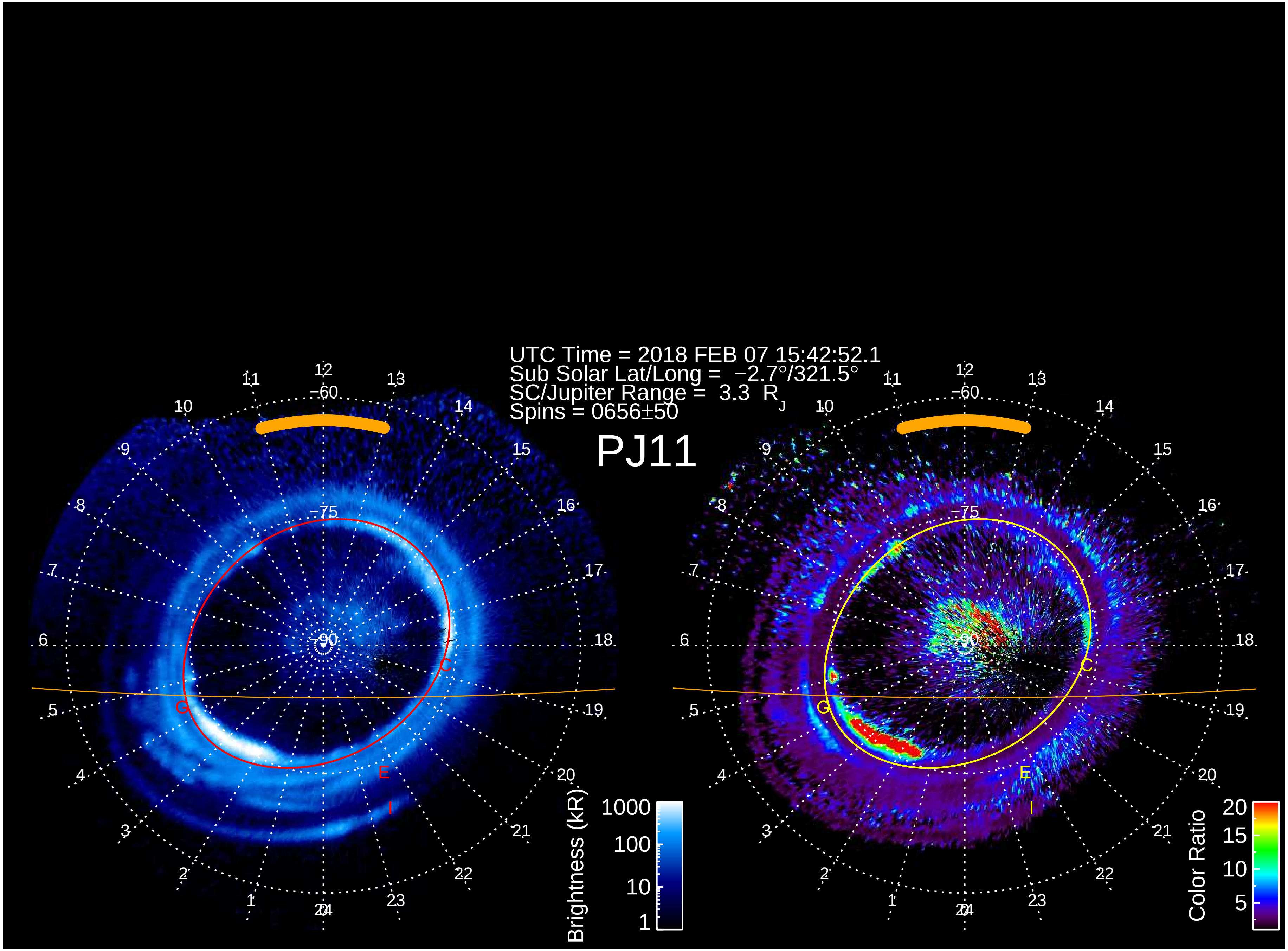

UTC Time = 2018 FEB 07 15:42:52.1
Sub Solar Lat/Long = −2.7°/321.5°
SC/Jupiter Range = 3.3 R_J
Spins = 0656±50
PJ11
Brightness (kR)
1000
100
10
1
Color Ratio
20
15
10
5

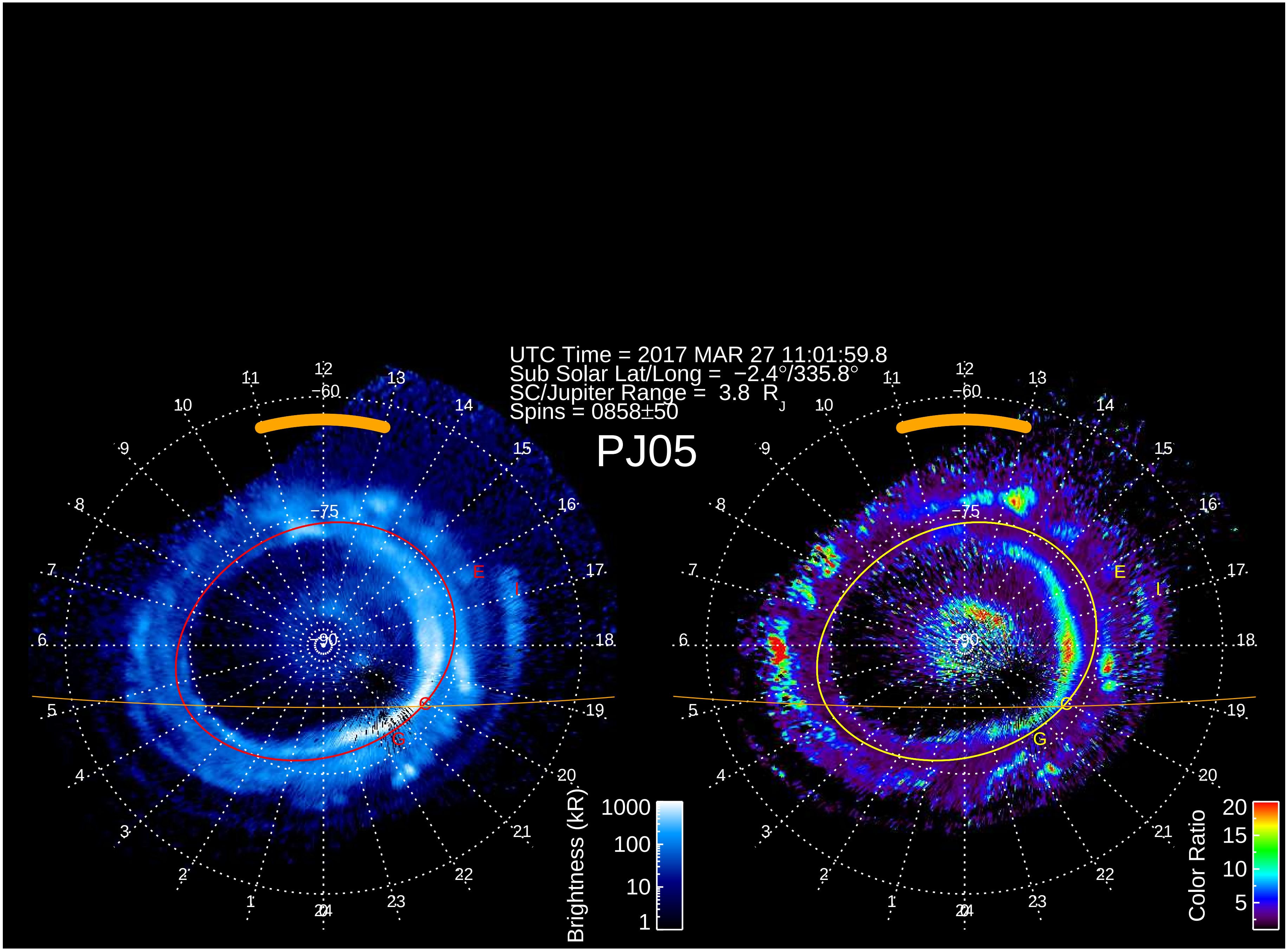

UTC Time = 2017 MAR 27 11:01:59.8
Sub Solar Lat/Long = −2.4°/335.8°
SC/Jupiter Range = 3.8 R_J
Spins = 0858±50
PJ05
Brightness (kR)
1000
100
10
1
Color Ratio
20
15
10
5

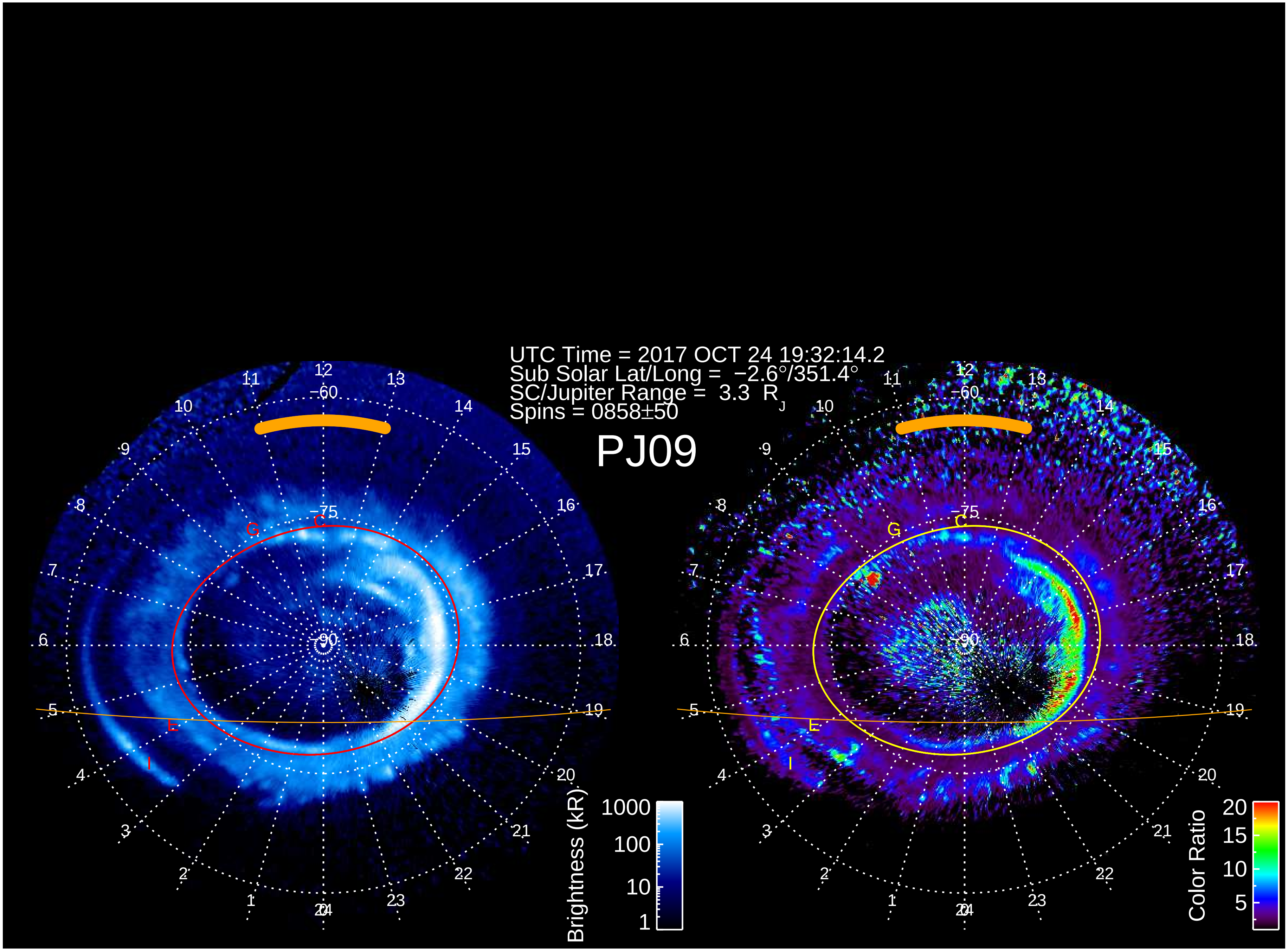

UTC Time = 2017 OCT 24 19:32:14.2
Sub Solar Lat/Long = −2.6°/351.4°
SC/Jupiter Range = 3.3 R$_J$
Spins = 0858±50
PJ09
Brightness (kR)
1000
100
10
1
Color Ratio
20
15
10
5

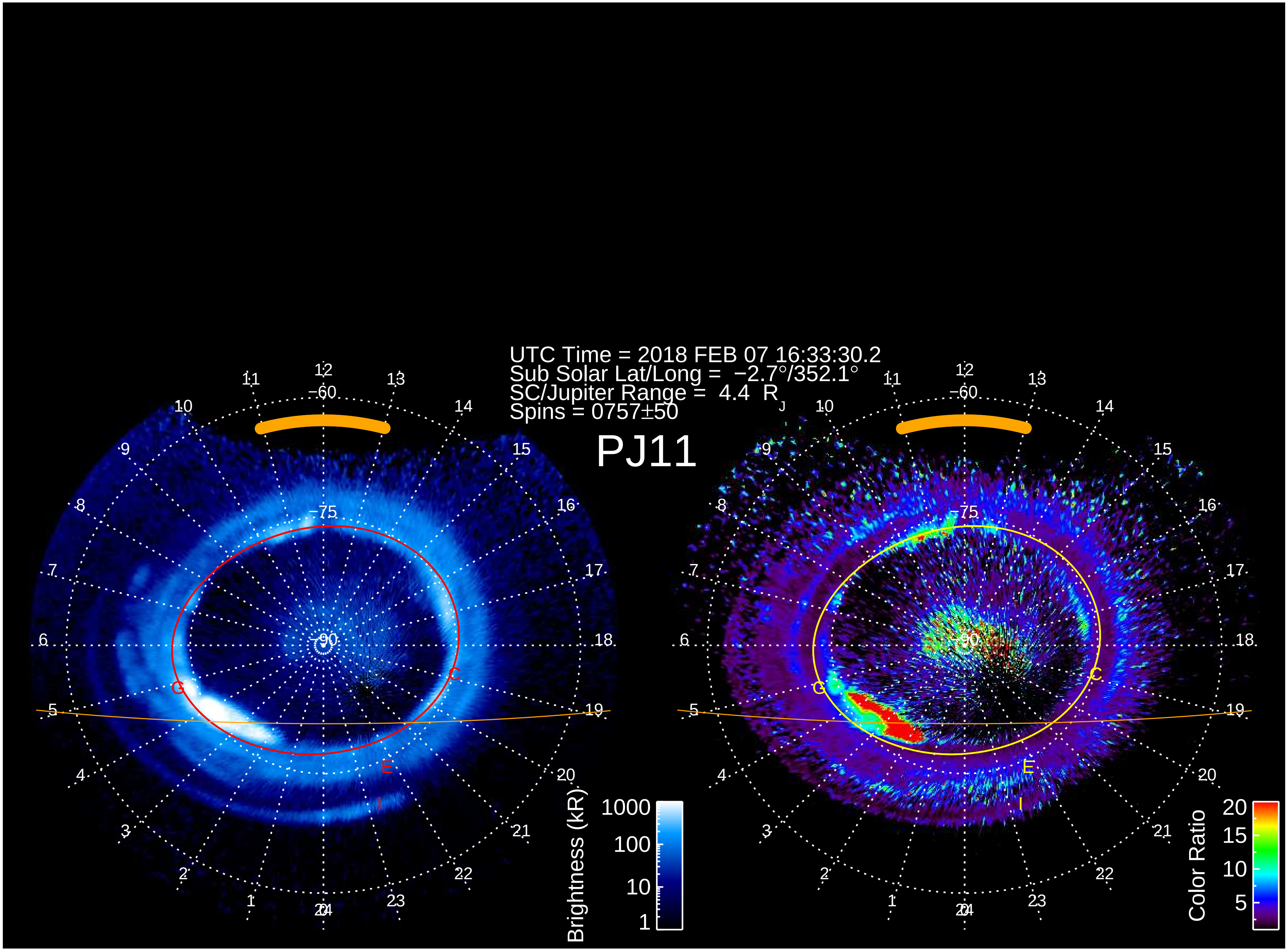

UTC Time = 2018 FEB 07 16:33:30.2
Sub Solar Lat/Long = −2.7°/352.1°
SC/Jupiter Range = 4.4 R_J
Spins = 0757±50
PJ11
Brightness (kR)
1000
100
10
1
Color Ratio
20
15
10
5

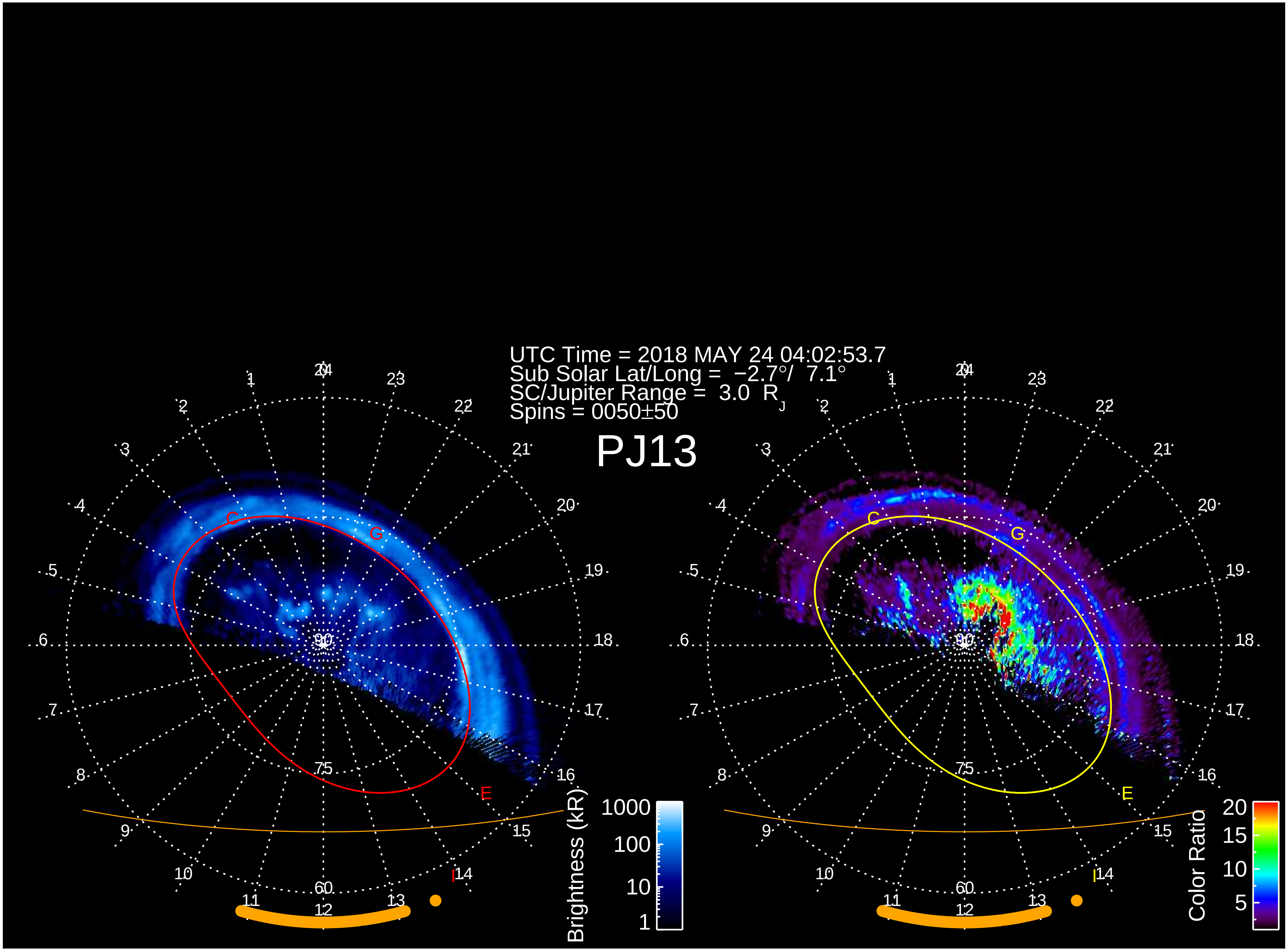

UTC Time = 2018 MAY 24 04:02:53.7
Sub Solar Lat/Long = −2.7°/ 7.1°
SC/Jupiter Range = 3.0 R_J
Spins = 0050±50
PJ13
Brightness (kR)
1000
100
10
1
Color Ratio
20
15
10
5

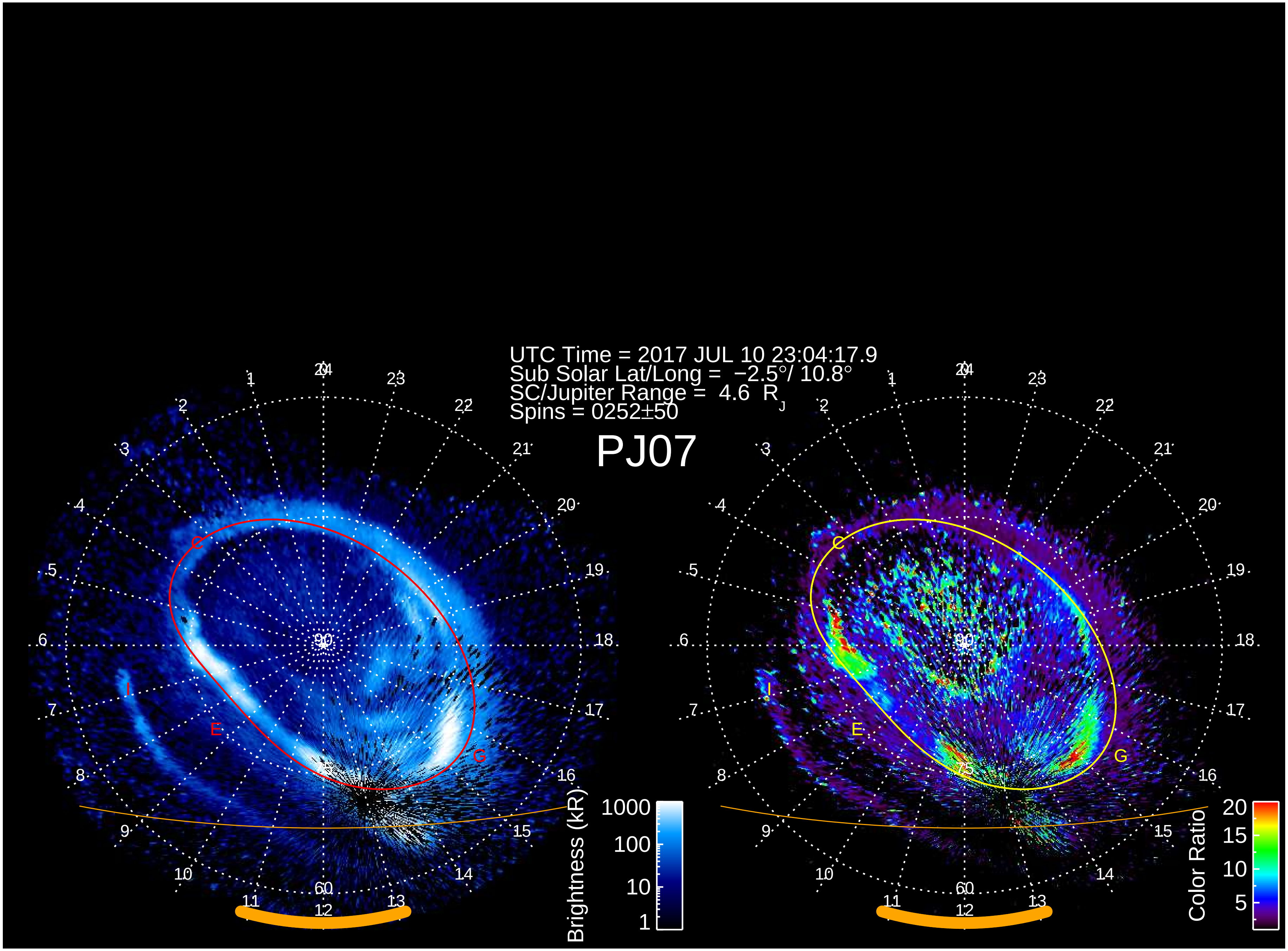
UTC Time = 2017 JUL 10 23:04:17.9
Sub Solar Lat/Long = −2.5°/ 10.8°
SC/Jupiter Range = 4.6 R_J
Spins = 0252±50
PJ07
Brightness (kR)
1000
100
10
1
Color Ratio
20
15
10
5

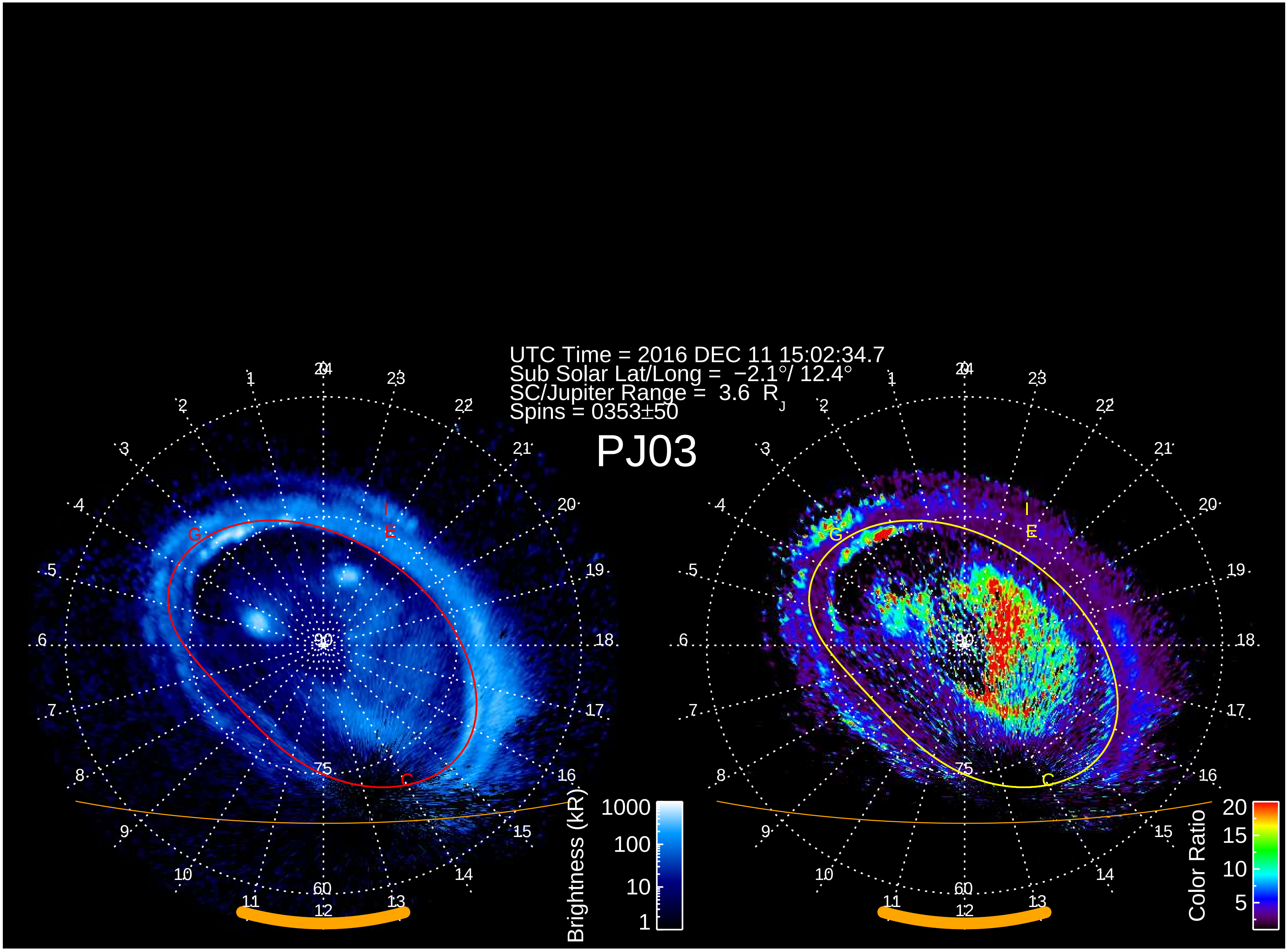

UTC Time = 2016 DEC 11 15:02:34.7
Sub Solar Lat/Long = −2.1°/ 12.4°
SC/Jupiter Range = 3.6 R$_J$
Spins = 0353±50
PJ03
Brightness (kR)
1000
100
10
1
Color Ratio
20
15
10
5

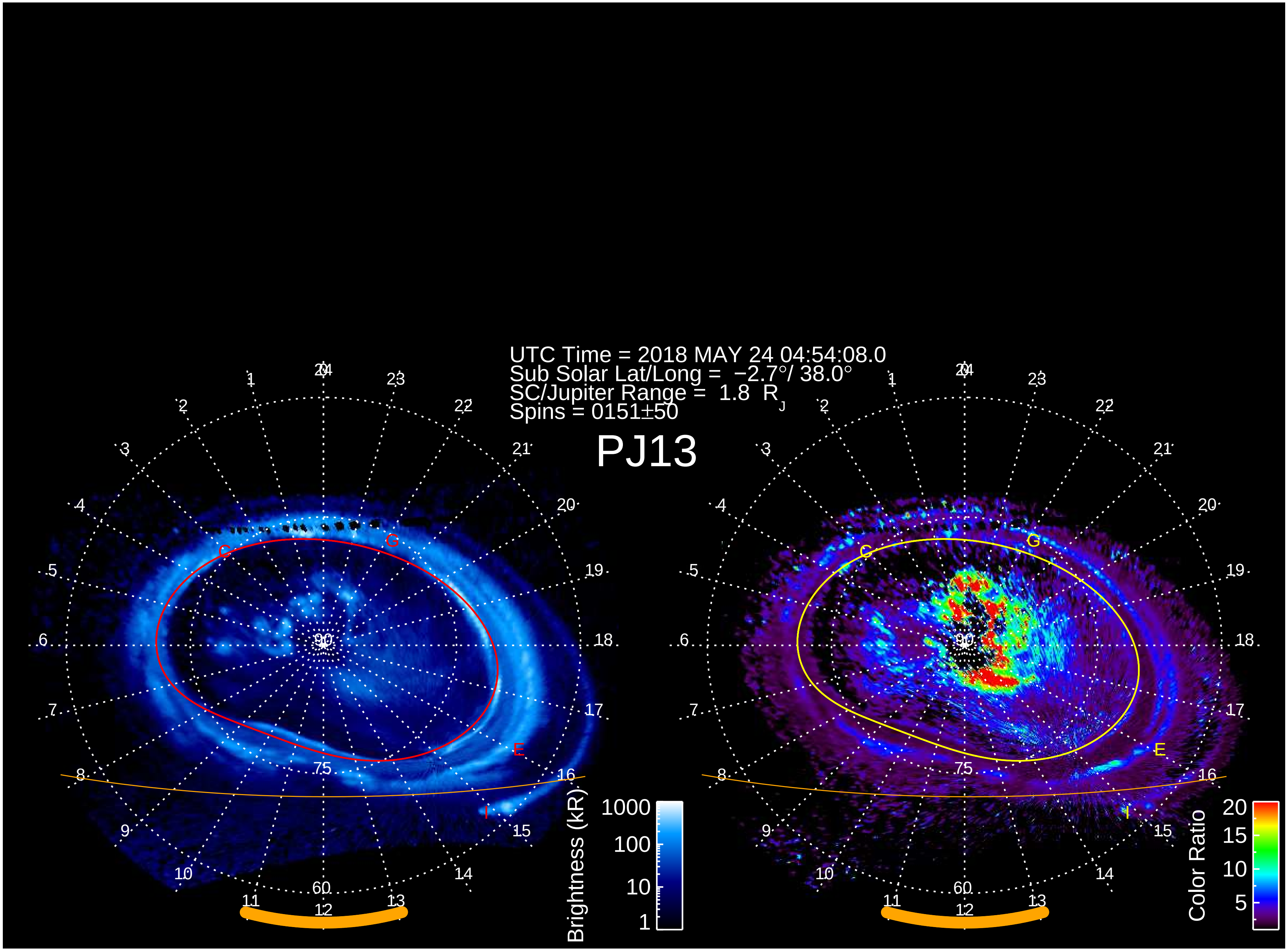
UTC Time = 2018 MAY 24 04:54:08.0
Sub Solar Lat/Long = −2.7°/ 38.0°
SC/Jupiter Range = 1.8 R$_J$
Spins = 0151±50
PJ13
Brightness (kR)
1000
100
10
1
Color Ratio
20
15
10
5

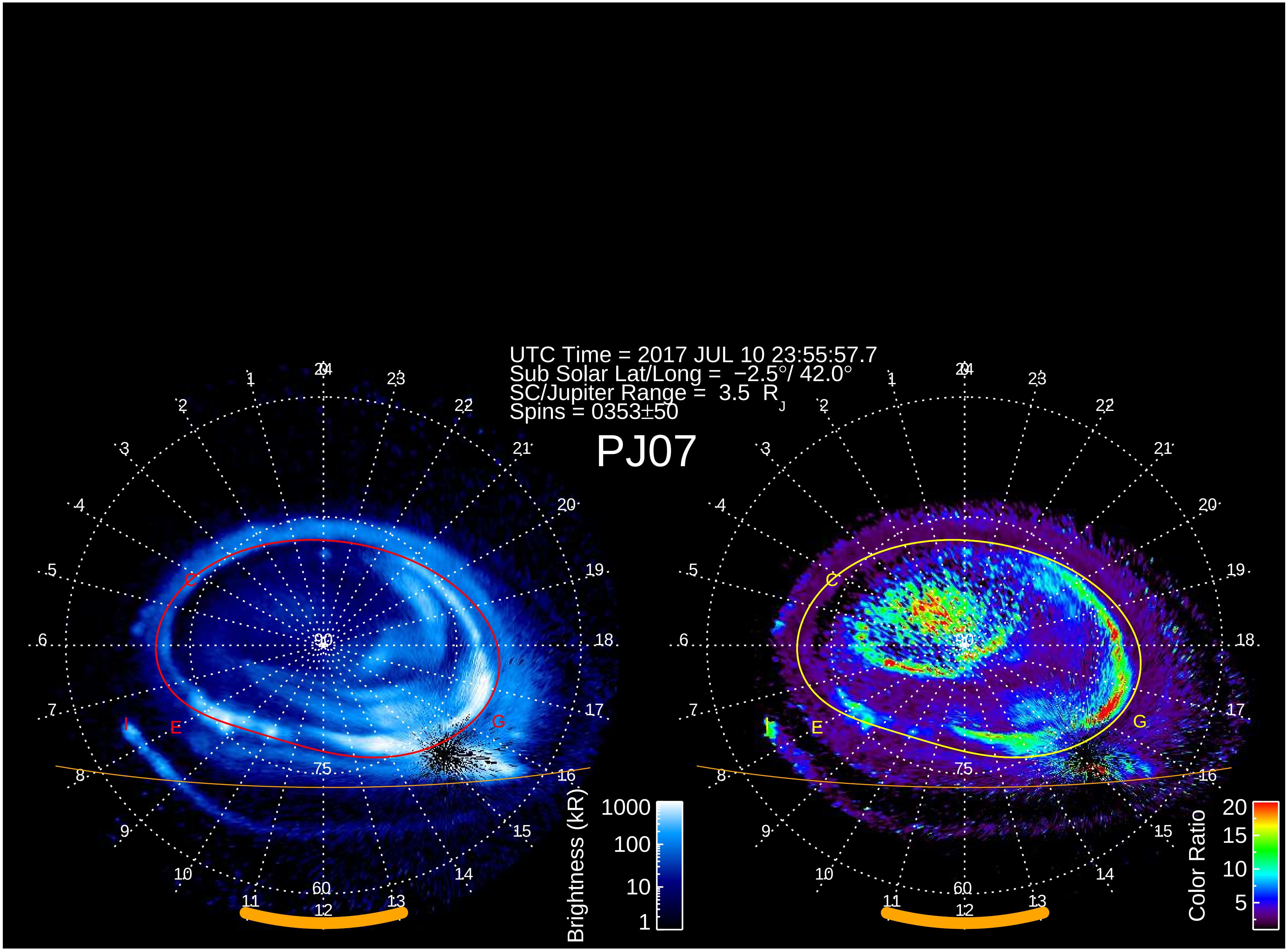

UTC Time = 2017 JUL 10 23:55:57.7
Sub Solar Lat/Long = −2.5°/ 42.0°
SC/Jupiter Range = 3.5 R_J
Spins = 0353±50
PJ07
C
E
I
G
75
60
90
Brightness (kR)
1000
100
10
1
Color Ratio
20
15
10
5

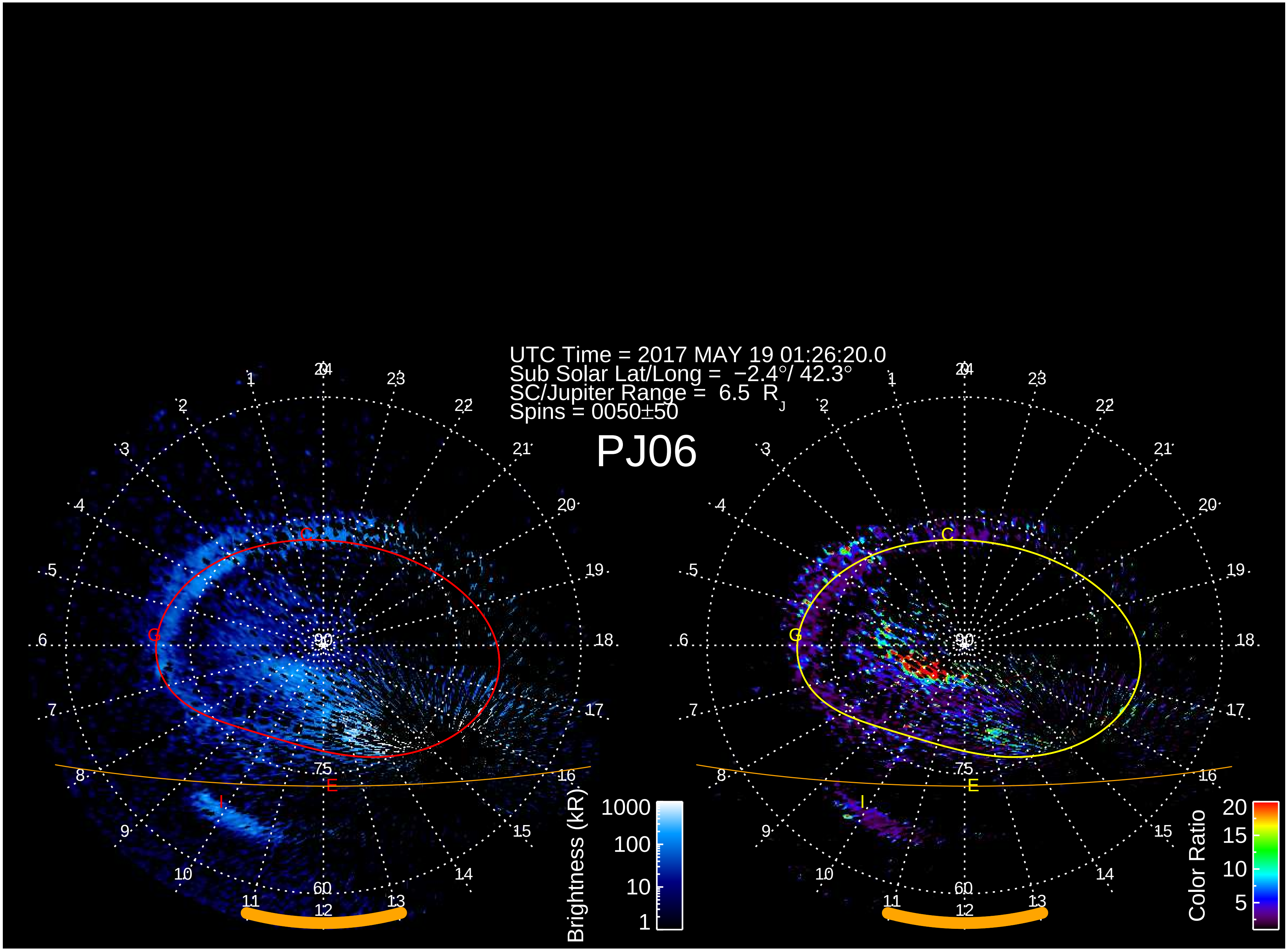
UTC Time = 2017 MAY 19 01:26:20.0
Sub Solar Lat/Long = −2.4°/ 42.3°
SC/Jupiter Range = 6.5 R_J
Spins = 0050±50
PJ06
Brightness (kR)
1000
100
10
1
Color Ratio
20
15
10
5

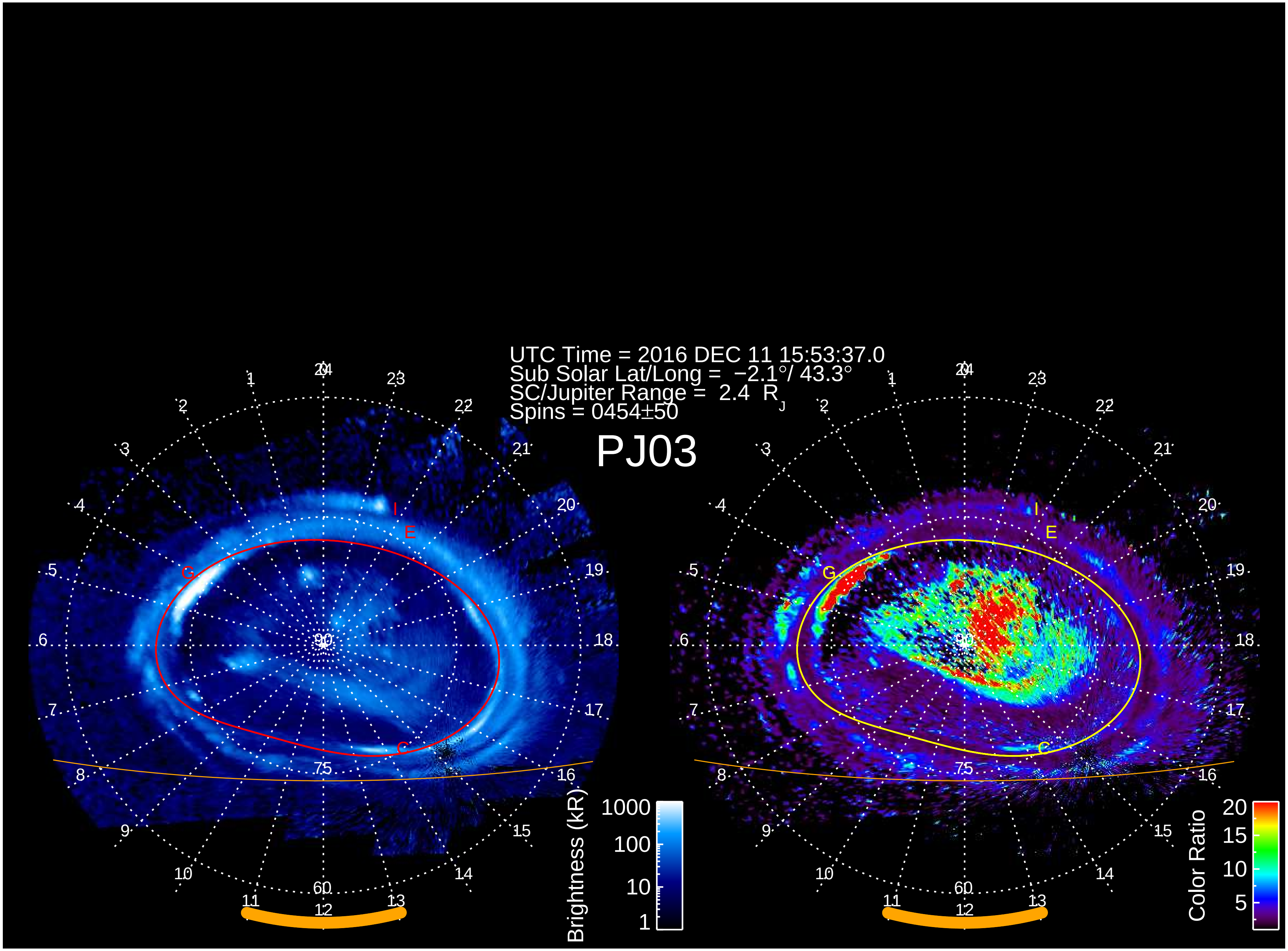
UTC Time = 2016 DEC 11 15:53:37.0
Sub Solar Lat/Long = −2.1°/ 43.3°
SC/Jupiter Range = 2.4 R_J
Spins = 0454±50
PJ03
Brightness (kR)
1000
100
10
1
Color Ratio
20
15
10
5

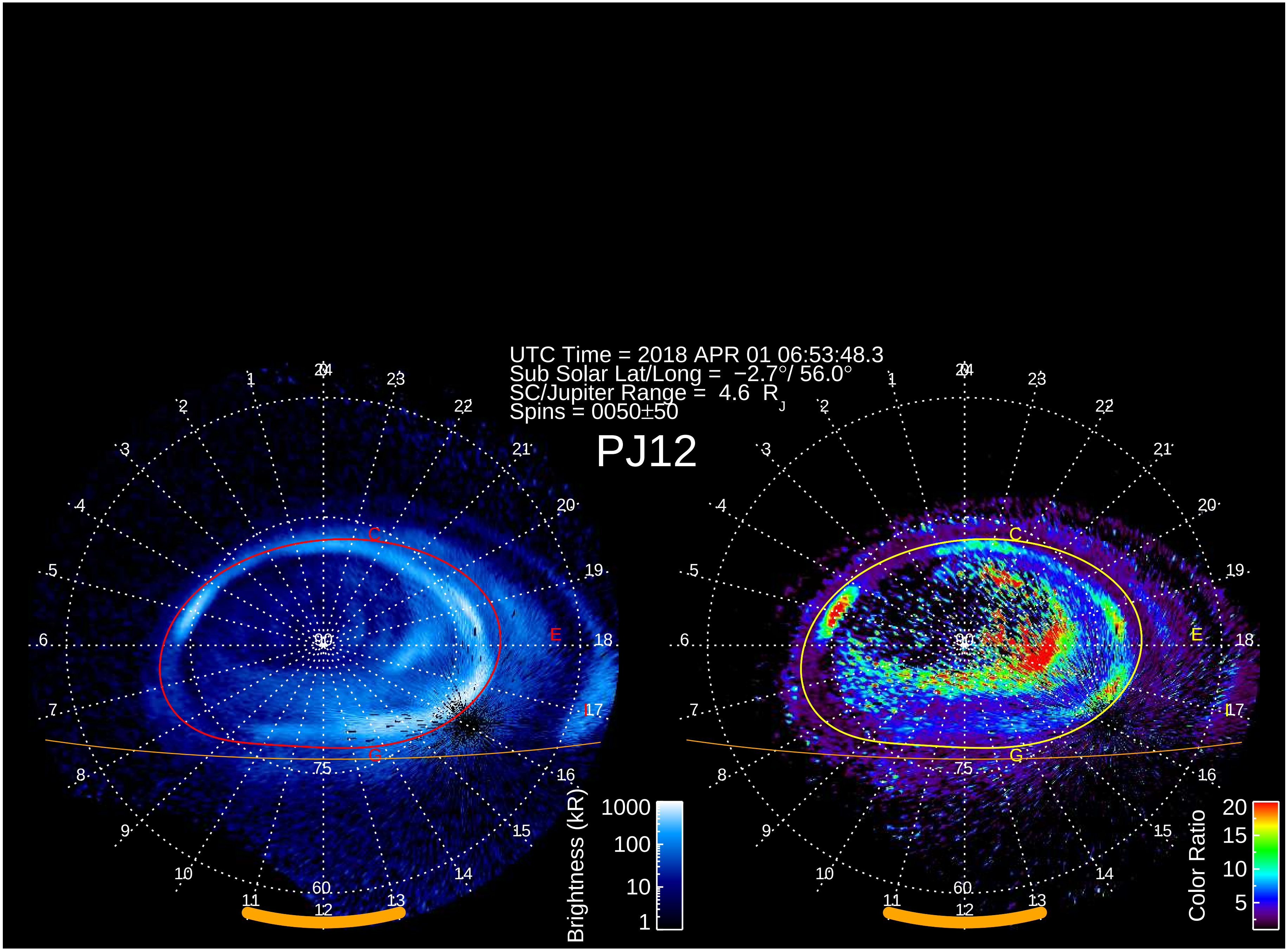

UTC Time = 2018 APR 01 06:53:48.3
Sub Solar Lat/Long = −2.7°/ 56.0°
SC/Jupiter Range = 4.6 R_J
Spins = 0050±50
PJ12
Brightness (kR)
1000
100
10
1
Color Ratio
20
15
10
5

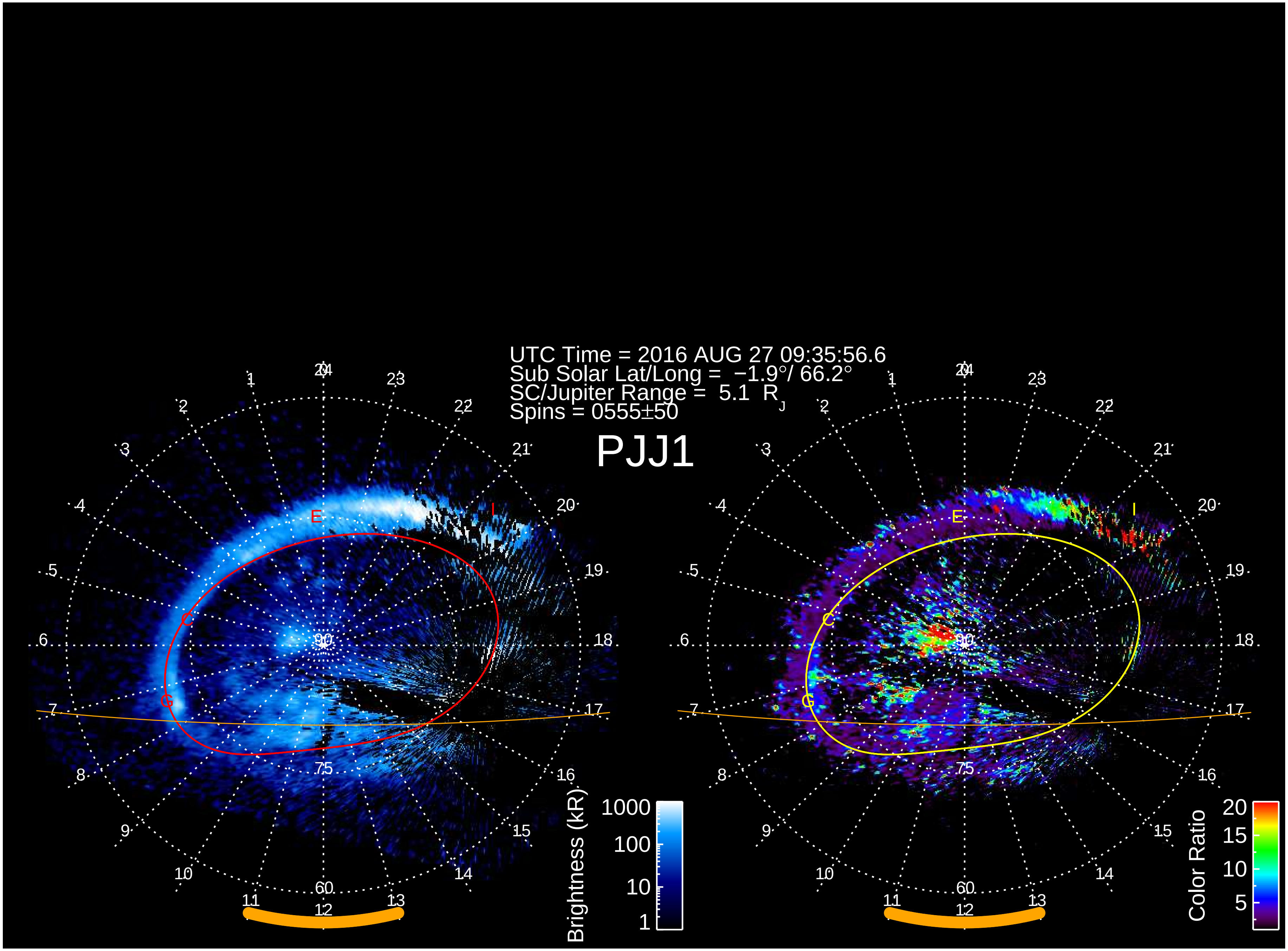
UTC Time = 2016 AUG 27 09:35:56.6
Sub Solar Lat/Long = −1.9°/ 66.2°
SC/Jupiter Range = 5.1 R_J
Spins = 0555±50
PJJ1
Brightness (kR)
1000
100
10
1
Color Ratio
20
15
10
5

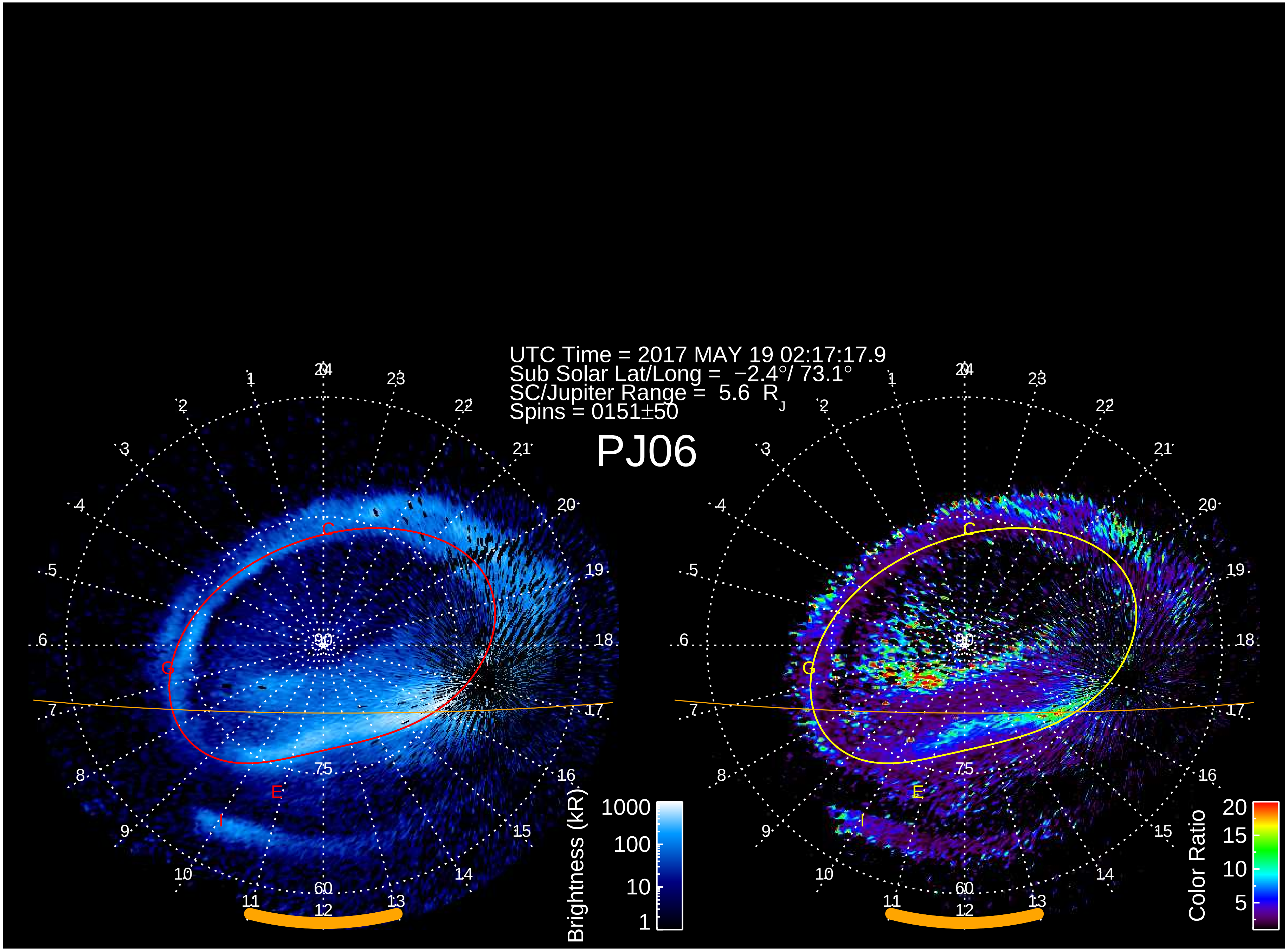

UTC Time = 2017 MAY 19 02:17:17.9
Sub Solar Lat/Long = −2.4°/ 73.1°
SC/Jupiter Range = 5.6 R$_J$
Spins = 0151±50
PJ06
Brightness (kR)
1000
100
10
1
Color Ratio
20
15
10
5

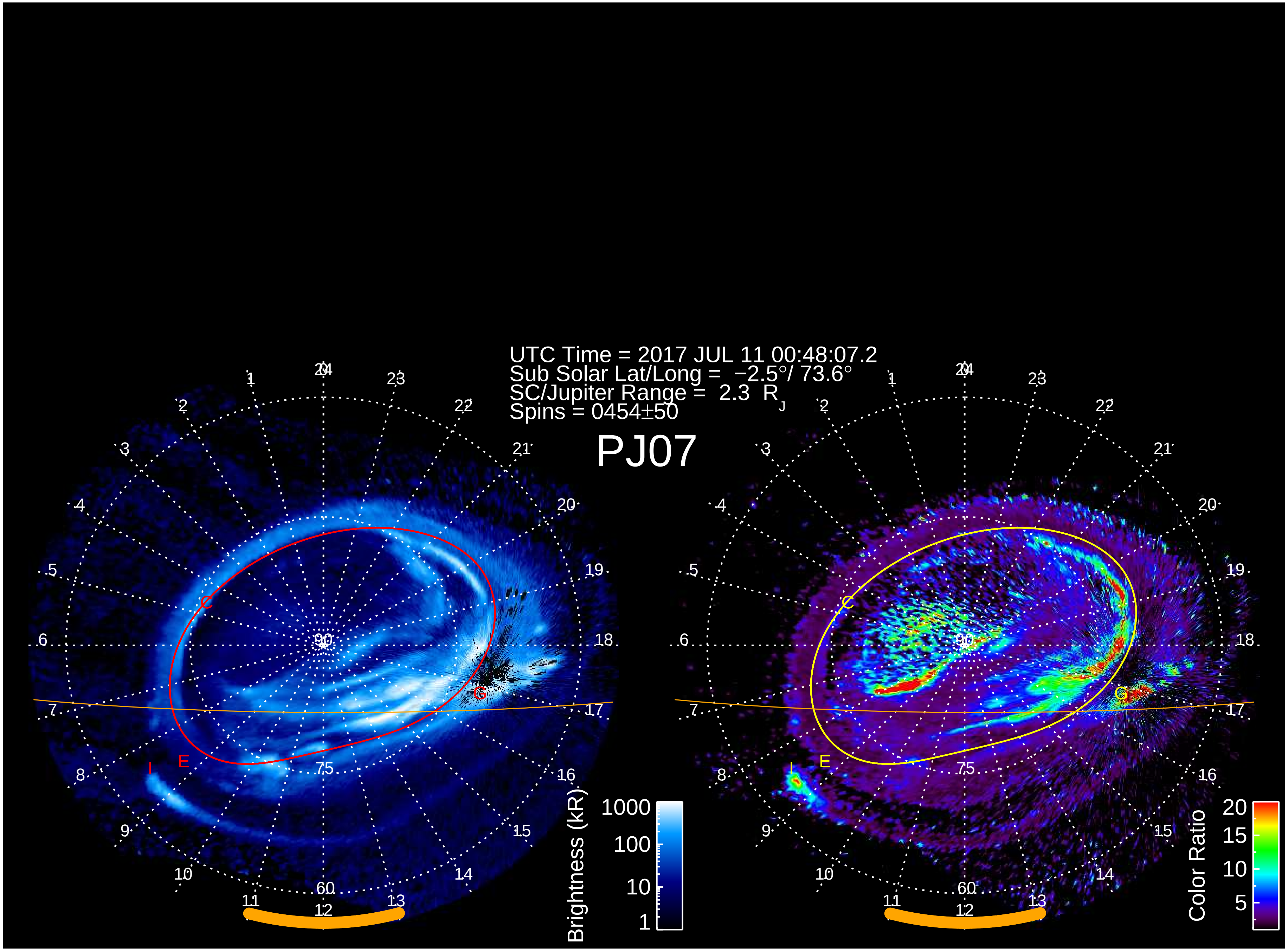
UTC Time = 2017 JUL 11 00:48:07.2
Sub Solar Lat/Long = −2.5°/ 73.6°
SC/Jupiter Range = 2.3 R_J
Spins = 0454±50
PJ07
Brightness (kR)
1000
100
10
1
Color Ratio
20
15
10
5
C
E
G
I
90
75
60

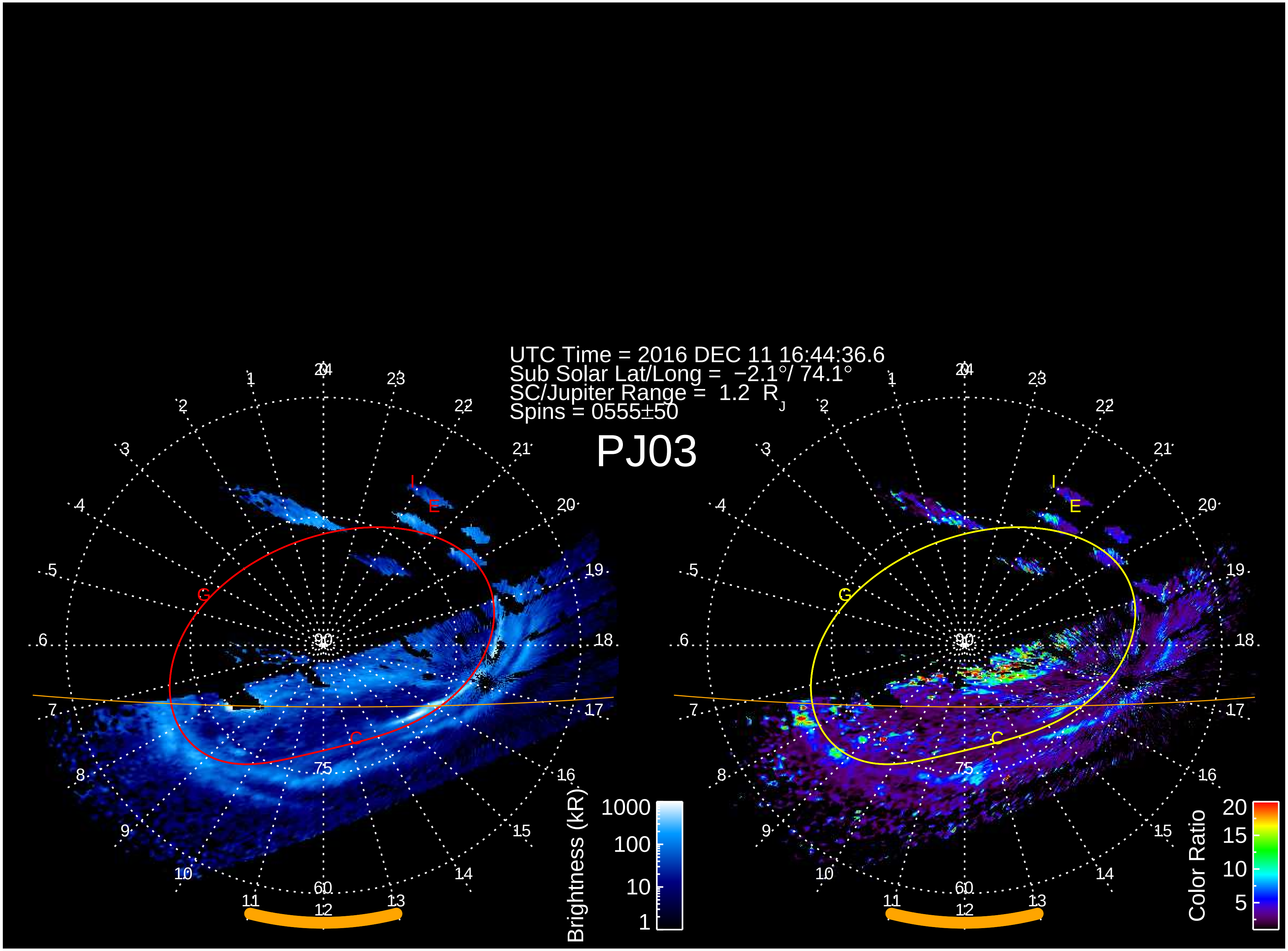

UTC Time = 2016 DEC 11 16:44:36.6
Sub Solar Lat/Long = −2.1°/ 74.1°
SC/Jupiter Range = 1.2 R_J
Spins = 0555±50
PJ03
Brightness (kR)
1000
100
10
1
Color Ratio
20
15
10
5

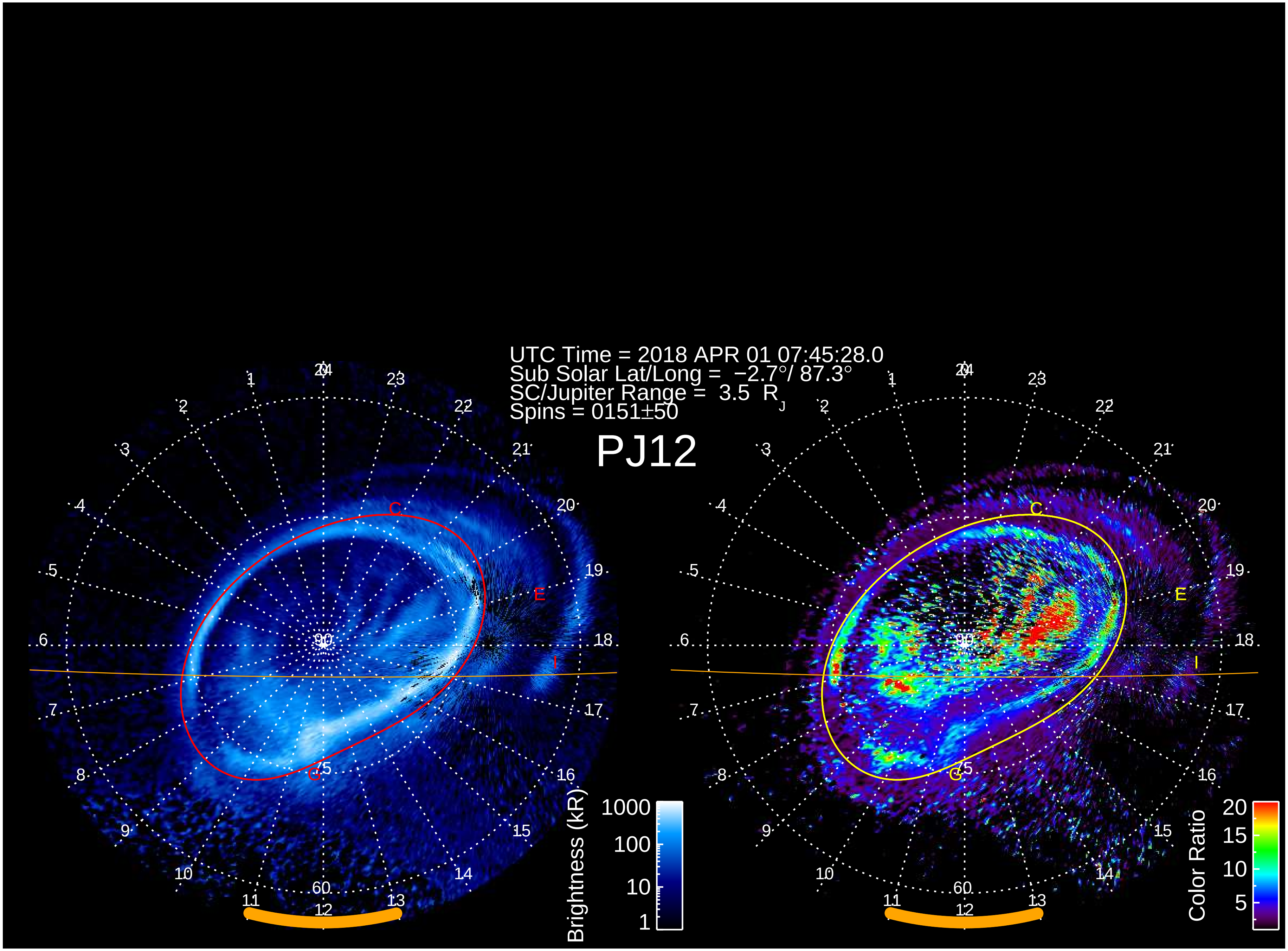
UTC Time = 2018 APR 01 07:45:28.0
Sub Solar Lat/Long = −2.7°/ 87.3°
SC/Jupiter Range = 3.5 R$_J$
Spins = 0151±50
PJ12
Brightness (kR)
1000
100
10
1
Color Ratio
20
15
10
5

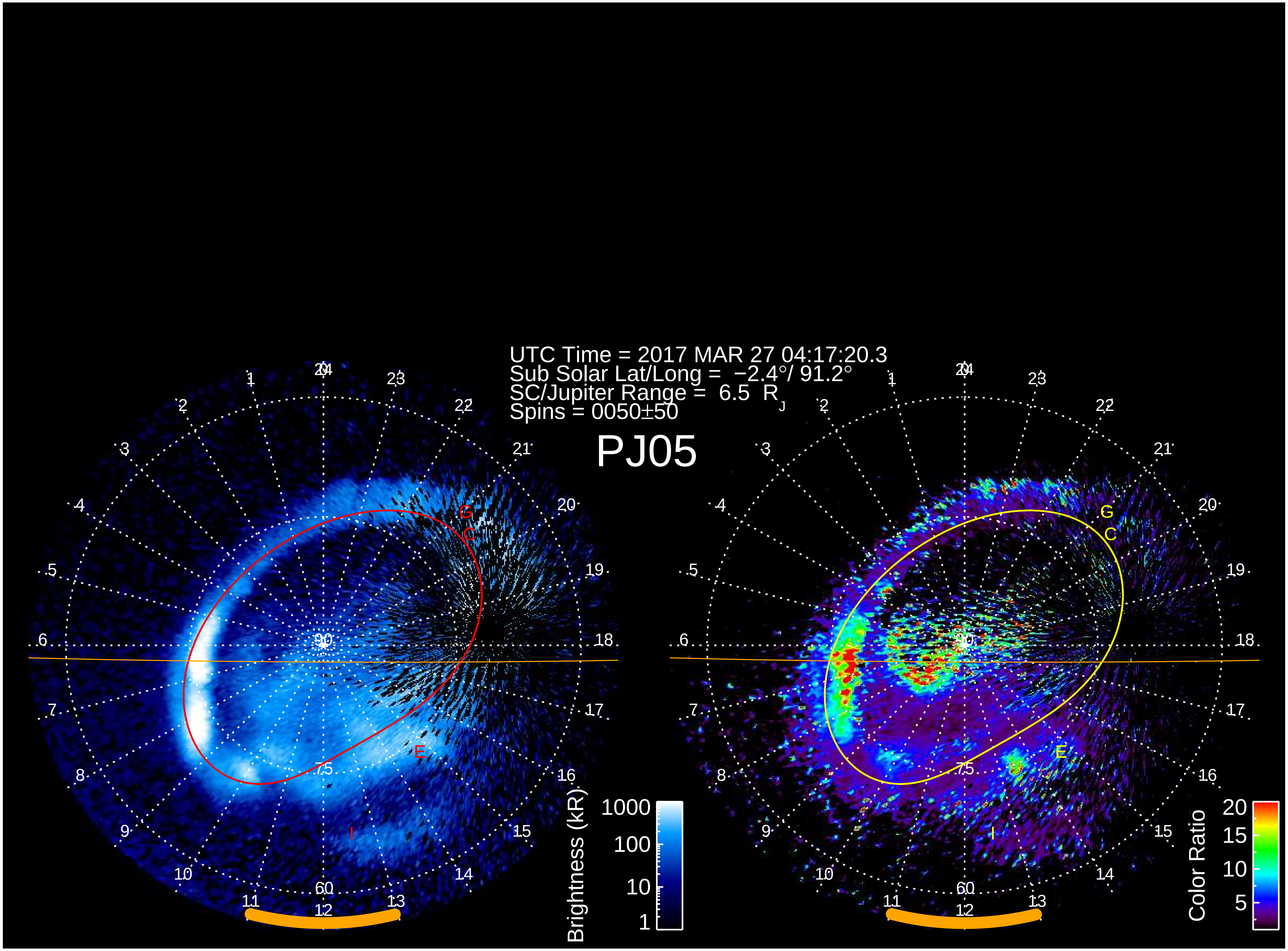

UTC Time = 2017 MAR 27 04:17:20.3
Sub Solar Lat/Long = −2.4°/ 91.2°
SC/Jupiter Range = 6.5 R_J
Spins = 0050±50
PJ05
Brightness (kR)
1000
100
10
1
Color Ratio
20
15
10
5

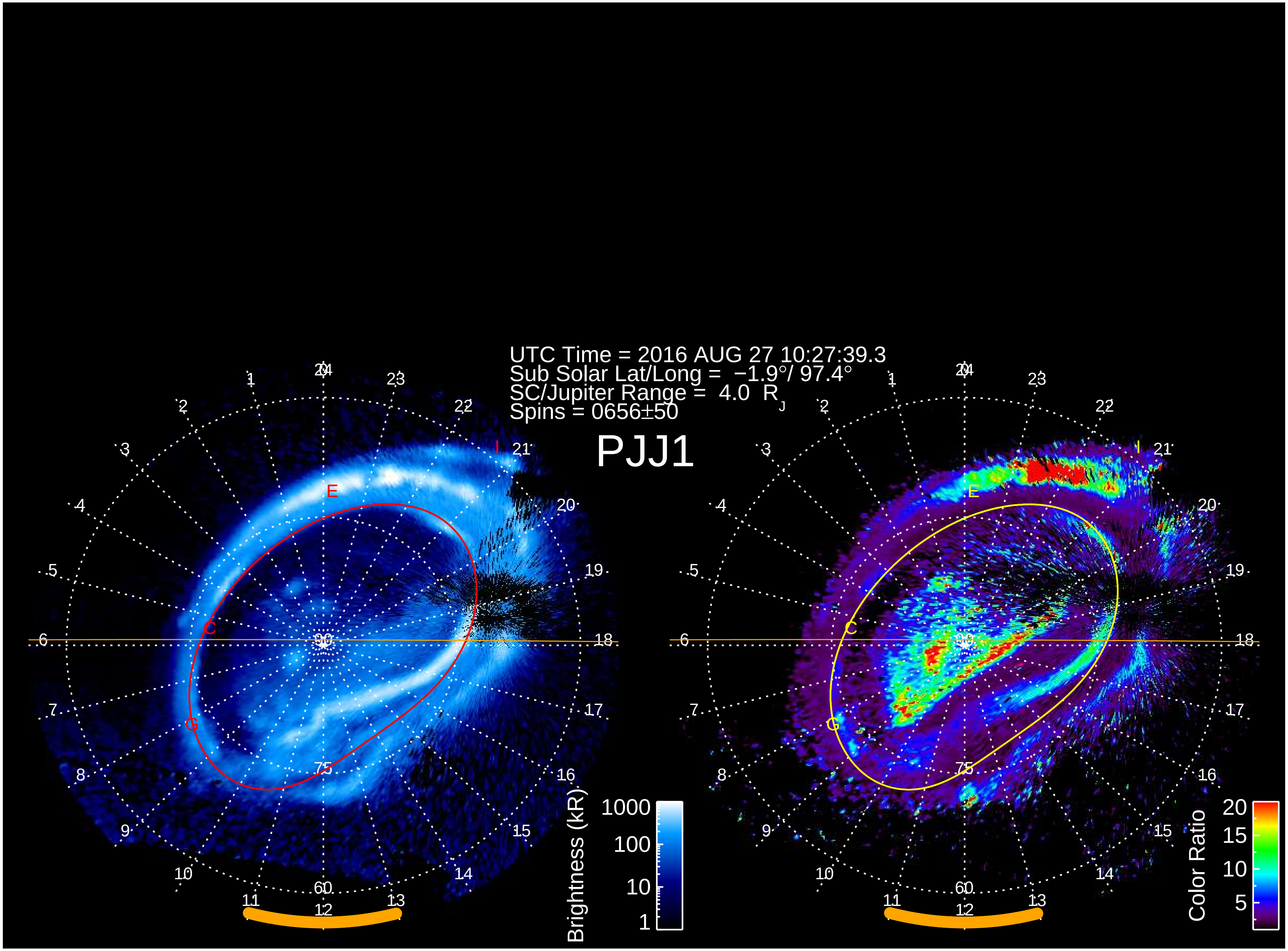
UTC Time = 2016 AUG 27 10:27:39.3
Sub Solar Lat/Long = −1.9°/ 97.4°
SC/Jupiter Range = 4.0 R_J
Spins = 0656±50
PJJ1
Brightness (kR)
1000
100
10
1
Color Ratio
20
15
10
5
E
C
G
I
60
75
90

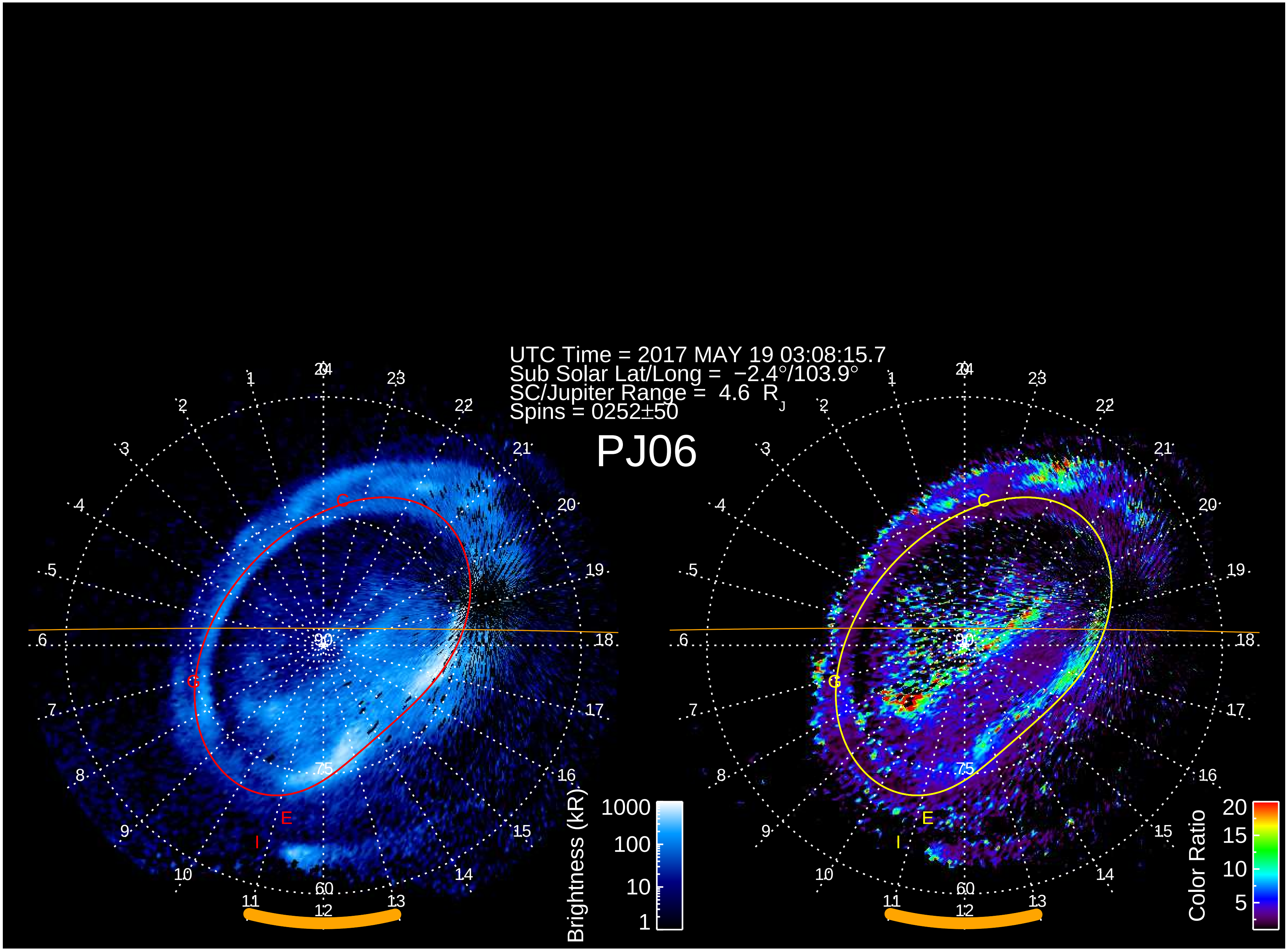
UTC Time = 2017 MAY 19 03:08:15.7
Sub Solar Lat/Long = −2.4°/103.9°
SC/Jupiter Range = 4.6 R_J
Spins = 0252±50
PJ06
Brightness (kR)
1000
100
10
1
Color Ratio
20
15
10
5

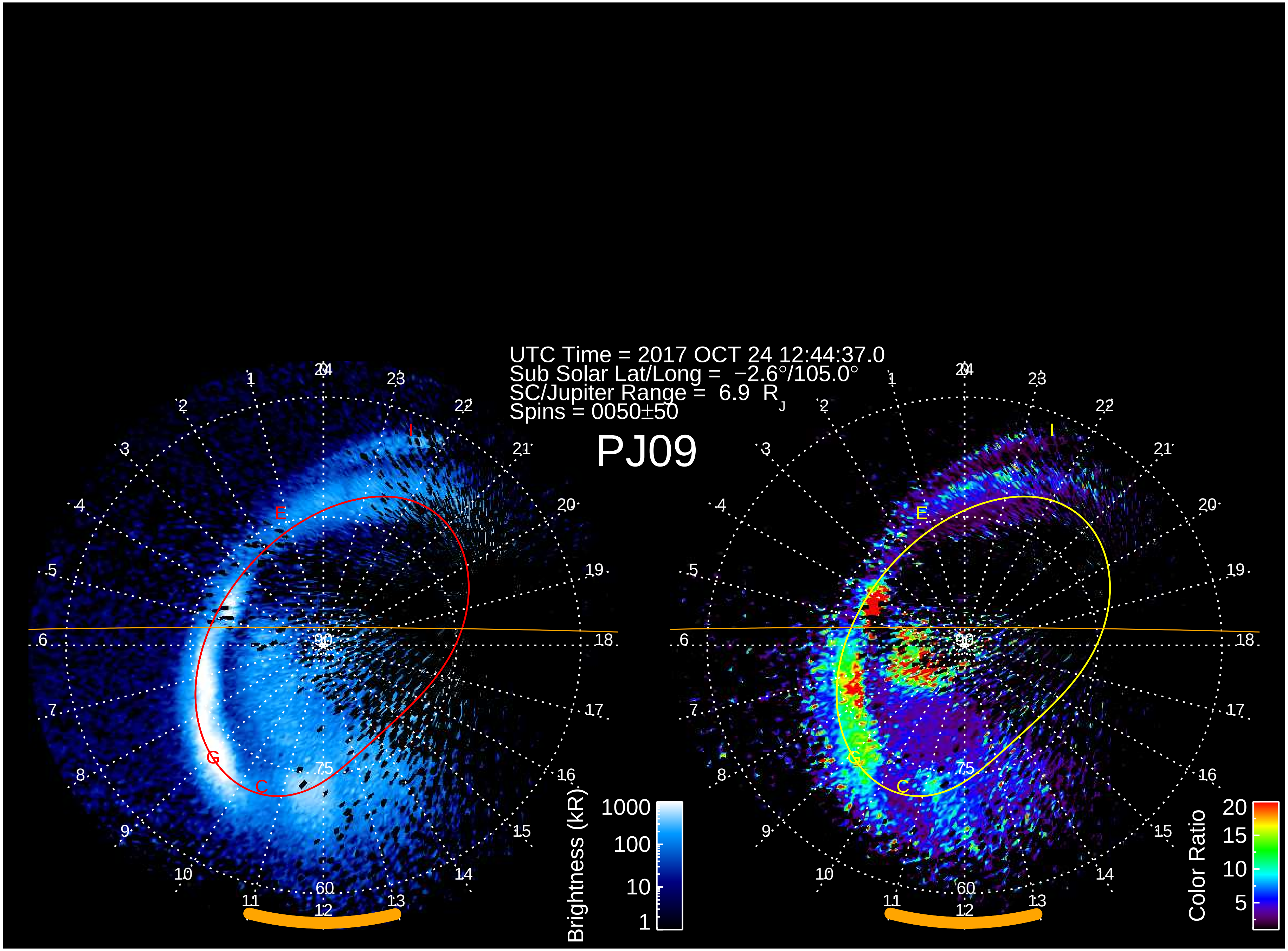

UTC Time = 2017 OCT 24 12:44:37.0
Sub Solar Lat/Long = −2.6°/105.0°
SC/Jupiter Range = 6.9 R_J
Spins = 0050±50
PJ09
Brightness (kR)
1000
100
10
1
Color Ratio
20
15
10
5

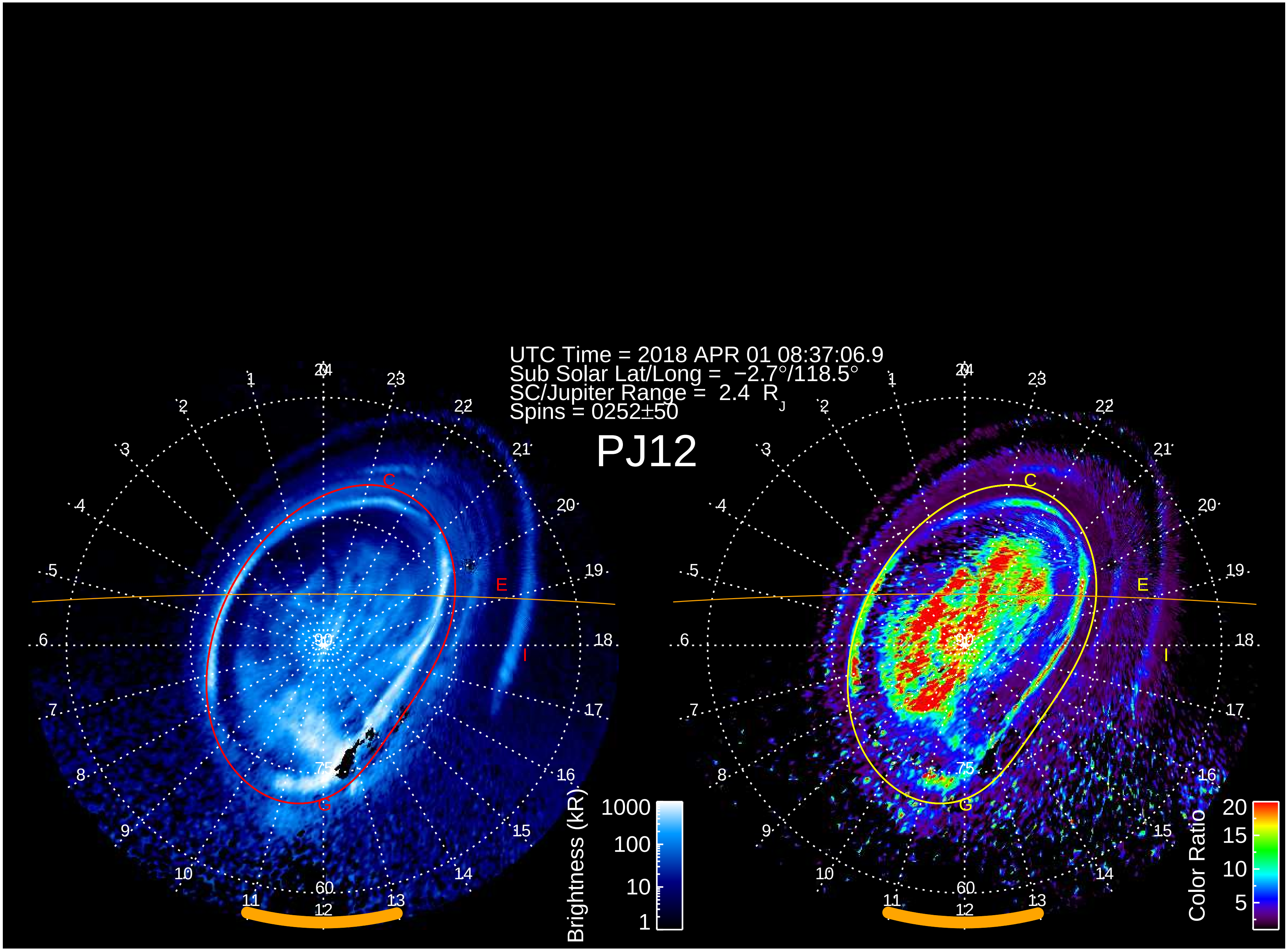
UTC Time = 2018 APR 01 08:37:06.9
Sub Solar Lat/Long = −2.7°/118.5°
SC/Jupiter Range = 2.4 R
J
Spins = 0252±50
PJ12
Brightness (kR)
1000
100
10
1
Color Ratio
20
15
10
5
C
E
I
G
75
60
90

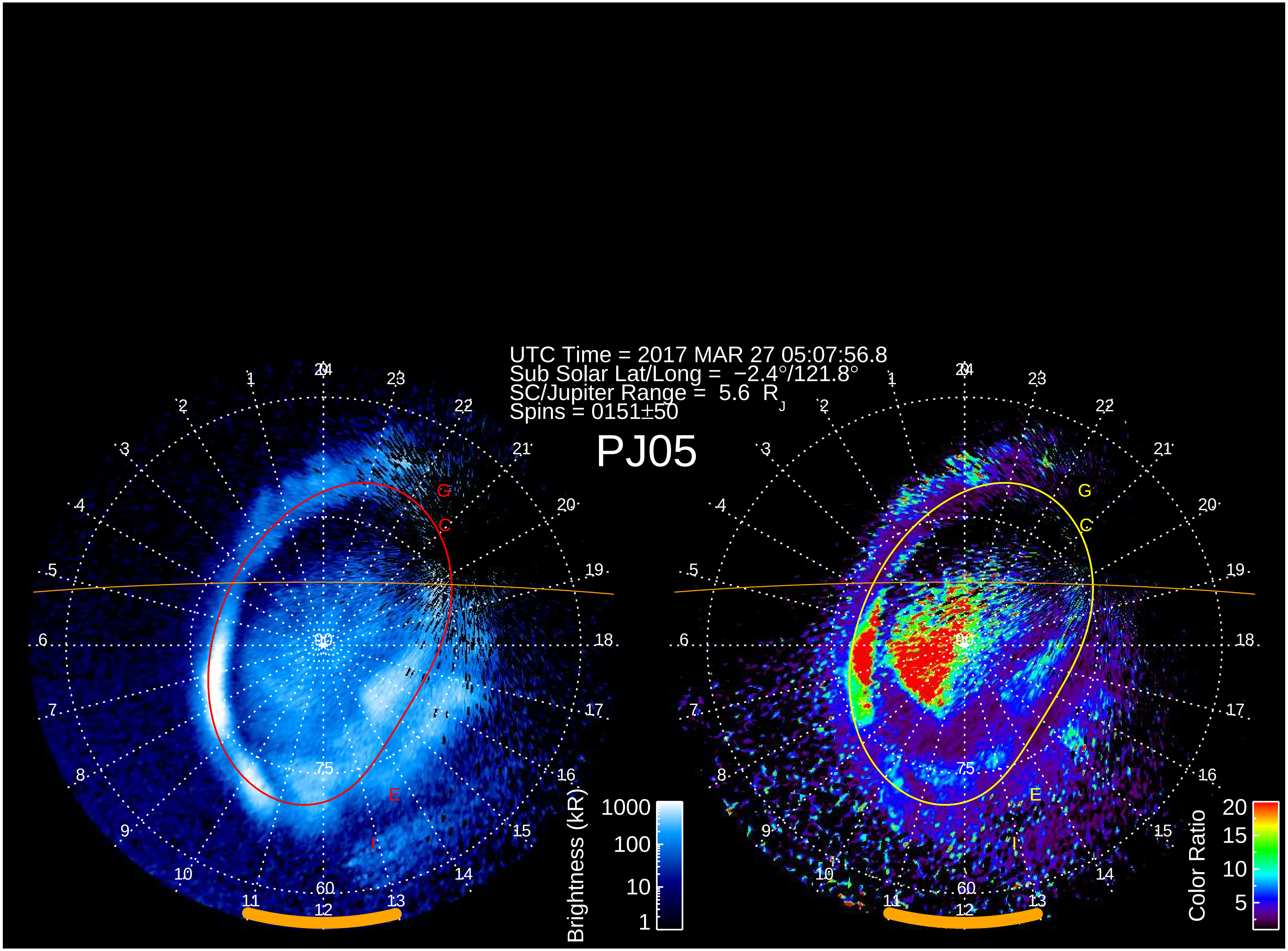

UTC Time = 2017 MAR 27 05:07:56.8
Sub Solar Lat/Long = −2.4°/121.8°
SC/Jupiter Range = 5.6 R$_J$
Spins = 0151±50
PJ05
Brightness (kR)
1000
100
10
1
Color Ratio
20
15
10
5
G
C
E
I

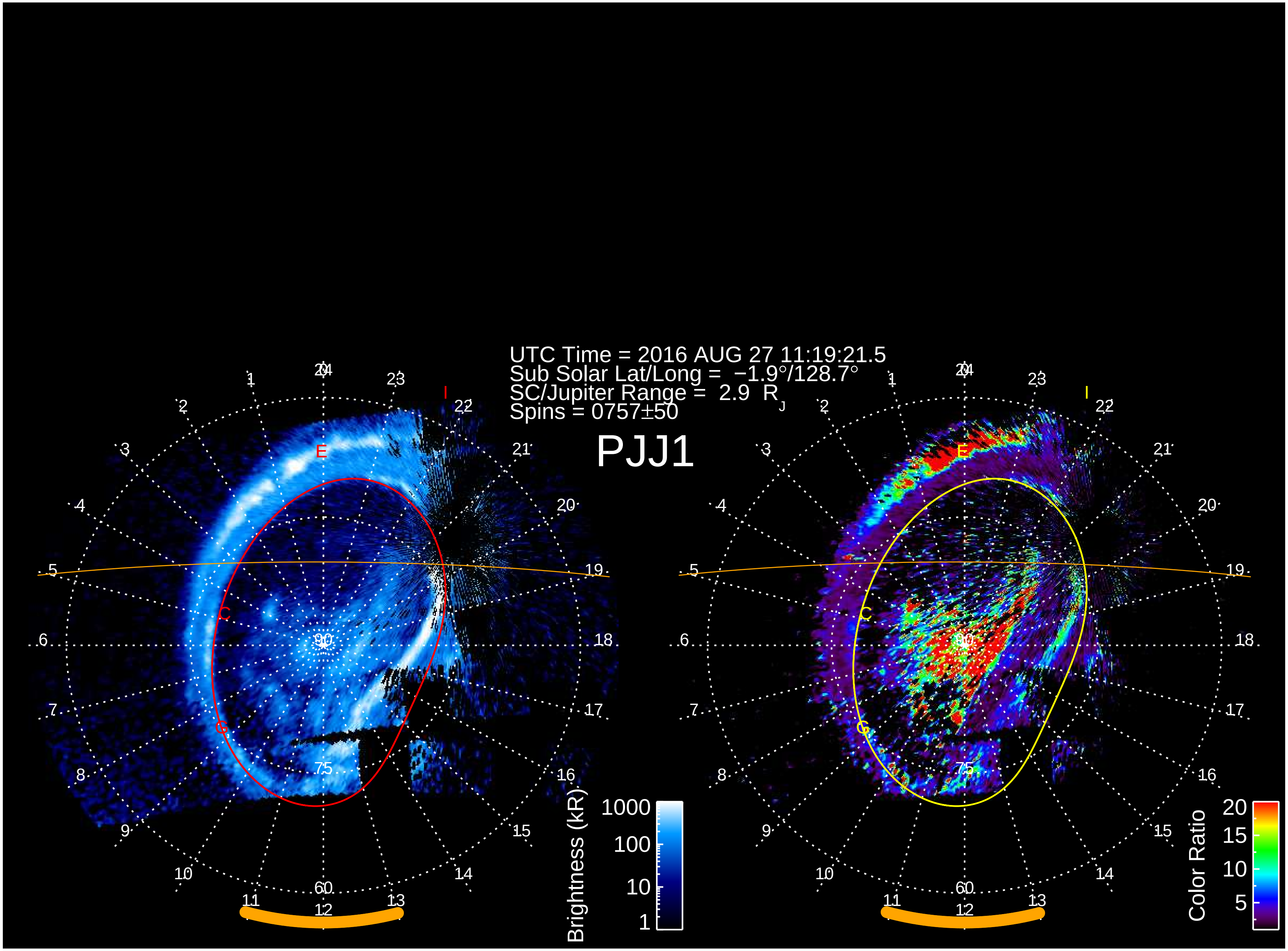

UTC Time = 2016 AUG 27 11:19:21.5
Sub Solar Lat/Long = −1.9°/128.7°
SC/Jupiter Range = 2.9 R
J
Spins = 0757±50
PJJ1
Brightness (kR)
1000
100
10
1
Color Ratio
20
15
10
5

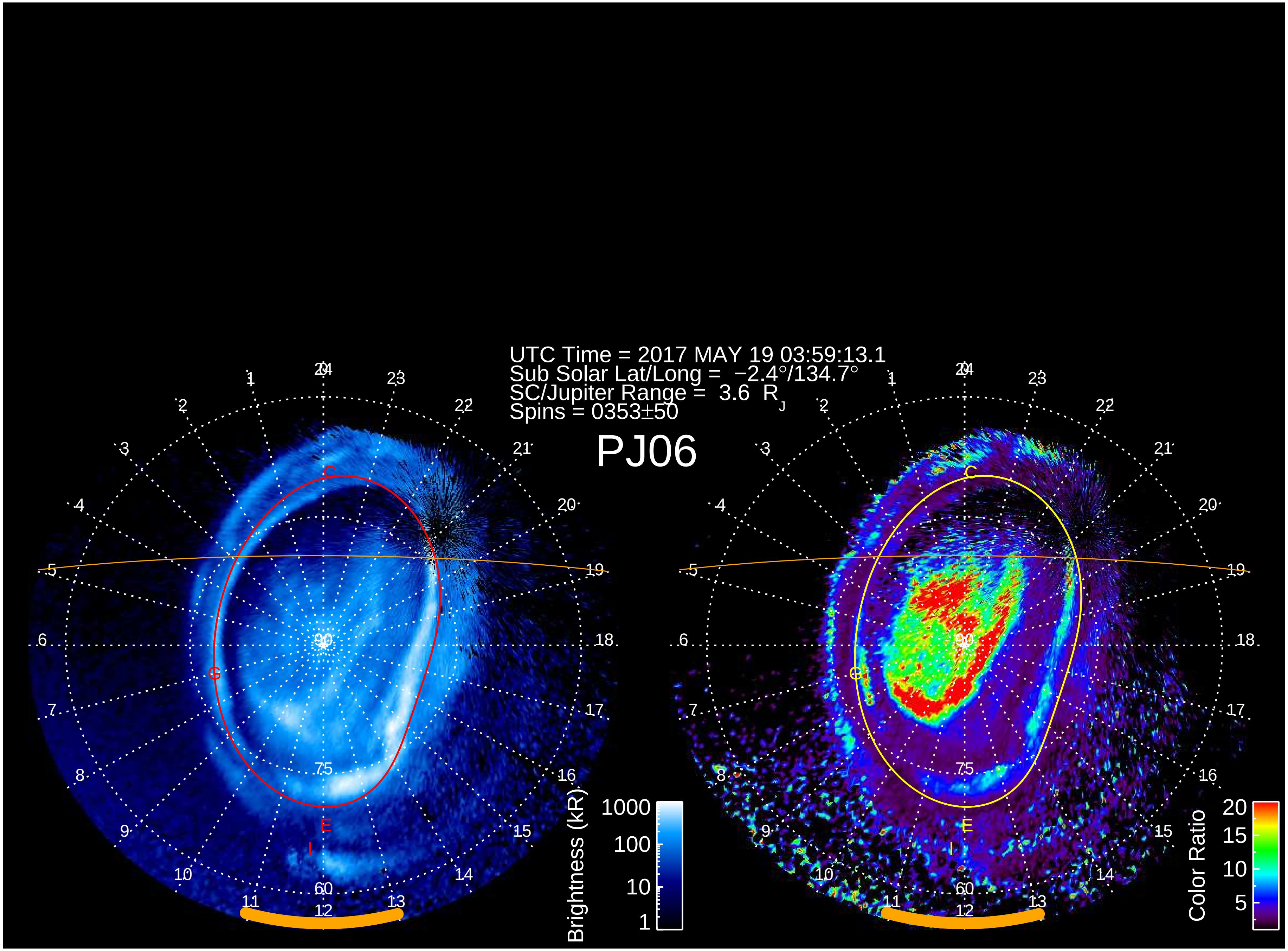
UTC Time = 2017 MAY 19 03:59:13.1
Sub Solar Lat/Long = −2.4°/134.7°
SC/Jupiter Range = 3.6 R$_J$
Spins = 0353±50
PJ06
Brightness (kR)
1000
100
10
1
Color Ratio
20
15
10
5

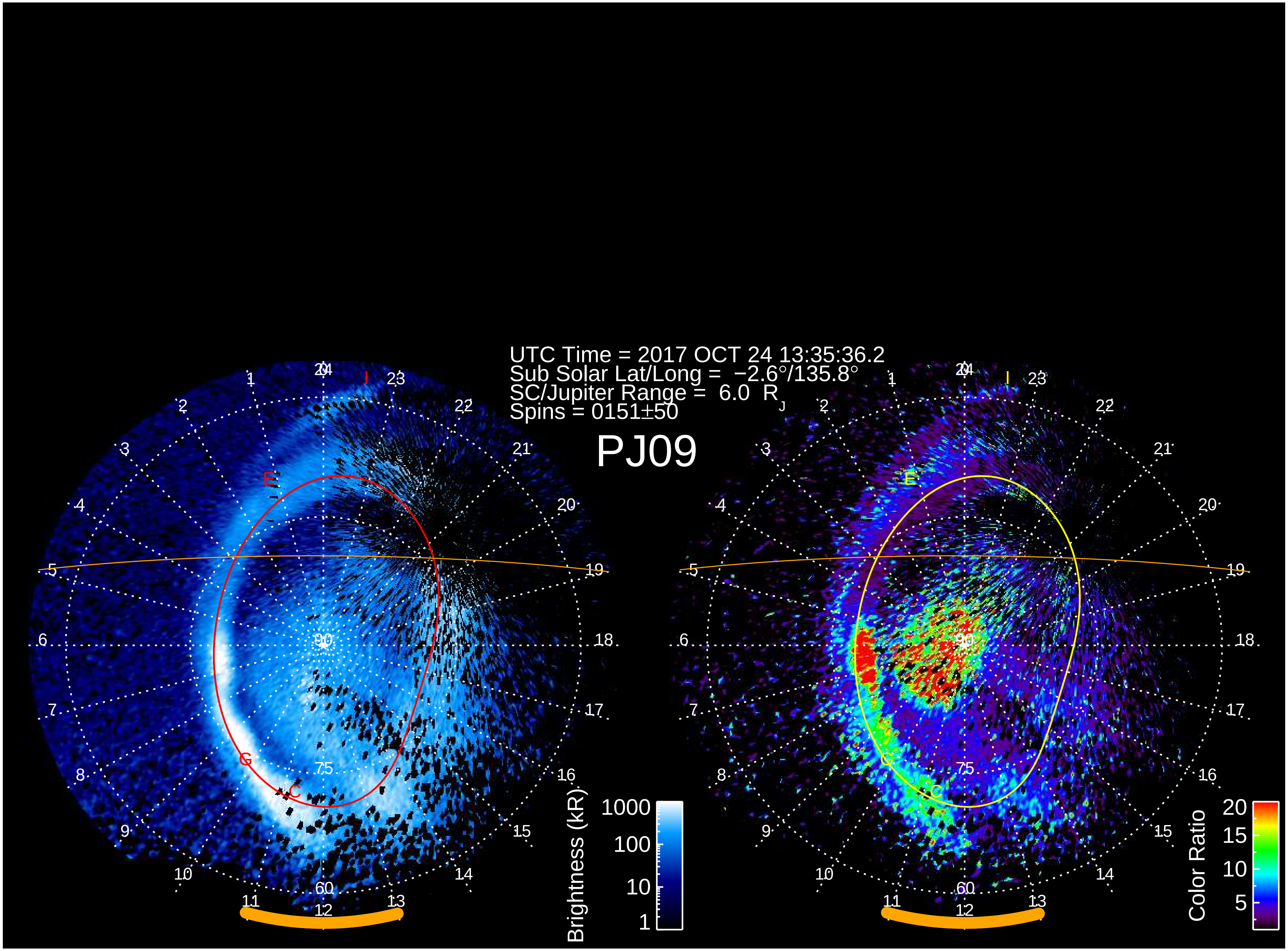

UTC Time = 2017 OCT 24 13:35:36.2
Sub Solar Lat/Long = −2.6°/135.8°
SC/Jupiter Range = 6.0 R_J
Spins = 0151±50
PJ09
Brightness (kR)
1000
100
10
1
Color Ratio
20
15
10
5

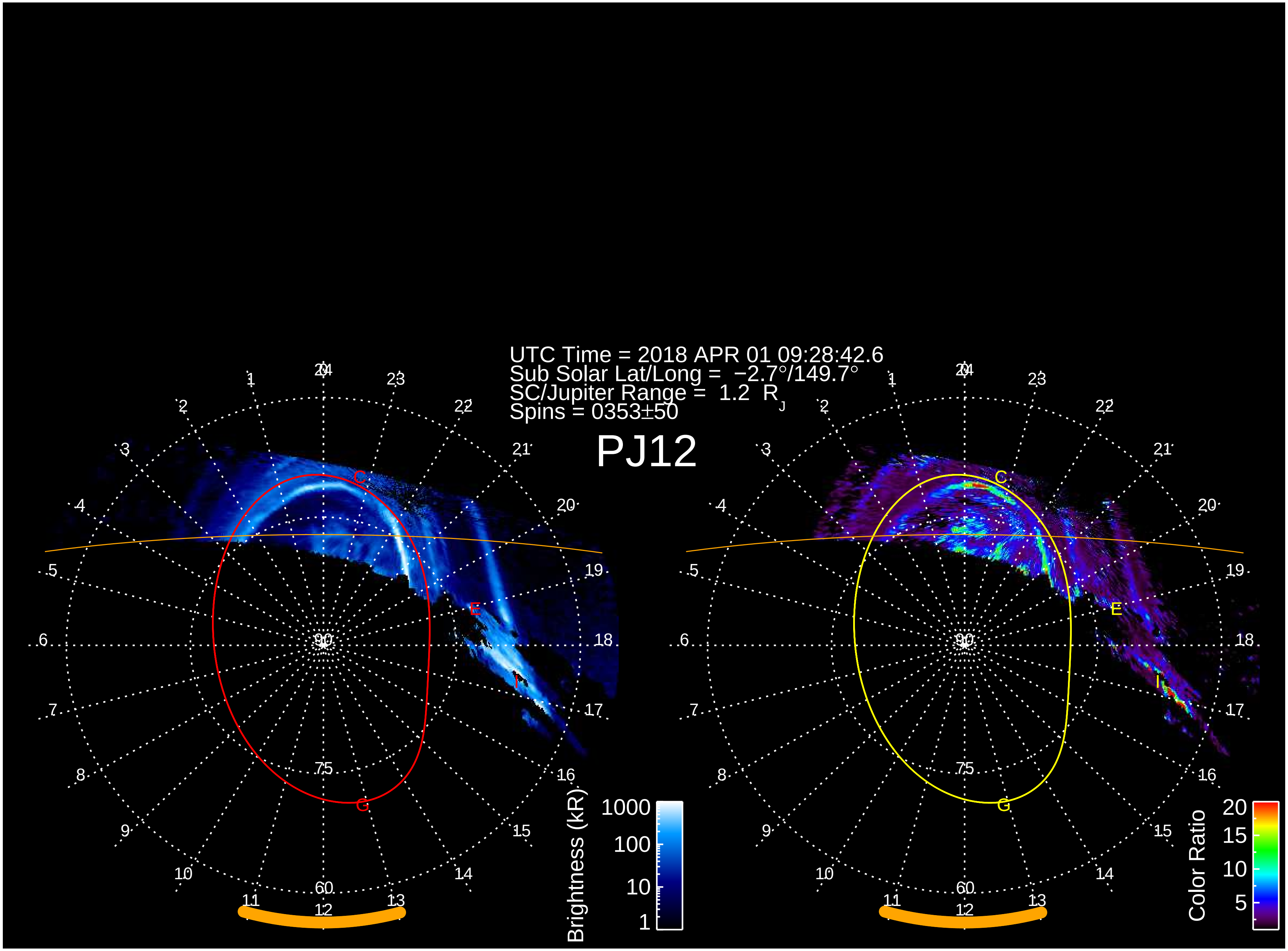

UTC Time = 2018 APR 01 09:28:42.6
Sub Solar Lat/Long = −2.7°/149.7°
SC/Jupiter Range = 1.2 R_J
Spins = 0353±50
PJ12
Brightness (kR)
1000
100
10
1
Color Ratio
20
15
10
5

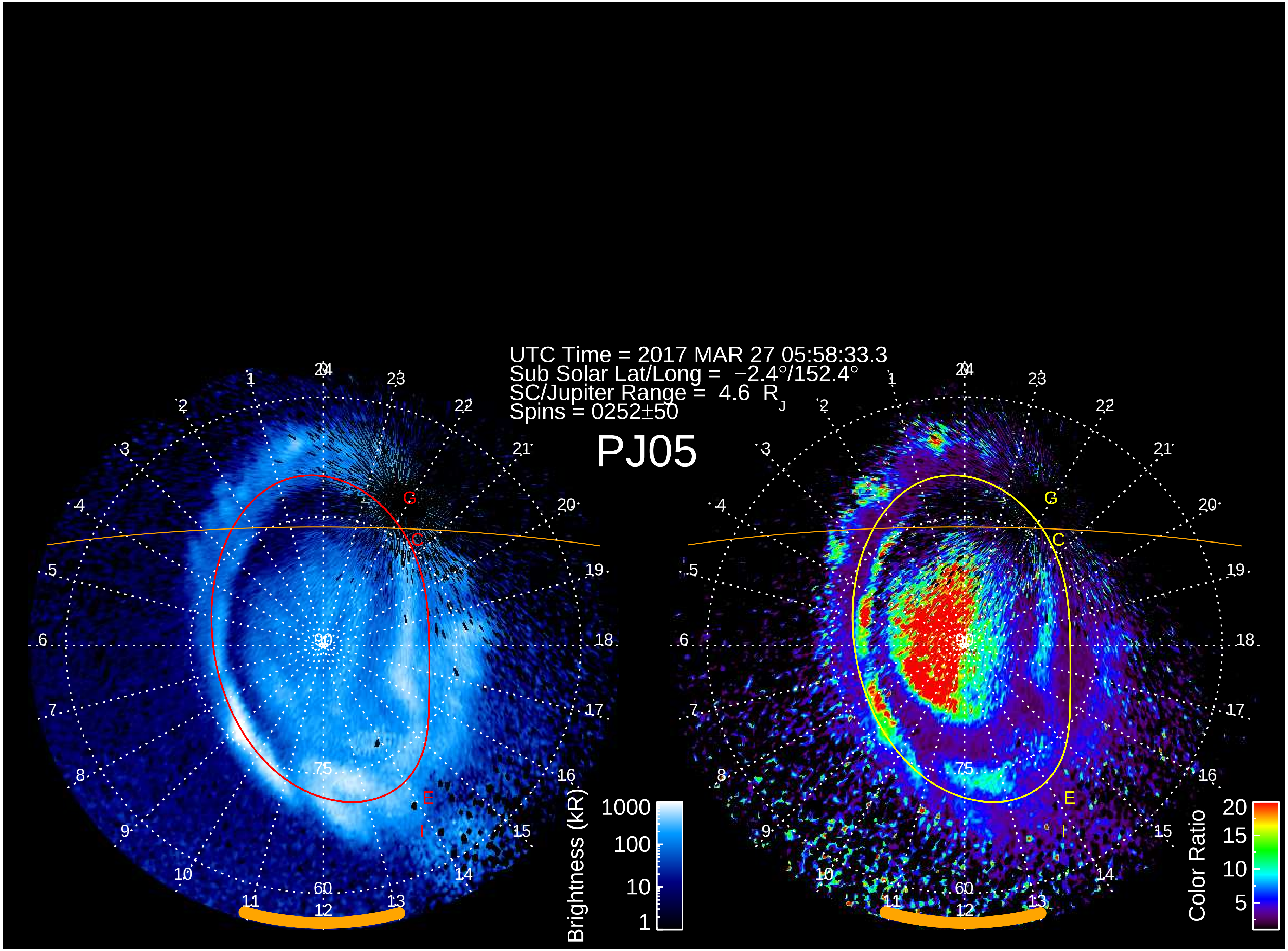
UTC Time = 2017 MAR 27 05:58:33.3
Sub Solar Lat/Long = −2.4°/152.4°
SC/Jupiter Range = 4.6 R
Spins = 0252±50
PJ05
Brightness (kR)
1000
100
10
1
Color Ratio
20
15
10
5
G
C
E
I
75
60
90

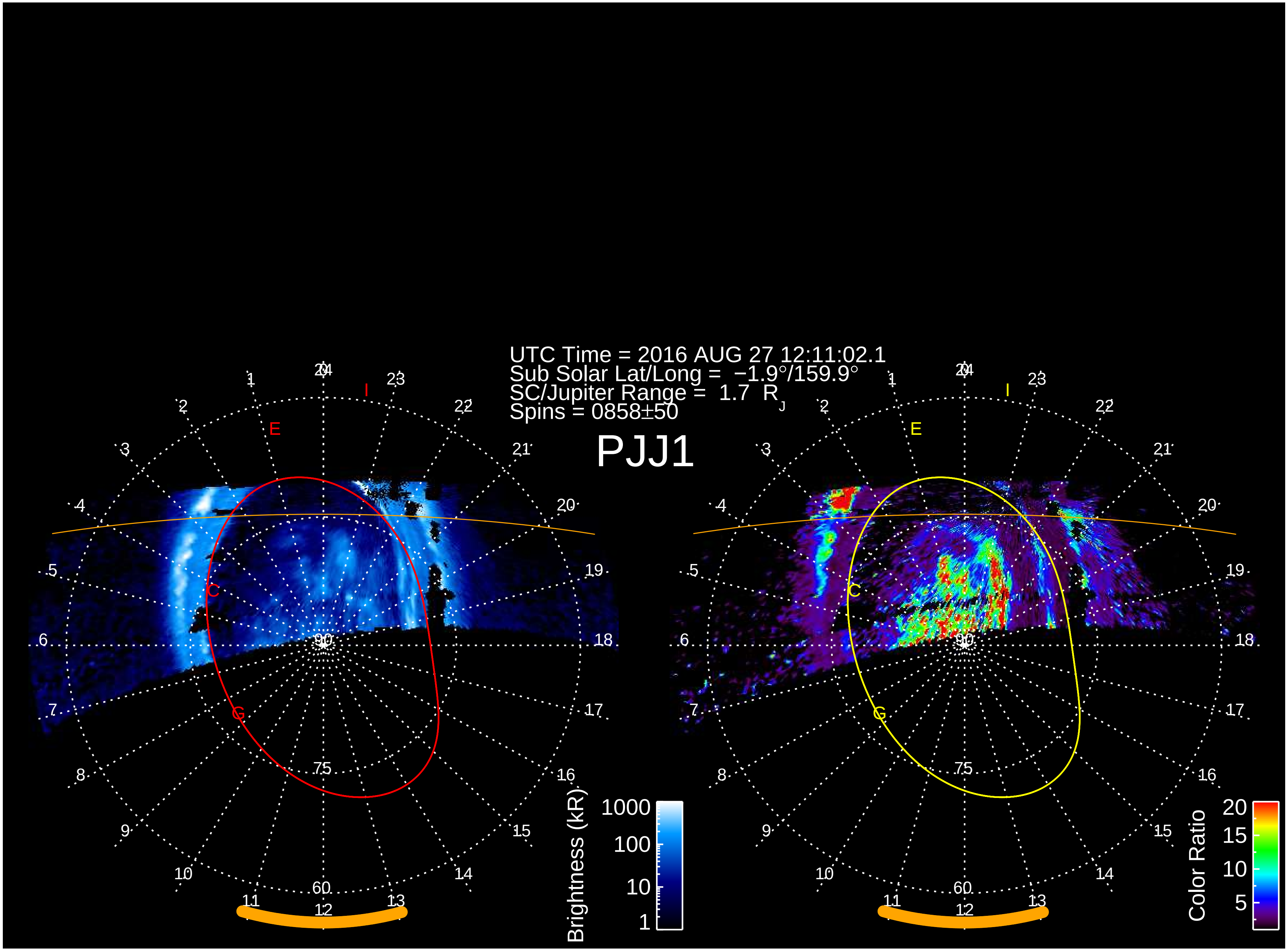
UTC Time = 2016 AUG 27 12:11:02.1
Sub Solar Lat/Long = −1.9°/159.9°
SC/Jupiter Range = 1.7 R_J
Spins = 0858±50
PJJ1
Brightness (kR)
1000
100
10
1
Color Ratio
20
15
10
5

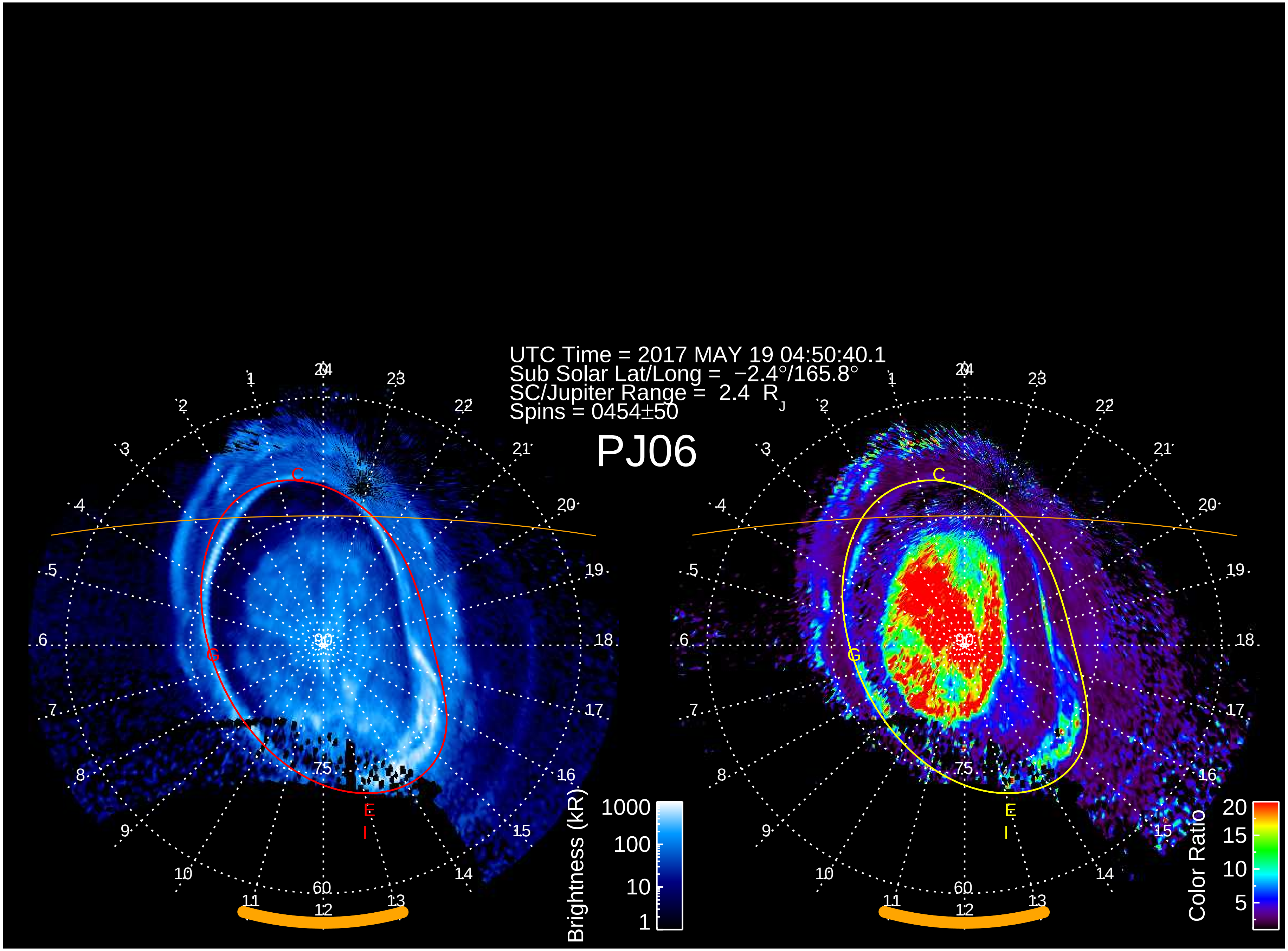

UTC Time = 2017 MAY 19 04:50:40.1
Sub Solar Lat/Long = −2.4°/165.8°
SC/Jupiter Range = 2.4 R$_J$
Spins = 0454±50
PJ06
Brightness (kR)
1000
100
10
1
Color Ratio
20
15
10
5

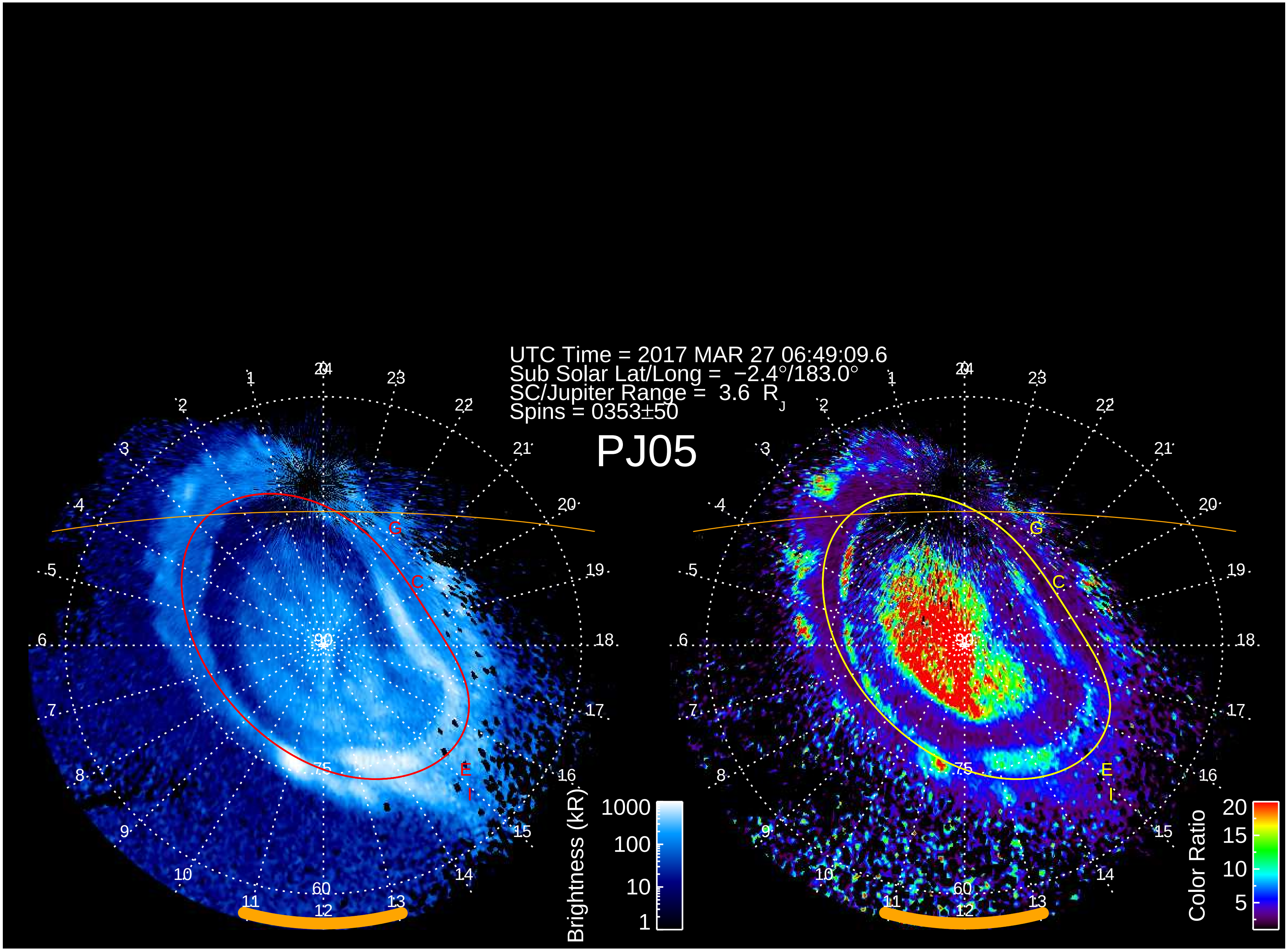
UTC Time = 2017 MAR 27 06:49:09.6
Sub Solar Lat/Long = −2.4°/183.0°
SC/Jupiter Range = 3.6 R$_J$
Spins = 0353±50
PJ05
Brightness (kR)
1000
100
10
1
Color Ratio
20
15
10
5

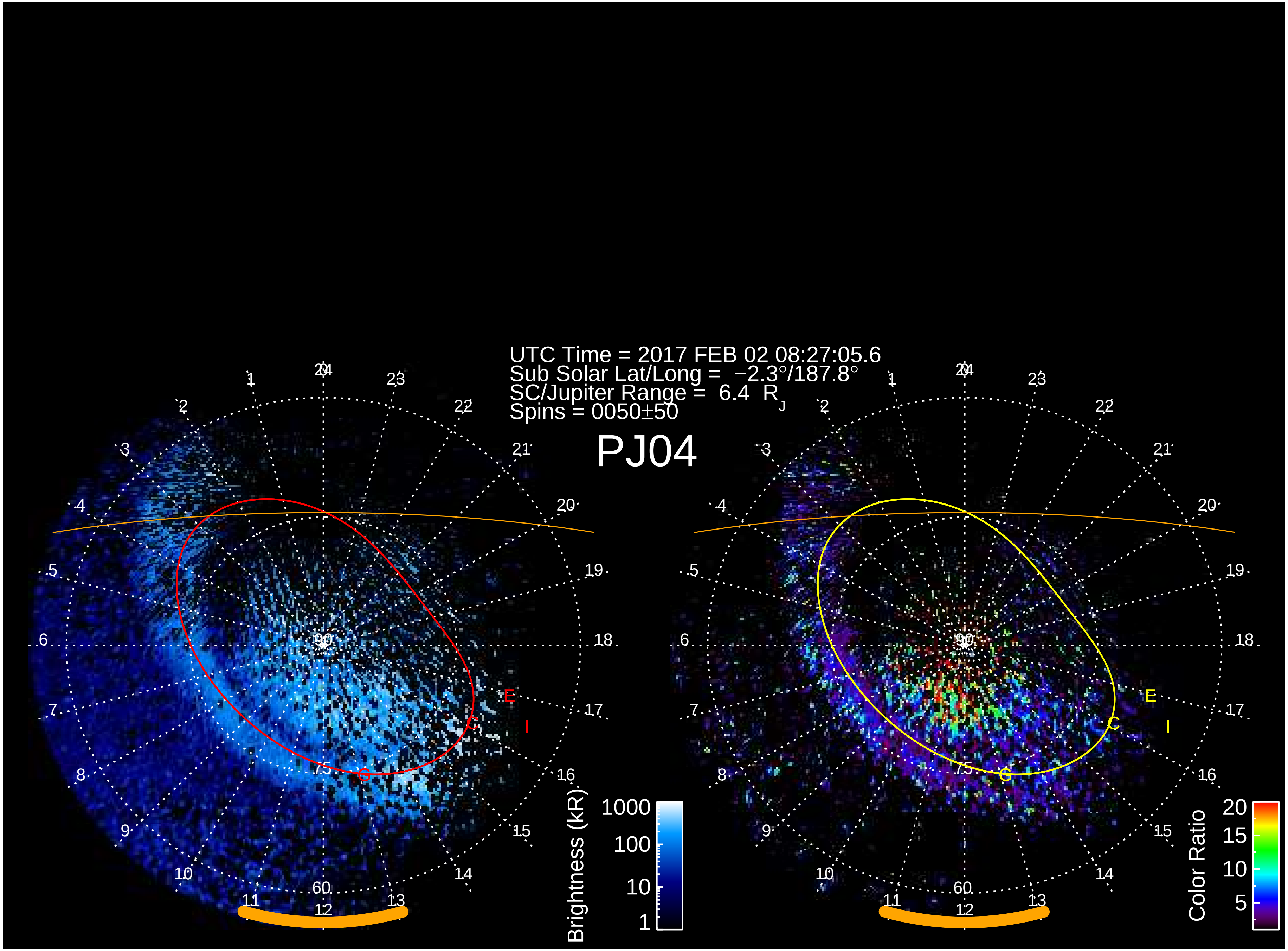
UTC Time = 2017 FEB 02 08:27:05.6
Sub Solar Lat/Long = −2.3°/187.8°
SC/Jupiter Range = 6.4 R_J
Spins = 0050±50
PJ04
Brightness (kR)
1000
100
10
1
Color Ratio
20
15
10
5

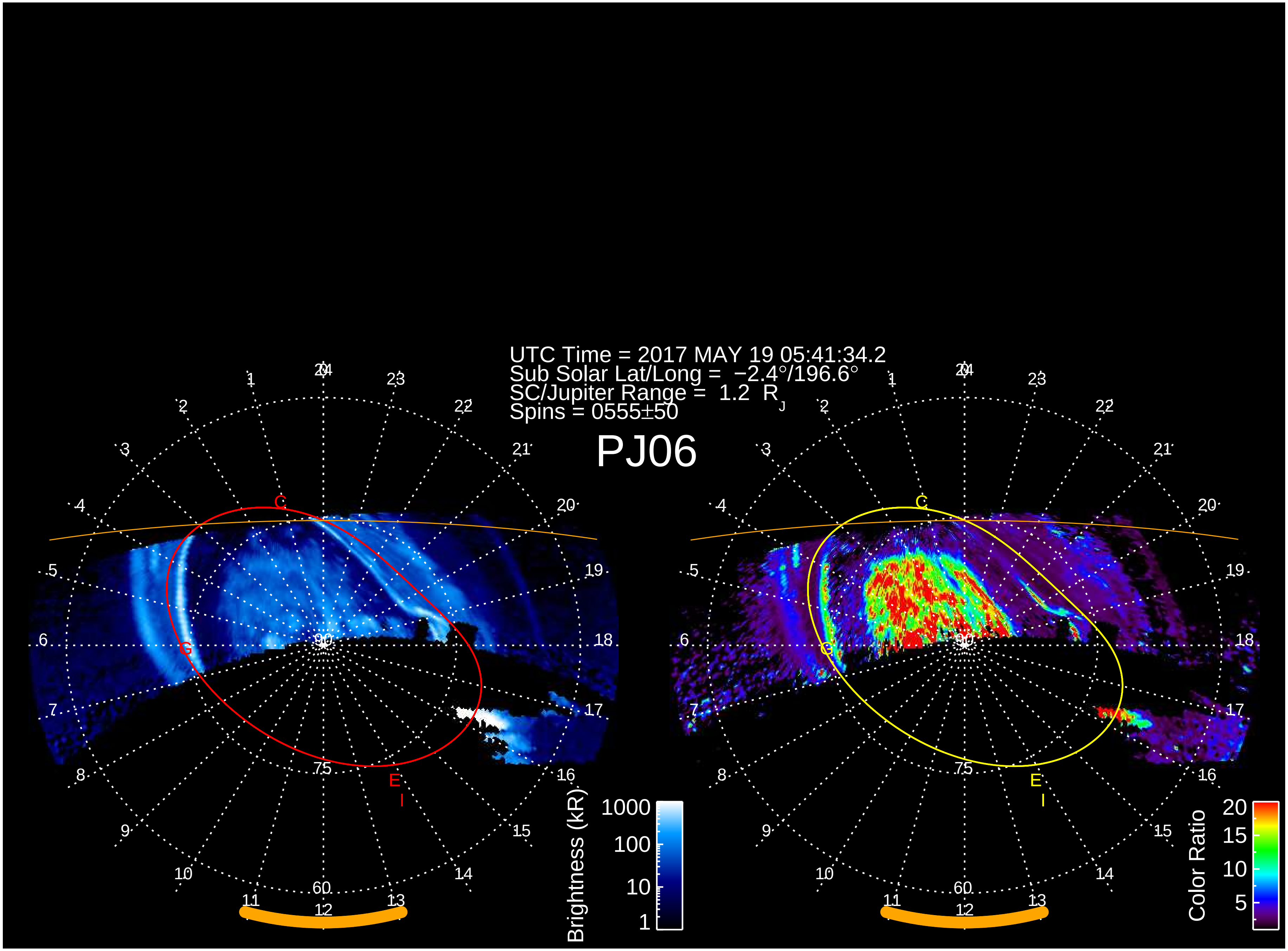
UTC Time = 2017 MAY 19 05:41:34.2
Sub Solar Lat/Long = −2.4°/196.6°
SC/Jupiter Range = 1.2 R_J
Spins = 0555±50
PJ06
Brightness (kR)
1000
100
10
1
Color Ratio
20
15
10
5

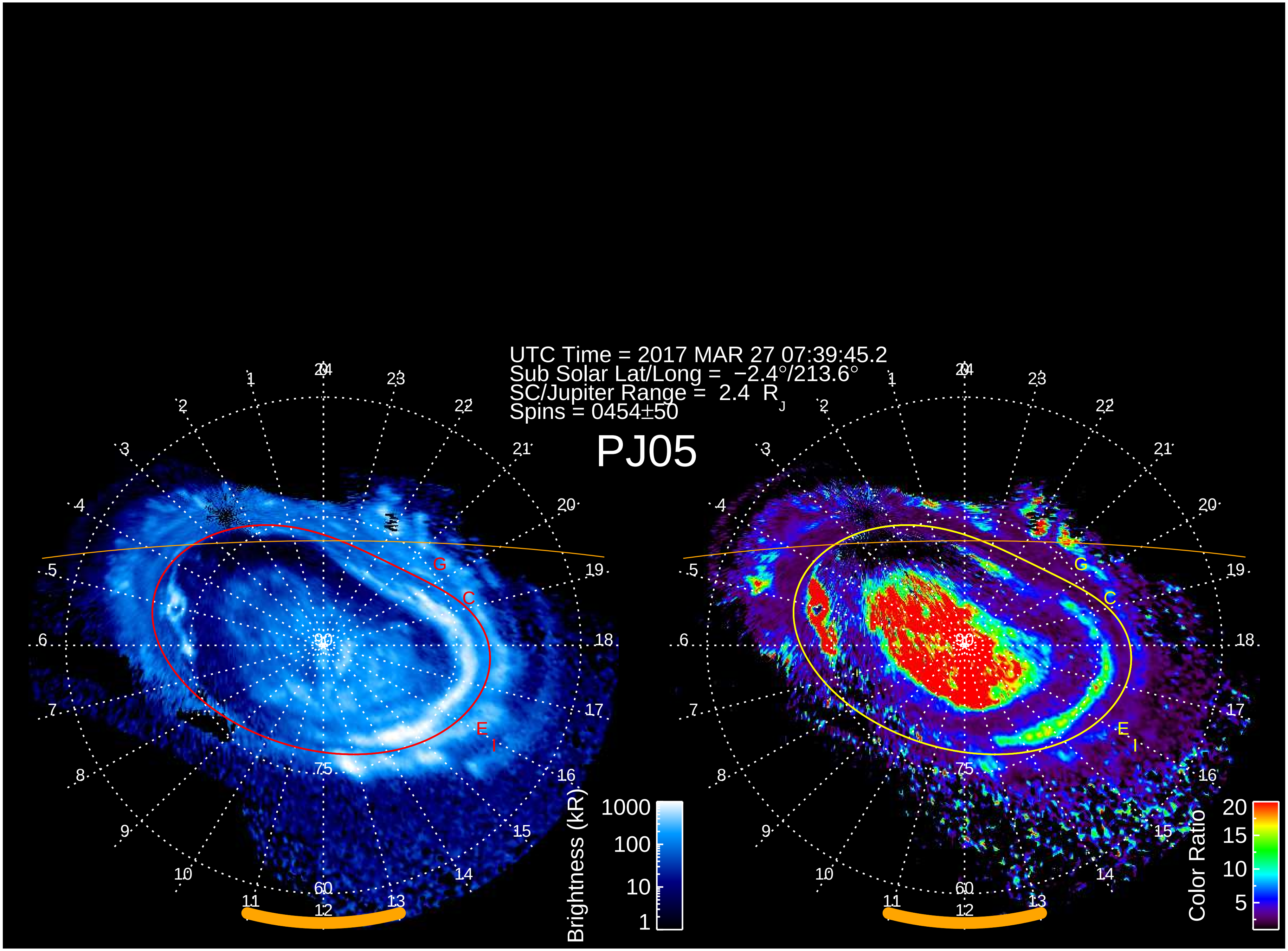

UTC Time = 2017 MAR 27 07:39:45.2
Sub Solar Lat/Long = −2.4°/213.6°
SC/Jupiter Range = 2.4 R$_J$
Spins = 0454±50
PJ05
Brightness (kR)
1000
100
10
1
Color Ratio
20
15
10
5
G
C
E
I

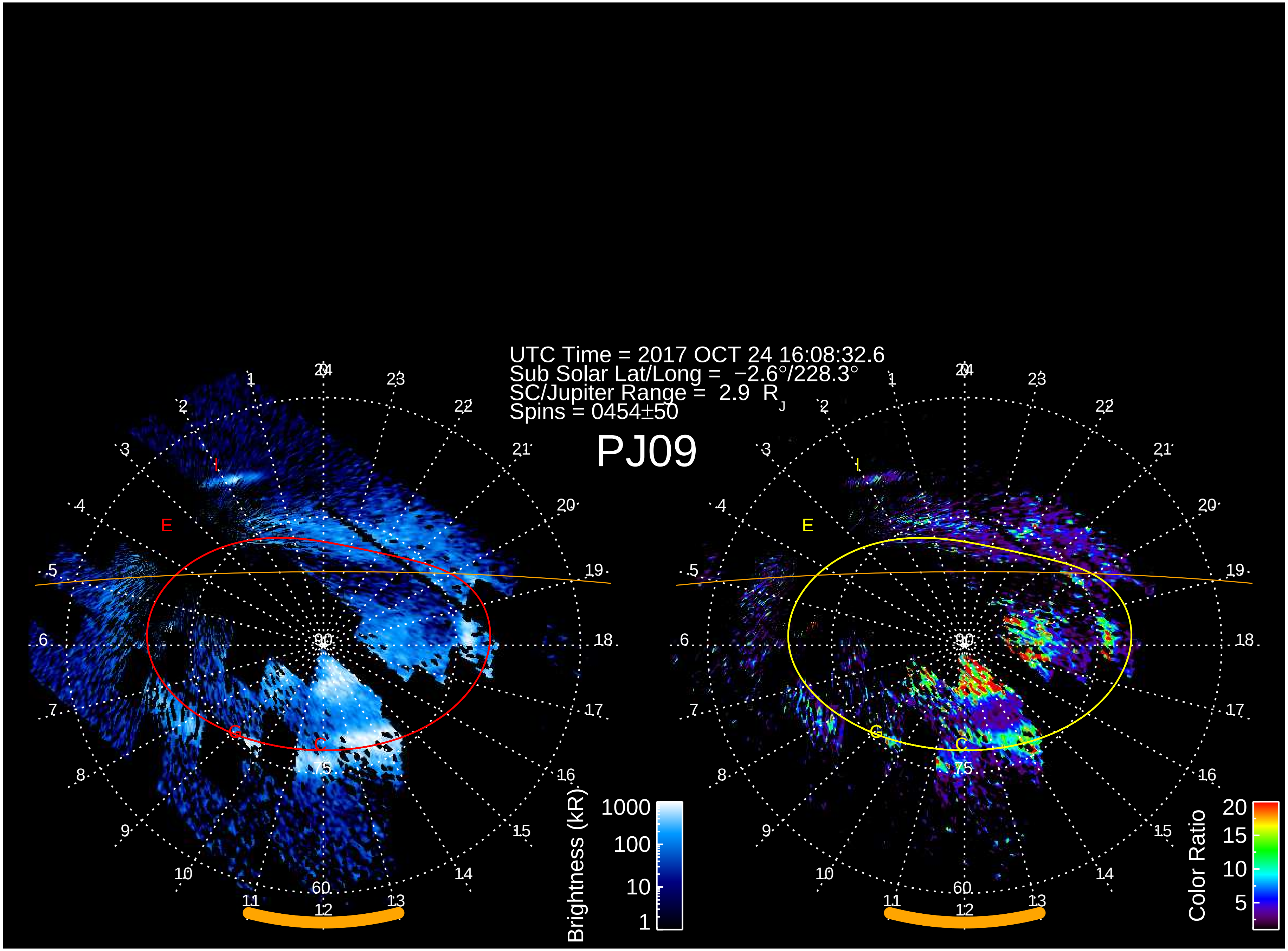
UTC Time = 2017 OCT 24 16:08:32.6
Sub Solar Lat/Long = −2.6°/228.3°
SC/Jupiter Range = 2.9 R_J
Spins = 0454±50
PJ09
Brightness (kR)
1000
100
10
1
Color Ratio
20
15
10
5

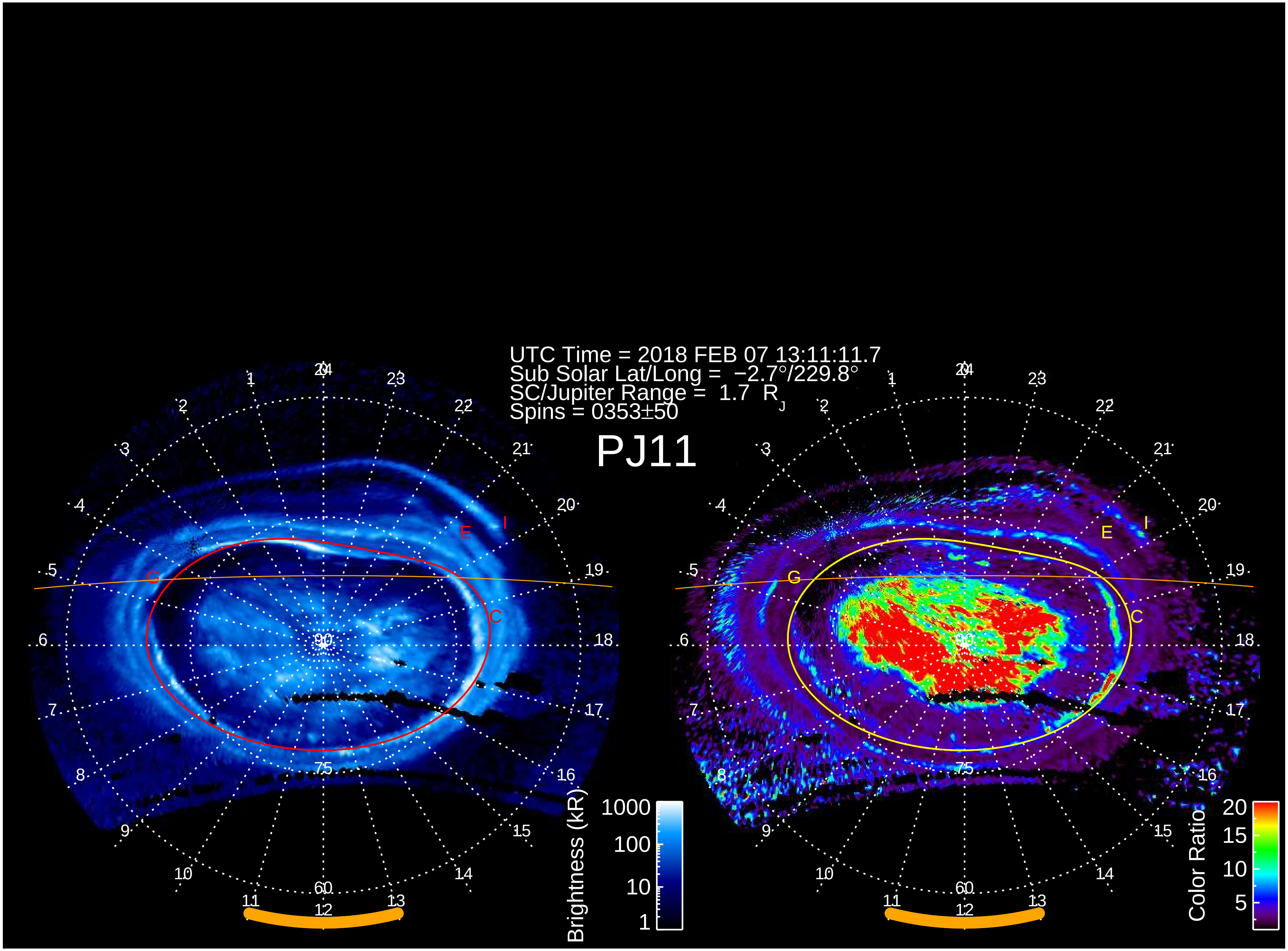

UTC Time = 2018 FEB 07 13:11:11.7
Sub Solar Lat/Long = −2.7°/229.8°
SC/Jupiter Range = 1.7 R_J
Spins = 0353±50
PJ11
Brightness (kR)
1000
100
10
1
Color Ratio
20
15
10
5

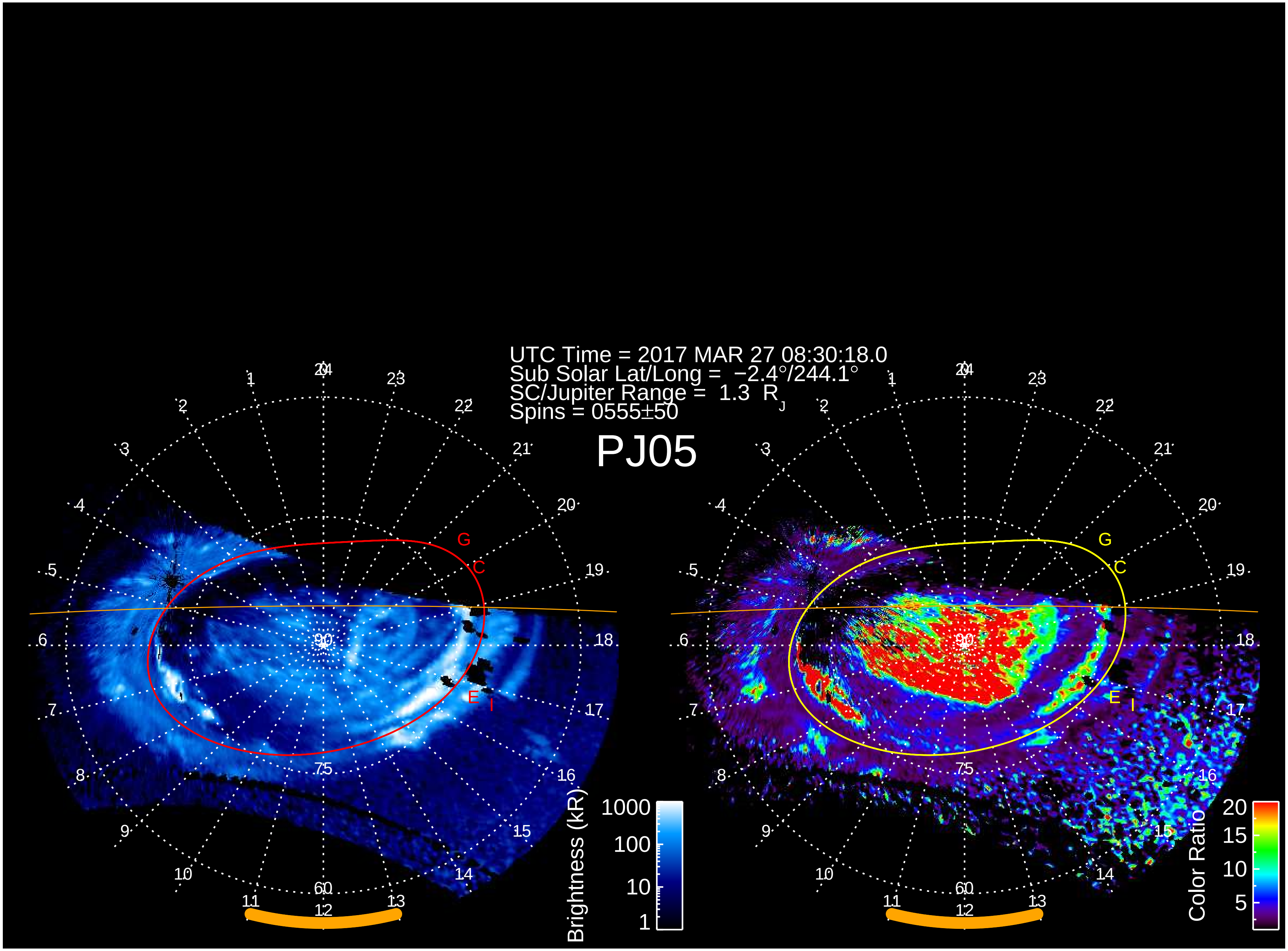

UTC Time = 2017 MAR 27 08:30:18.0
Sub Solar Lat/Long = −2.4°/244.1°
SC/Jupiter Range = 1.3 R_J
Spins = 0555±50
PJ05
Brightness (kR)
1000
100
10
1
Color Ratio
20
15
10
5
G
C
E
I

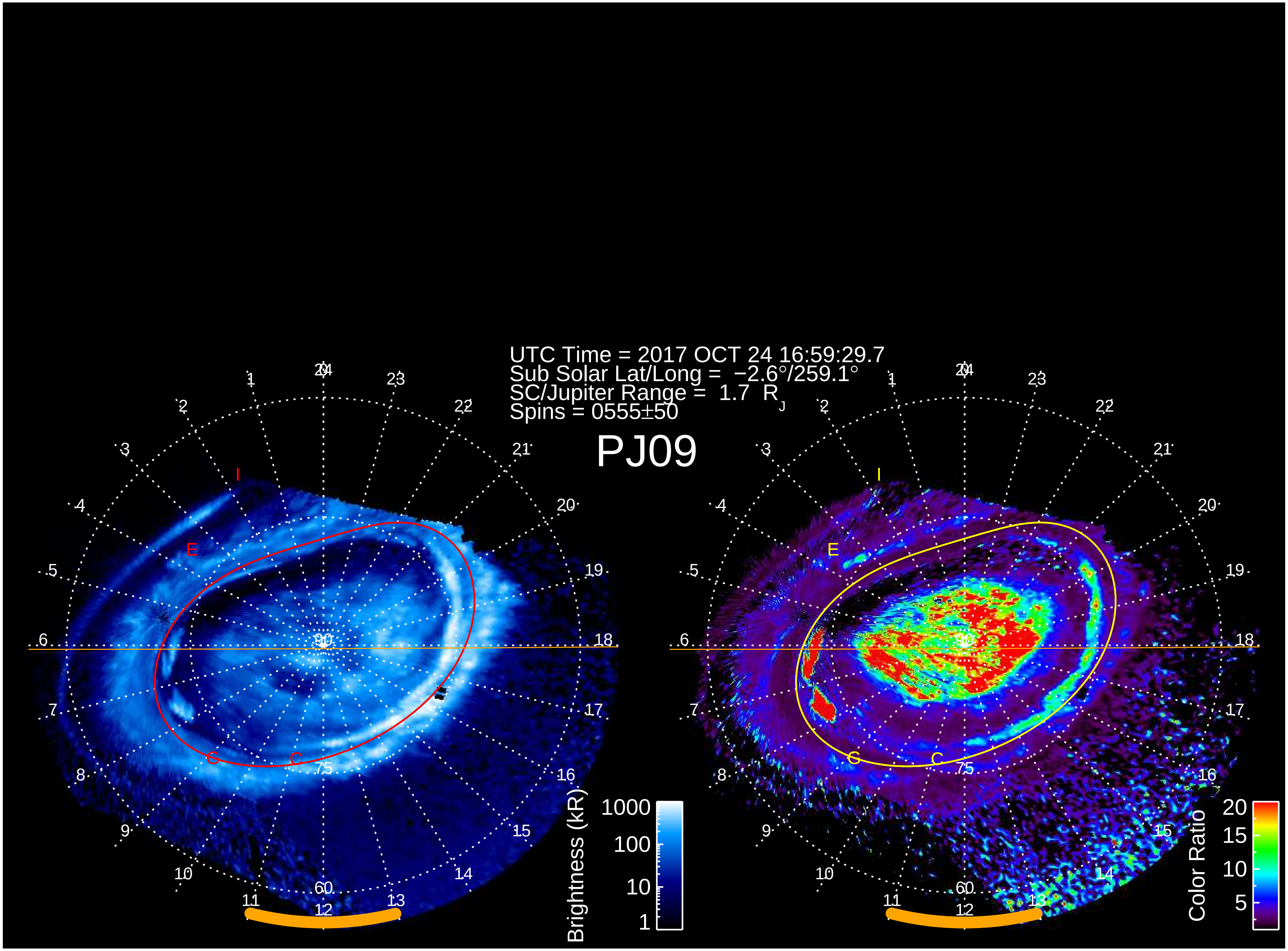

UTC Time = 2017 OCT 24 16:59:29.7
Sub Solar Lat/Long = −2.6°/259.1°
SC/Jupiter Range = 1.7 R$_J$
Spins = 0555±50
PJ09
Brightness (kR)
1000
100
10
1
Color Ratio
20
15
10
5

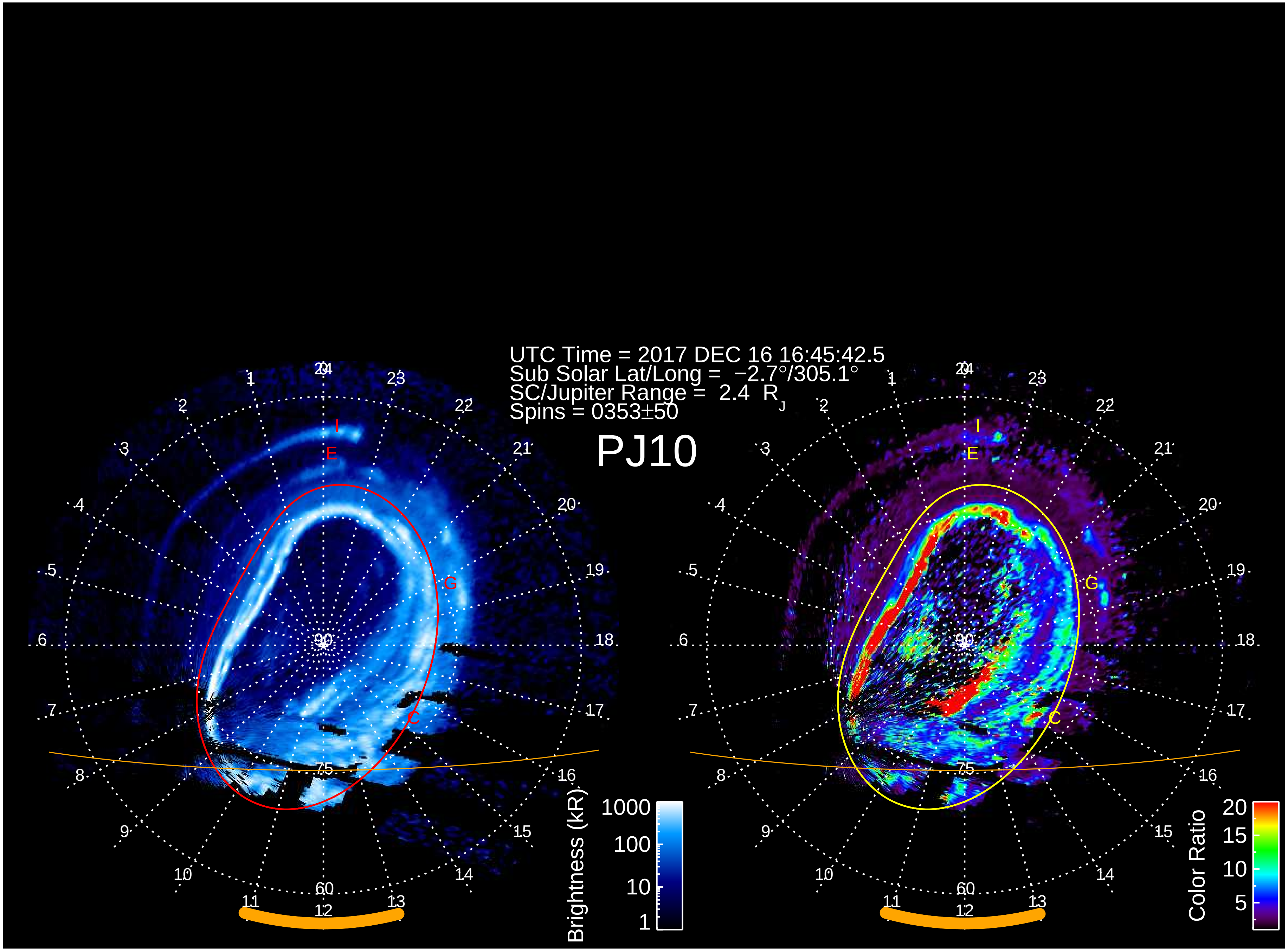
UTC Time = 2017 DEC 16 16:45:42.5
Sub Solar Lat/Long = −2.7°/305.1°
SC/Jupiter Range = 2.4 R_J
Spins = 0353±50
PJ10
Brightness (kR)
1000
100
10
1
Color Ratio
20
15
10
5

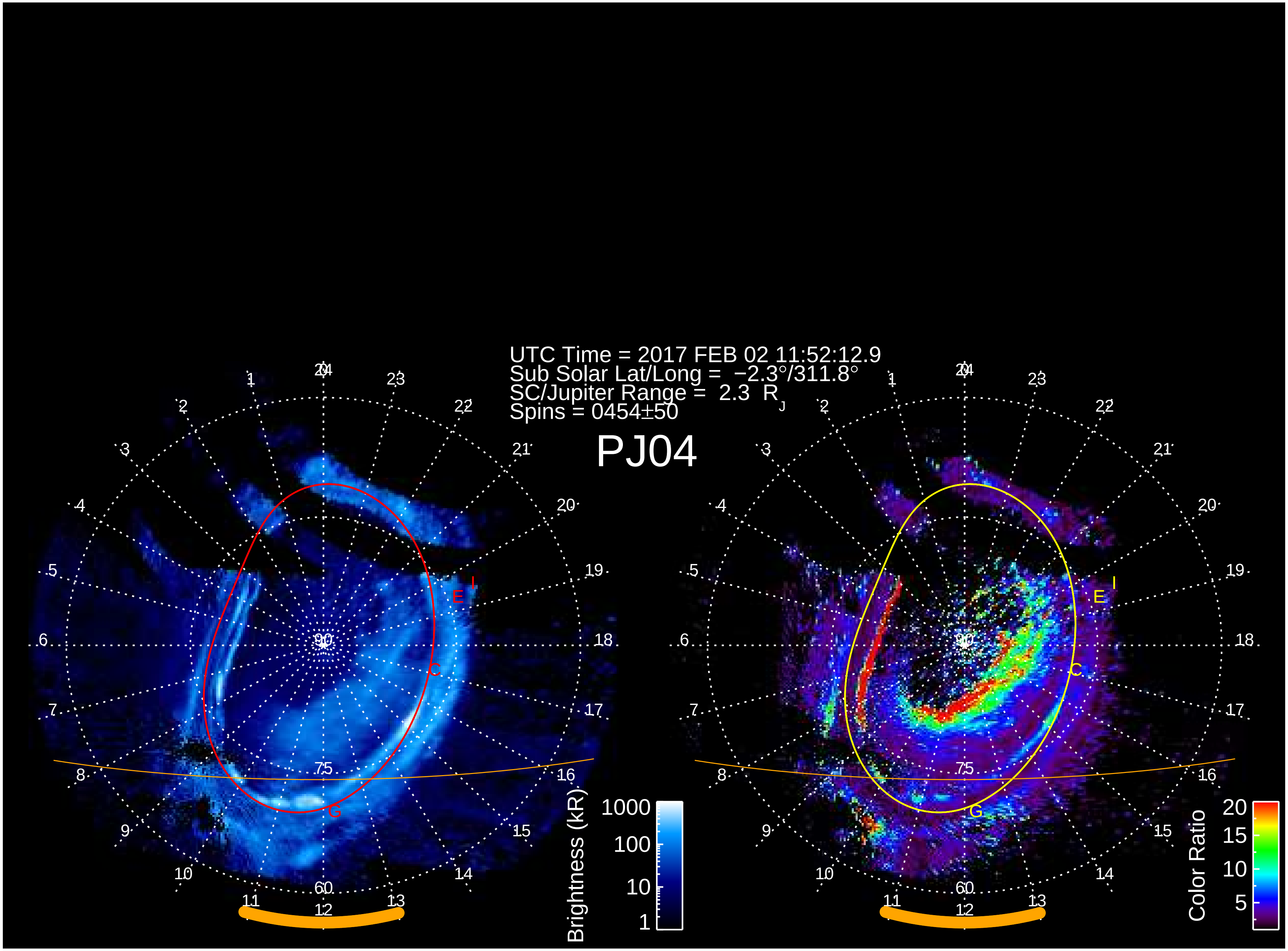
UTC Time = 2017 FEB 02 11:52:12.9
Sub Solar Lat/Long = −2.3°/311.8°
SC/Jupiter Range = 2.3 R_J
Spins = 0454±50
PJ04
Brightness (kR)
1000
100
10
1
Color Ratio
20
15
10
5

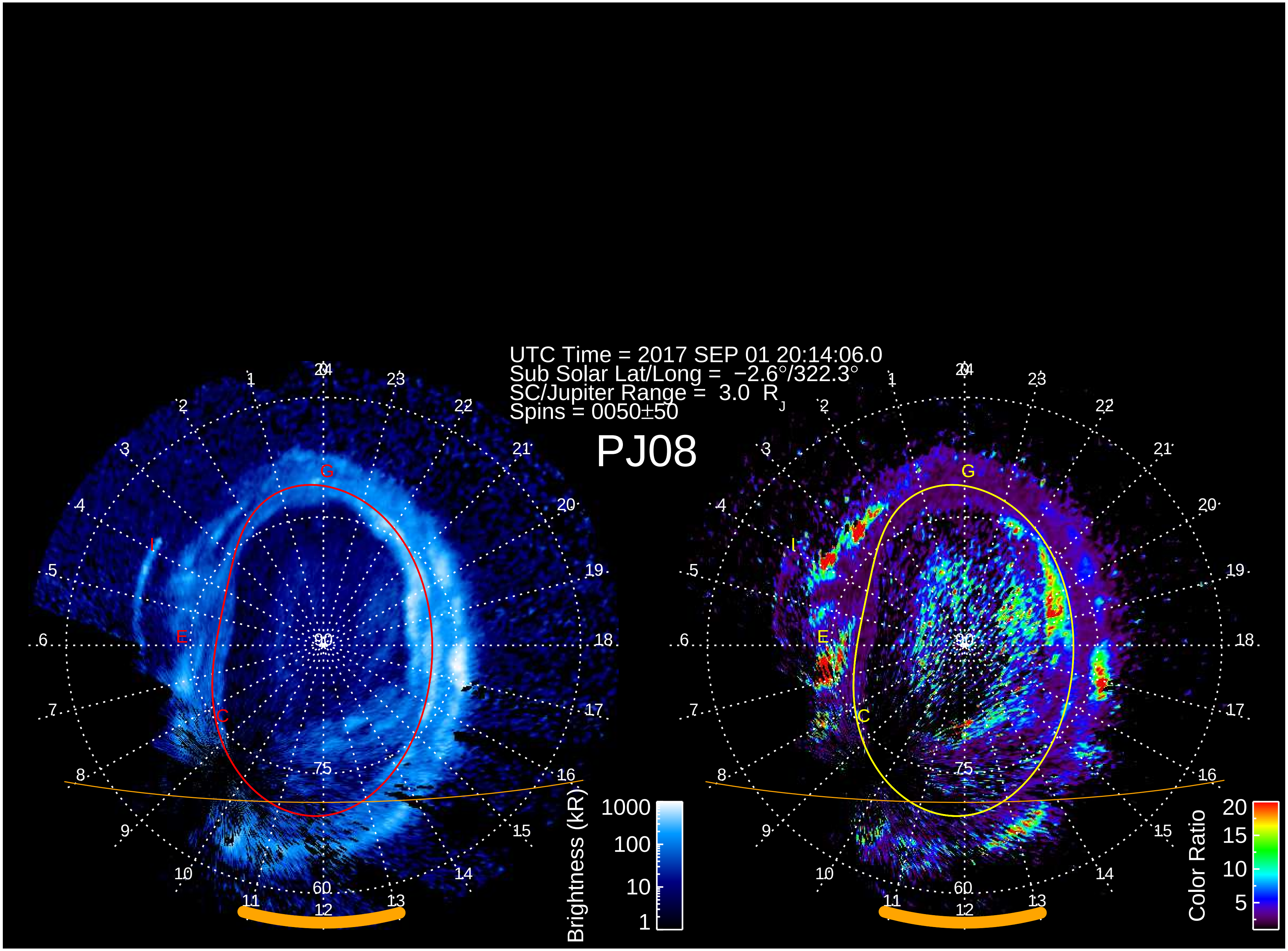

UTC Time = 2017 SEP 01 20:14:06.0
Sub Solar Lat/Long = −2.6°/322.3°
SC/Jupiter Range = 3.0 R_J
Spins = 0050±50
PJ08
Brightness (kR)
1000
100
10
1
Color Ratio
20
15
10
5
G
I
E
C

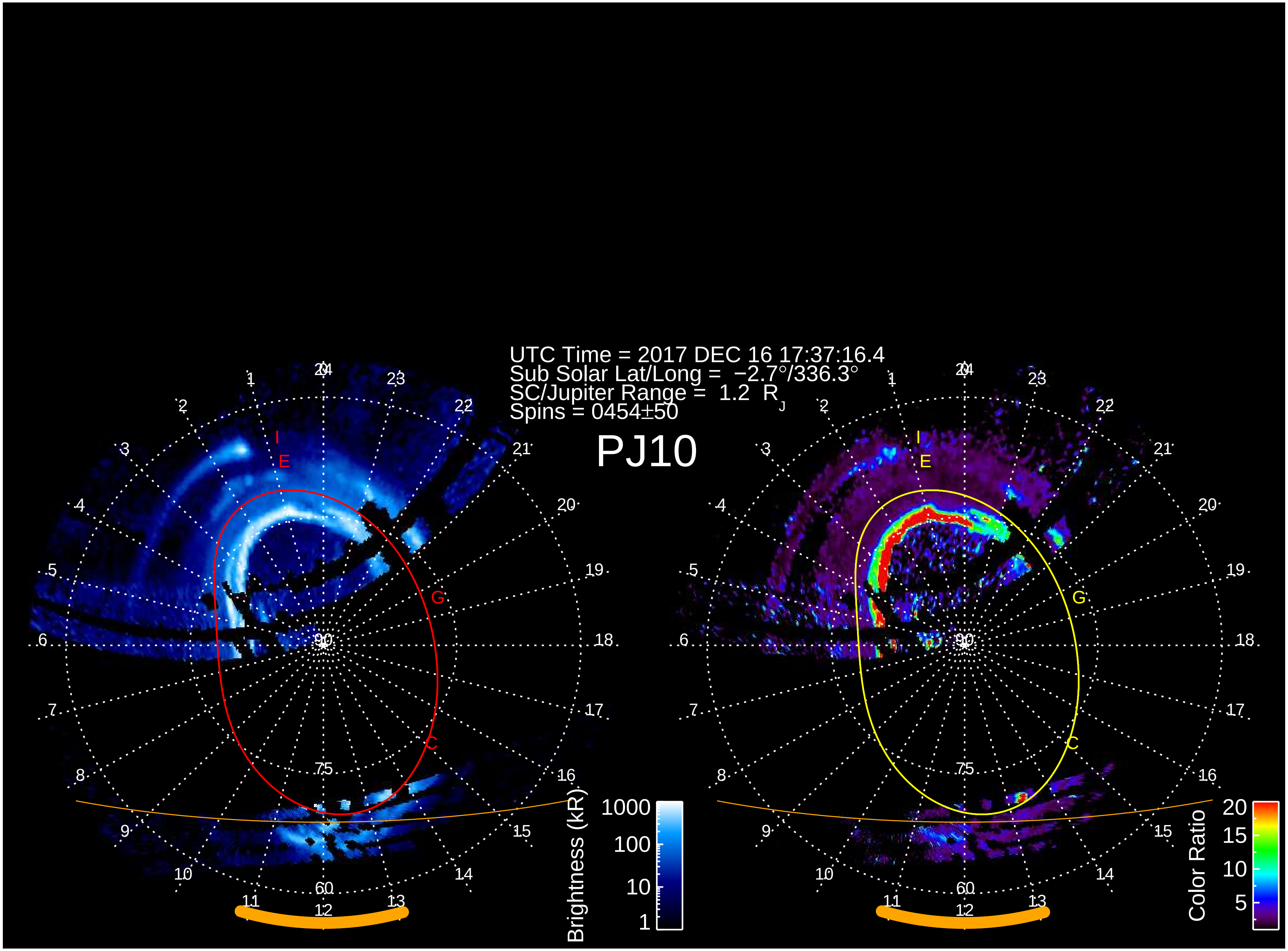

UTC Time = 2017 DEC 16 17:37:16.4
Sub Solar Lat/Long = −2.7°/336.3°
SC/Jupiter Range = 1.2 R_J
Spins = 0454±50
PJ10
Brightness (kR)
1000
100
10
1
Color Ratio
20
15
10
5

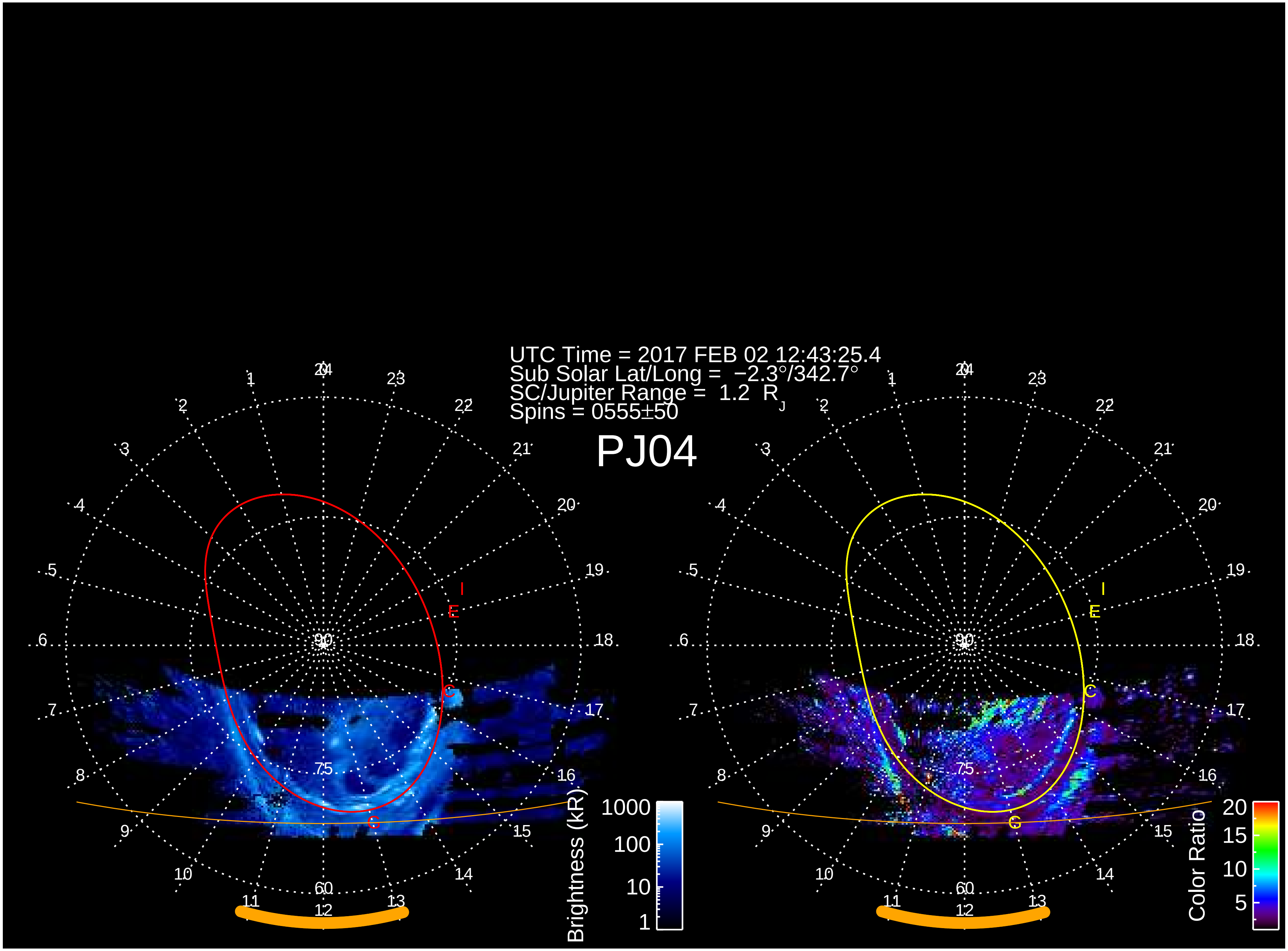
UTC Time = 2017 FEB 02 12:43:25.4
Sub Solar Lat/Long = −2.3°/342.7°
SC/Jupiter Range = 1.2 R_J
Spins = 0555±50
PJ04
Brightness (kR)
1000
100
10
1
Color Ratio
20
15
10
5

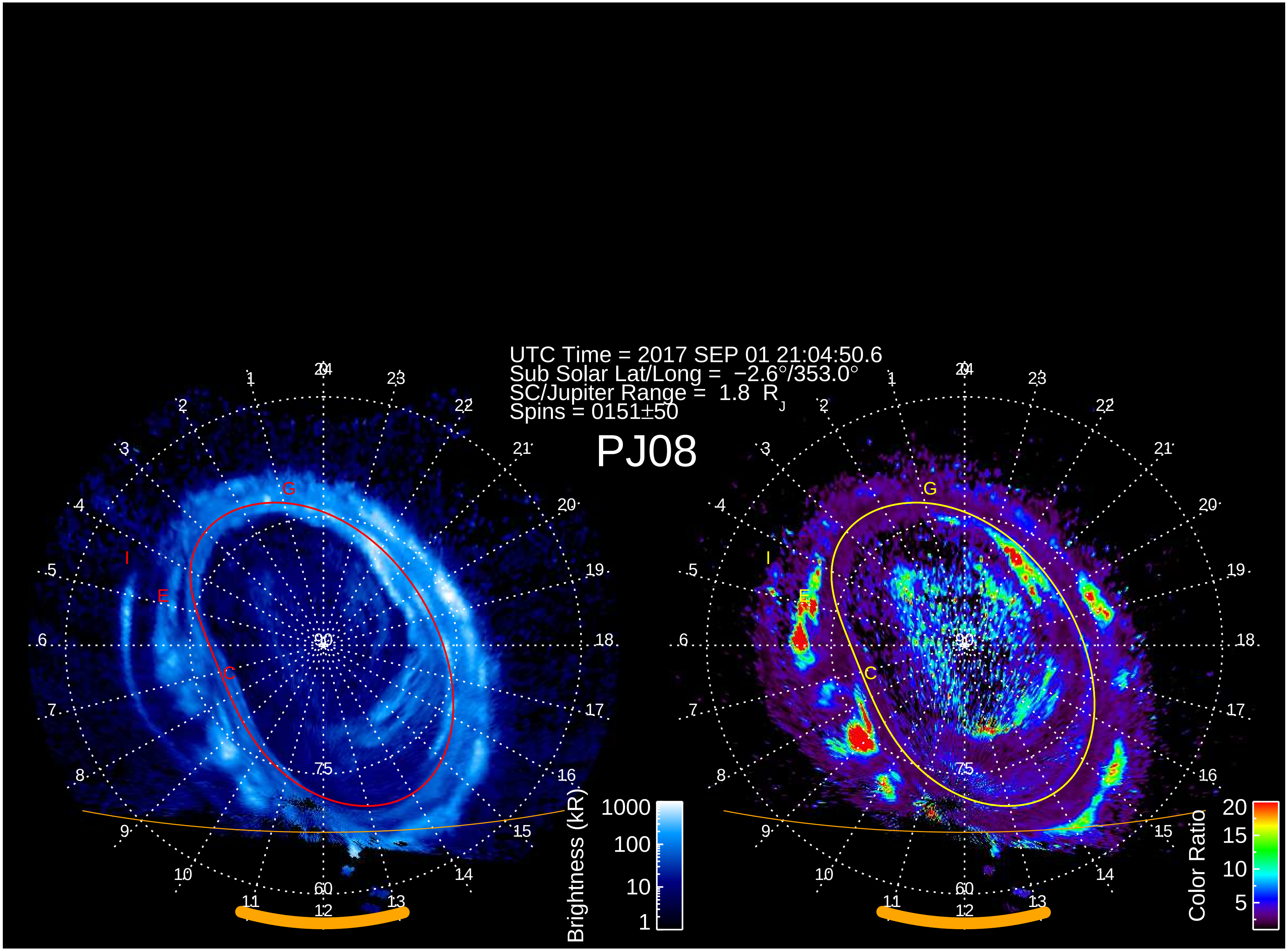
UTC Time = 2017 SEP 01 21:04:50.6
Sub Solar Lat/Long = −2.6°/353.0°
SC/Jupiter Range = 1.8 R_J
Spins = 0151±50
PJ08
G
I
E
C
75
60
90
Brightness (kR)
1000
100
10
1
Color Ratio
20
15
10
5